Intracellular Cargo Transport by Single-Headed Kinesin Motors

by

Kristin I. Schimert

A dissertation submitted in partial fulfillment
of the requirements for the degree of
Doctor of Philosophy
(Biophysics)
in The University of Michigan
2018

Doctoral Committee:

Professor Kristen J. Verhey, Chair
Assistant Professor Michael A. Cianfrocco
Associate Professor Ryoma Ohi
Associate Professor Ajit P. Joglekar
Associate Professor Sarah Veatch

Kristin I. Schimert

ORCID iD: 0000-0001-9209-7986

To my parents

ACKNOWLEDGMENTS

I gratefully acknowledge the many people in my life who have been instrumental in my scientific training and personal support.

First, my PhD adviser, Professor Kristen Verhey. I cannot imagine a better mentor, scientifically or personally. Thank you for welcoming me into your lab, for helping me step outside my comfort zone to think about science in a different way, for encouraging me to be confident, and for setting an example in everything you do. You are my hero. You inspire so many people and are living proof that it is very possible to be both an amazing scientist AND human. When I have felt like something was the end of the world, you convinced me that it would be ok (which is a nontrivial task). I cannot adequately express how grateful I am to have you as a mentor. I wish I could work for you forever.

My thesis committee: Kristen Verhey, Mike Cianfrocco, Puck Ohi, Ajit Joglekar, Sarah Veatch, and Barry Grant. Thank you for your patience, enthusiasm, feedback, and great ideas. As a younger graduate student, I never would have guessed that I would eventually enjoy committee meetings, but I did. I will really miss our discussions.

The Verhey lab. We can go from commiserating to laughing to communicating a thousand words with a single look. I love our community and how we accept each other's neuroses. Thank you for creating such a fun, supportive, helpful environment in which to do science. Thank you especially to Breane Budaitis, who has been an amazing colleague, collaborator, and friend. I feel so lucky to have coworkers who are

also stellar friends. Not everyone can say they WANT to continue to hang out with their coworkers after work. And as I said about The Boss, I also wish I could work with you forever.

Wei Cheng and the Cheng lab, for teaching me many things and being great labmates.

Thank you to the people who trained me during lab rotations, especially Stephen Norris, Jin Kim, Yuanjie Pang, and Yubing Sun.

My collaborators, Nikki Reinemann and Matt Lang. Thank you for being so patient and willing to try a million different things until we got our experiments to work. Thank you also for hosting us for a week at Vanderbilt with lots of motors and hot chicken.

The Department of Cell and Developmental Biology, which has welcomed me and given me a home. Thank you to all the administrative staff for treating me like a CDB student. Diane Fingar, Mara Duncan, Billy Tsai, and their labs. Thank you for your feedback during weekly joint group meetings and for being great people. Thank you to Noemi Mirkin, Ari Gafni, and Michal Zochowski from the Biophysics Program for their support.

Thank you to Ahmet Yildiz and the Yildiz lab, for introducing me to motors and microscopy as an undergraduate, allowing me to explore and pursue an interesting project independently, and setting an extremely high bar for lab environment. Each of you taught me so much science and made a lasting impact on me. I miss all of you a lot.

Fred Gittes for introducing me to biophysics and specifically single-molecule biophysics. I still miss your energetic lectures. David Pevovar, my high school physics teacher, who instilled in me a love of physics and whose classes I still remember better than I remember what I did last week.

My friends, who have stood by me in summer and winter seasons, literally

and metaphorically, to celebrate and to mourn. Thank you for always being there. Thank you for forgiving me when I periodically go MIA and for tracking me down, bringing me food and coffee, and making me laugh. I've been so fortunate to have incredible, supportive friends throughout my life. My graduate school friends have been integral to my sanity.

Thank you to everyone who has put up with my incessant photography (with varying amounts of patience)... Someday, when none of us can remember anything, these pictures can be our memories. Thank you for helping create those memories.

My partner in crime, Jon, who has unnatural levels of patience and has always accepted me as-is. Thank you for cooking for me and sending me thousands of dog pictures/videos to cheer me up on bad days. It's a shockingly effective tactic. Thank you for listening to my long, rambling stories and for genuinely caring and encouraging me. Being in a long-distance relationship for 6 years is not easy, but the fact that we made it speaks for itself.

My dogs, who are my sunshine and inspired me to graduate so I could get one of my own.

Thank you to my family, who has constantly supported me throughout my life and always pushed me to excel in math and science. Thank you for loving me unconditionally, for chatting with me at odd hours, and for dealing with me and my nonsense for 29 years. You have encouraged me through low and high points and I am forever grateful. I would not be here without you and this dissertation is dedicated to you.

TABLE OF CONTENTS

LIST OF FIGURES

Figure

ABSTRACT

Kinesins are cytoskeletal motor proteins that transport cargoes along microtubules in eukaryotic cells. Motors in the kinesin superfamily share a highly conserved structure containing two motor domains that dimerize through a coiled-coil stalk. The canonical view is that dimerization is required for kinesin's processive motility and force generation, as the two motor domains of a dimer step along the microtubule lattice in a tightly coordinated manner. However, whether dimerization is required for intracellular transport remains unknown. Here, we address this issue using a combination of *in vitro* and cellular assays to directly compare dimeric motors across the kinesin-1, -2, and -3 families to their monomeric forms. Surprisingly, we find that monomeric motors across different kinesin families are able to work in teams to drive peroxisome dispersion in cells. However, peroxisome transport requires minimal force output, and we find that most monomeric motors are significantly less efficient at dispersion of the Golgi complex, a high-load cargo. Strikingly, monomeric versions of the kinesin-2 family motors KIF3A and KIF3B are able to drive Golgi dispersion in cells, and teams of monomeric KIF3B motors can generate up to 11 pN of force in an optical trap. The ability of KIF3B to work in teams enabled us to test the impact of monomer length on collective cargo transport and force generation. We demonstrate that increasing the motor-to-cargo distance results in a decreased efficiency of cellular cargo transport and a decreased speed and force output *in vitro*. Together, these results suggest that dimerization of kinesin motors is not required for intracellular transport; however, it enables motor-to-motor coordination and high force generation

regardless of motor-to-cargo distance. Dimerization is thus critical for cellular transport events that require an ability to generate or withstand high forces. Our findings lend insight into the minimal requirements and mechanical modulators of collective kinesin cargo transport.

CHAPTER I

Introduction

Introduction: the cytoskeleton

Cells are the most basic building blocks of life. However, the cell itself is a complex, crowded factory of intricately intertwined processes. These processes are coordinated in time and space to maximize the efficiency of the factory.

For many processes, random diffusion is insufficient to achieve this coordination, especially in the crowded, viscous cytoplasm (Fulton, 1982). Thus, eukaryotic cells have evolved a strategy using molecular motors, or motor proteins, to move molecules from one location to another along the cytoskeleton (Ross et al., 2008). The cytoskeleton is a network of filaments that provides the structure and spatial organization of the cell (Fletcher and Mullins, 2010).

The eukaryotic cytoskeleton is composed of microtubules, actin filaments, and intermediate filaments (Fletcher and Mullins, 2010). The microtubule and actin filaments act as tracks for motor proteins and allow the cell to overcome the limits of diffusion (Figure 1.1). Microtubules (shown in green in Figure 1.1) and actin filaments (F-actin, herein referred to as actin, shown in red in Figure 1.1) are linear polymers composed of tubulin and globular actin subunits, respectively. Both have a polarity that arises from the directional assembly of their subunits (Li and Gundersen, 2008). Most eukaryotic cells are arranged with their microtubule plus (fast-growing) ends at

the cell periphery and their minus (slow-growing) ends near the nucleus. Likewise, actin plus ends are oriented toward the cell periphery and minus ends are pointing inward toward the cell center. Intermediate filaments do not have polarity and do not support the directional motility of motors (Fletcher and Mullins, 2010).

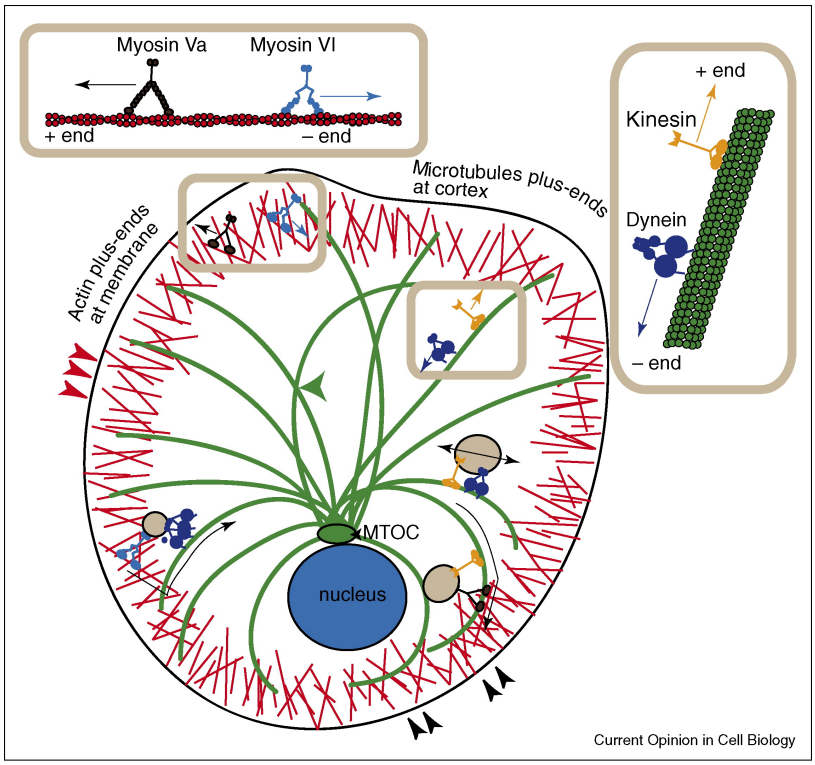

Figure 1.1: **Cartoon representation of motor proteins and vesicular cargo transport in the cell.**
Myosin family motors, myosin Va (dark brown) and myosin VI (light blue), walk along actin filaments (red) at the cortex. Myosin Va walks toward the F-actin plus end, which is oriented toward the membrane. Myosin VI walks toward the minus end of F-actin, toward the cell interior. Microtubule-based motors include the kinesin family motors (orange) and cytoplasmic dynein (violet). Kinesin motors walk to the plus ends of microtubules (green), which are oriented toward the actin cortex. Dynein motors walk toward the minus end of the microtubule, which is located at the microtubule-organizing center (MTOC, green) near the cell nucleus (blue). F-actin and microtubules cross at the cell cortex, as highlighted by black arrowheads (lower right). F-actin cross in the cortex, highlighted by the red arrowheads (left). Microtubules can intersect other microtubules highlighted by the green arrowhead (center). Vesicular cargo (tan) can bind to myosin VI and dynein to switch from actin-based to microtubule-based motion while being transported into the cell interior (lower left). Vesicles can bind kinesin and myosin Va to switch from microtubule-based to actin-based motion in order to be transported to the cell cortex (lower right). Vesicles traveling on microtubules can experience a tug of war from kinesin and dynein simultaneously bound (right). Reprinted from Ross et al., 2008, with permission.

1.1 Cytoskeletal motor proteins

Cytoskeletal motor proteins are enzymes that convert chemical energy from adenosine triphosphate (ATP) hydrolysis into mechanical work (Knight and Molloy, 1999; Vale and Milligan, 2000). For motor proteins involved in intracellular transport, the mechanical work results in their directional movement along cytoskeletal tracks. This movement facilitates a large number of critical cellular functions ranging from division of the genome to the daughter cells to signaling in the brain to contraction of muscles (Hirokawa et al., 2010). There are three classes of motor proteins in eukaryotic cells: kinesin, myosin, and dynein (Figure 1.2).

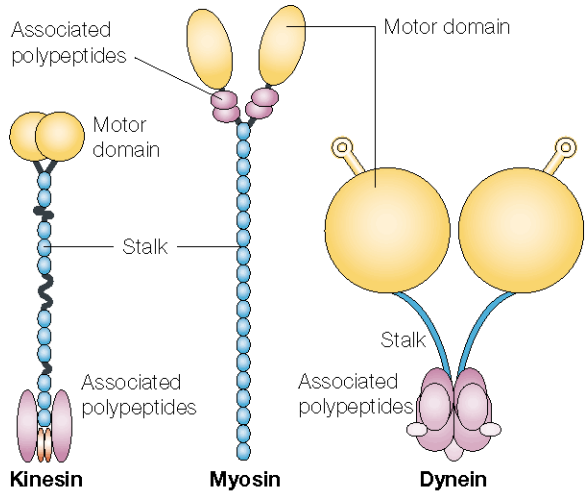

Figure 1.2: **Overview of three molecular motor prototypes.**
The actin-based motor skeletal muscle myosin in the centre is flanked by the microtubule motors conventional kinesin on the left and cytoplasmic dynein on the right. All three motors consist of a dimer of two heavy chains whose catalytic domains are shown in yellow, whereas the stalks, which form extended coiled-coils in both myosin and kinesin, are shown in blue. Associated polypeptides (four light chains in skeletal muscle myosin, two light chains in conventional kinesin, and a complex set of intermediate, light-intermediate and light chains in dynein) are shown in purple. The antennae extending from the dynein heads contain the microtubule binding site, which in myosin and kinesin is part of the compact head. (Drawn roughly to scale.) Reprinted from Woehlke and Schliwa, 2000, with permission.

Dynein and kinesin carry out long-range transport along microtubule highways, whereas myosin moves shorter distances along actin roads. All three motor types contain globular motor domains (often called "heads" and shown in yellow in Figure 1.2) that are responsible for both ATP hydrolysis and track binding. They also contain a stalk domain, usually a coiled-coil structure, that enables oligomerization of polypeptides into dimers and tetramers. Finally, they contain a "tail" domain that can bind to associated polypeptides and confers functional/cargo specificity.

Over the last few decades, diverse experimental approaches have revealed a multitude of data on the enzymatic, kinetic, motility, and mechanical properties of all three motor classes (Vale, 2003). Like other enzymes, cytoskeletal motors can be described according to their processivity; chemical or kinetic processivity is the ability to undergo multiple rounds of ATP hydrolysis before detaching from their track, whereas mechanical processivity is the ability to take successive steps along their track before detaching (Cross, 2004; Chowdhury, 2013). Some motors are highly processive and some are nonprocessive. All three types of motors hydrolyze one molecule of ATP per step they take along their track (Schnitzer and Block, 1997; Visscher et al., 1999; Sakamoto et al., 2008; Mallik et al., 2004). Their affinity for their track also changes depending on the stage of their catalytic cycle (Cross, 2004; Wang et al., 2015; Hackney, 1996).

All three classes of cytoskeletal motor proteins are considered to be superfamilies with large numbers of polypeptides encoding motors of that class. For example, in the human genome there are 45 genes encoding kinesin motor proteins, as defined by the presence of a kinesin motor domain (Verhey and Hammond, 2009). The kinesin motor domains of these polypeptides are highly similar, but it is thought that the divergent sequences in their motor domains give rise to strikingly different motility properties, such as speed, run length, and stall force, and that these motility properties are tuned for the cellular function of the particular motor. One goal in the field

is to understand how the biophysical properties of a motor translate to its behavior in the cell.

Myosins and kinesins are thought to have evolved from a common ancestor (Kull et al., 1996, 1998). Indeed, they share many features and structural homology. Their motor domains include common core structural elements, with the nucleotide-binding site on the opposite side as the filament-binding site. Interestingly, myosins and kinesins exhibit reversed kinetics during interaction with their track; kinesins bound to ADP are in a weak microtubule-binding state, whereas myosins bound to ADP are in a strong actin-binding state. Dyneins are unrelated to myosins and kinesins and are members of the AAATPase family (Vale, 2003; Bhabha et al., 2016).

1.2 Experimental approaches: from *in vitro* to cellular assays

Over the years, several *in vitro* experimental approaches have been instrumental in revealing the enzymatic, kinetic, motility, and mechanical properties of all three motor classes. In this section, I introduce these assays and describe their benefits and drawbacks.

1.2.1 Single-molecule motility assays

In vitro motility assays were first developed by Sheetz and Spudich (1983) for myosin and Vale et al. (1985) for kinesin. These demonstrated ATP-dependent, motor-driven movement of beads or filaments. Motility assays were later modified to observe filament movement by single or low numbers of motors adsorbed on a coverslip (Howard et al., 1989; Uyeda et al., 1991). However, the motility of the individual motors responsible for filament movement remained unclear. Single-molecule motility assays enabling the direct observation of fluorescently labeled motors without a cargo were later developed by Funatsu et al. (1995) for myosin and Vale et al. (1996) for kinesin. These assays have provided remarkably detailed insight into the motility

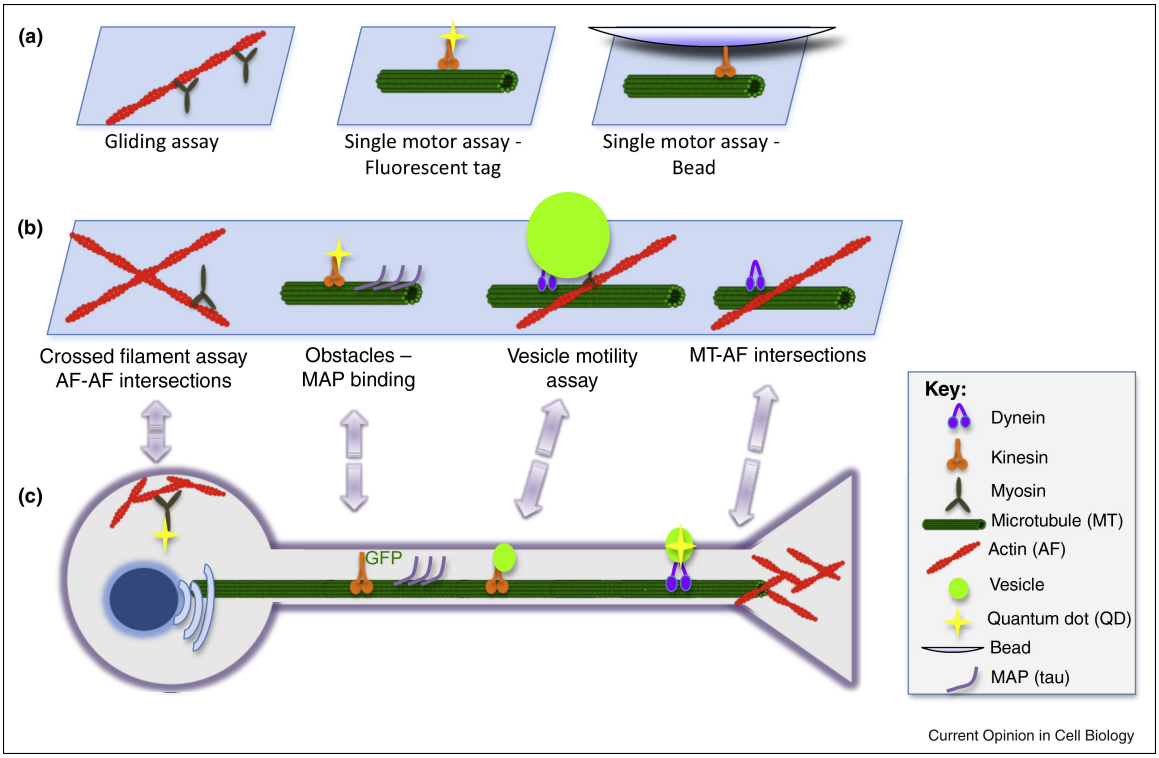

Figure 1.3: **Modeling intracellular motility with in vitro assays.**
(a) Gliding assays for all three types of molecular motors (myosins, kinesins, and dynein) involve attaching the motor to a glass microscope slide and monitoring the translocation of either actin filaments or microtubules across the surface upon addition of ATP. Sliding velocity, ATP dependence and some indications of population dynamics can be obtained. Single motor assays involve an inverse configuration: the actin filament or microtubule is attached to the glass surface and the movement of the motor is monitored, either directly via a fused fluorescent tag such as GFP, organic fluorophore or a quantum dot. This approach yields nanometer resolution, allowing the measurement of step size and angular changes during translocation. In single motor assays with beads, motors are attached to small polymer spheres that are easily observed by differential interference contrast or phase microscopy. This configuration can be used in an optical trap to measure step size, processivity and stall force. Additionally, multiple motors of the same or different types can be bound to the same bead to study collective motor activity. (b) Closer approximations of the cellular environment can be developed in crossed filament assays. In these assays, the translocation and/or switching of motors can be monitored through actinactin (AFAF), microtubulemicrotubule (MTMT), and microtubuleactin filament (MTAF) intersections. Other obstacles to motility can be bound to cytoskeletal filaments, such as the microtubule-associated protein (MAP), tau. While bead assays provide information on motor dynamics, monitoring vesicle motility in vitro provides insight into the coordinate regulation of motors bound to their natural cargos. (c) Finally, direct measurements of motility in a cell, such as the neuron shown here, can be made by expressing GFP-labeled motors, or by introducing motors or probes into the cell through pinocytosis or endocytosis.
Reprinted from Holzbaur and Goldman, 2010, with permission.

mechanisms of cytoskeletal motors, allowing the measurement of individual motor properties such as speed, run length, and microtubule on-rate.

A flow chamber is constructed, usually with double-sided tape attaching a glass coverslip to a glass microscope slide. Solutions are flowed into the narrow chamber, which holds ~ 10 uL liquid. First, microtubules are adhered to the coverslip, either via nonspecific adsorption or by specific binding of, for example, biotinylated microtubules to a streptavidin-coated surface. Next, the remaining surface is blocked with an inert protein such as BSA or casein to reduce background. Finally, motors are flowed into the chamber and an imaging/motility buffer containing ATP is added either with the motor or immediately afterward. A schematic is shown in Figure 1.3 A, center.

Total internal reflection fluorescence (TIRF) is commonly used to generate an evanescent field in the region adjacent to the interface between the glass coverslip and the solution in the flow chamber, which have different refractive indices (Axelrod, 1981, 1989). This evanescent field intensity decays exponentially with distance, restricting the region of fluorescence excitation to ≈ 100 nm above the coverslip surface. Thus, only fluorophores near the interface are excited, such as fluorescently labeled motors on the microtubule. This reduces background fluorescence from outside the focal plain, increasing the signal-to-noise ratio.

The development of techniques like Fluorescence Imaging One-Nanometer Accuracy (FIONA) ushered in a new era of motor imaging analysis. In FIONA, the center of a fluorophore's diffraction-limited point-spread-function is localized with nanometer accuracy by fitting it to a Gaussian function, allowing the tracking of individual motor domains to elucidate their stepping pattern with subsecond resolution. Using FIONA, Yildiz et al. showed that myosin V walks hand-over-hand with 37 nm center-of-mass steps (Yildiz et al., 2003) and kinesin-1 walks hand-over-hand with 8.3 nm center-of-mass-steps (Yildiz et al., 2004).

The reductionism of these assays enables high spatial and temporal resolution but also oversimplifies *in vivo* conditions. These assays do not recapitulate the complexity of the cellular environment. For example, microtubule-associated proteins, post-translational modifications, adapter proteins, and cytoplasmic crowding are not included in standard *in vitro* motility assays. These assays also only provide readouts of single motors without cargo. Furthermore, the fluorescent tags required to visualize them can affect their motility properties, so careful probe selection is required (Norris et al., 2015).

1.2.2 Optical trapping

The ability to exert and measure forces using an optical trap or optical tweezers has revolutionized the motors field. For a review, see Spudich et al. (2011a). This assay offers many of the benefits of the motility assays described above, but with the added control of mechanical manipulation and readout. It also allows for studies on nonprocessive motors (Molloy et al., 1995). Many seminal findings on all three classes of motor proteins – for example Miyata et al. (1995) for myosin, Block et al. (1990) and Visscher et al. (1999) for kinesin, and Mallik et al. (2004) for dynein – were possible only through the use of optical trapping of beads with single motors. These assays can also report on force generation when multiple motors of the same or different type are coupled to the same bead (Jamison et al., 2010, 2012).

Ashkin et al. first demonstrated optical trapping of dielectric particles with a single-beam gradient force trap in 1986 (Ashkin et al., 1986). A single-beam trap can be decomposed into two orthogonal forces: 1) the scattering force, which is proportional to the light intensity and points in the direction of the beam, pushing objects out of the trap; 2) the gradient force, which is proportional to the gradient of the light intensity and points in the direction of the intensity gradient (toward the beam focus), pulling objects into the trap.

For motors applications, a high-power infrared laser beam is used to capture a dielectric bead that is bound to motors. When the trapped bead moves out of the trap center, the gradient force acts like a Hookean spring and pulls it back to the trap center with a force of F = -kx, where F is the force, k is the spring constant or trap stiffness, and x is the displacement from the center (Bustamante et al., 2011).

Two types of optical trap geometries are commonly used in the motor field. Force clamps, which use a feedback loop to adjust the position of the beam to maintain a constant force on the trapped bead, allow for mechanochemical measurements such as velocity and step size at constant external load (Visscher et al., 1999). On the other hand, position clamps maintain the bead position, enabling detachment or stall force measurements over short distances as the motor displaces the bead from the trap center (Svoboda and Block, 1994). These are often combined with bright-field or fluorescence microscopy to visualize the bead and filament (Spudich et al., 2011b).

Several strategies have been used for bead attachment, including nonspecific adsorption, chemical crosslinking, biotin/streptavidin linkages, and antibody/antigen linkages. It is critical to ensure that the linkage to the bead does not affect the motor activity, which is especially risky in the case of nonspecific adsorption because of the lack of control over motor orientation. Bead size is an important consideration for both biological and optical reasons. Ideally, the bead should mimic endogenous cargo, but there are tradeoffs even for sizes within this range. Large beads ($\sim$1 um) are easier to trap and allow higher trap stiffness. Smaller beads are harder to trap but can resolve faster events (Spudich et al., 2011b).

Despite the exquisitely detailed information this assay yields, there are limitations (Mehta et al., 1997). First, the static immobilization of motors on the bead surface is distinct from the endogenous membrane-bound cargoes that allow motor diffusion. Some groups have performed optical trapping assays with lipid-coated beads, lipid droplets (Bartsch et al., 2013), or purified native cargoes (Barak et al.,

2013; Hendricks et al., 2014) to overcome this. Another potential problem is optical damage of the biological sample caused by the high-power laser beam (Neuman et al., 1999; Landry et al., 2009). Surface effects can also arise from using beads that are too large or have certain coatings (Spudich et al., 2011a).

1.2.3 Microtubule or actin gliding assays

In vitro gliding assays were first developed in 1985 by Vale et al. in their seminal paper identifying kinesin from giant squid axoplasm (Vale et al., 1985). Shortly thereafter, Kron and Spudich applied this idea to myosin and actin filaments using a purified system (Kron and Spudich, 1986). Microtubule or actin filament gliding assays are now commonly used to assess multi-motor function, but they have also been adapted for studying single motors (Howard et al., 1989).

A flow chamber is constructed as in the above two assays, usually with double-sided tape, to form a narrow channel between a glass coverslip and a glass microscope slide. Motors are immobilized on the glass coverslip through specific binding (Berliner et al., 1994), immunoadsorption (Post et al., 2002), or nonspecific adsorption (Howard et al., 1989) such that their motor domains are facing up into solution. Fluorescent microtubules or actin are flowed in and are propelled by the lawn of immobilized motors, giving them the appearance of gliding along the surface; this is a different frame of reference than the single-molecule motility assays described above. A schematic is shown in Figure 1.3 A, left.

Kymographs of filament position over time are generated and their speed is indicative of how well that motor works in teams. Whether a motor is processive can also be determined by examining gliding as a function of motor density. For example, one group observed reduced gliding velocity at low motor densities for non-processive yeast class V myosins but not for processive chick myosin-Va (Reck-Peterson et al., 2001). Lastly, the directionality of a motor can also be deduced by using polarity-

marked filaments in gliding assays (Tseng et al., 2018).

Limitations of this assay include the non-physiological geometry: endogenous motors in cells are able to diffuse in the lipid bilayer of their cargo, not immobilized on a flat surface. Furthermore, adsorption to the coverslip surface may change motility properties or partially denature the motors, yielding different results depending on the motor-coverslip binding strategy.

1.2.4 Cellular assays

Although the above assays have given unprecedented insight into the enzymatic, kinetic, motility, and mechanical properties of purified motor proteins, there is also great interest in evaluating the motility and cooperation of motors in a cellular environment where motors must navigate a complex cytoskeleton (e.g. intersecting filaments) in a viscoelastic environment (Veigel and Schmidt, 2011).

An important step forward in this direction was the ability to image motor proteins at the single-molecule level in cells. There are many difficulties with imaging motors in cells, including how to fluorescently label the motor to sufficiently track motility above the noise of the cellular environment. Cai et al. demonstrated tracking of fluorescently tagged kinesins at the single-molecule level in the cytoplasm of live cells (Cai et al., 2007). This work revealed the important result that individual kinesin-1 motors move with an average speed and run length that agree in cells and *in vitro*.

The authors later extended this work using two-color tracking to investigate kinesin motility on heterogeneous microtubules in COS-7 cells (Cai et al., 2009). They showed that kinesin-1 motors prefer stable microtubules marked by post-translational modifications, whereas specific motors from the kinesin-2 and -3 families are not selective. These results, inaccessible by *in vitro* methods, revealed a novel strategy for the cell to segregate trafficking events based on microtubule diversity. It would

be interesting to examine the microtubule roadmap in other cell types and with other kinesin motors in the future. For myosins, another group developed an *ex vivo* motility assay using detergent-extracted cells and showed that the actin cytoskeleton also regulates unconventional myosins through distinct track selection in different cell types (Brawley and Rock, 2009).

Optical trapping has also been performed in cells, combining high resolution force measurements with the native cellular environment. Pioneered by Ashkin et al. (1990), optical trapping in cells has been used to study transport by kinesin (Shubeita et al., 2008; Rai et al., 2013), myosin (Nambiar et al., 2009), and dynein (Blehm et al., 2013; Rai et al., 2013). Some studies have utilized latex beads phagocytosed into macrophages to dissect transport by endogenous motors on a membrane-bound cargo (Hendricks et al., 2012; Leidel et al., 2012; Rai et al., 2013). Other groups have used lipid droplets as the cargo (Shubeita et al., 2008; Leidel et al., 2012). Although measuring endogenous motors certainly has advantages, it is also impossible to be certain of their identity, and many assumptions inevitably go into these studies.

The next significant development was the ability to image motor proteins transporting cargoes in cells. Utilizing the FKBP-rapalog-FRB heterodimerization system, Kapitein et al. developed a generic approach to probe the activity of specific motors in cells by inducibly recruiting them to peroxisomes (Kapitein et al., 2010b). This assay enables the study of selected motors with membrane-bound cargoes in the native cellular environment and can be used for a wide variety of questions. In Chapter 3, I describe the application of this assay to several questions about kinesin cooperativity in teams.

The native cellular environment provides both the advantages and disadvantages of these assays. It is useful to have the cellular complexity, but it comes at the expense of control and resolution. A disadvantage of studies in cells is the lack of control over parameters such as motor number, which can be more finely tuned

in vitro. However, recent studies have taken large strides toward this, using genetic approaches to control receptor density on the peroxisome surface with a doxycycline-inducible system (Efremov et al., 2014). They were also able to modulate cargo size, another important parameter affecting multi-motor transport.

In the following sections, I will cover some of the seminal findings on the myosin and kinesin superfamilies that have used these experimental techniques.

1.3 Myosins

Myosin motor proteins move along actin filaments in eukaryotic cells. They are essential for muscle contraction, cell division, cell migration, membrane trafficking, and vesicle transport. Myosin mutations can lead to a variety of diseases including deafness, cardiomyopathy, hydrocephalus, neuronal malfunction, and intestinal disease (Hartman and Spudich, 2012).

The myosin superfamily, shown in Figure 1.4, is divided into fifteen different classes based on phylogenetic analysis (Sellers, 2000). They share a conserved motor domain that binds to actin and hydrolyzes ATP. After the motor domain, there is a neck domain that binds to light chains or calmodulin, which provide rigidity. The neck acts as a lever arm and provides the power stroke for motility by swinging relative to the motor domain in response to ATP hydrolysis; this is known as the swinging neck-lever model (Uyeda et al., 1996). Finally, the tail domains vary considerably between families (Sellers, 2000). These associate with adapter proteins or anchor the motor domain to specific cargoes, facilitating various cellular functions.

The founding family of myosins is known as conventional myosin or myosin II and includes both muscle and non-muscle motors. These operate in large arrays, forming bipolar filaments. Individual myosin II motors have a low duty ratio, or fraction of their ATPase cycle spent associated with actin, which makes them effective for working in teams.

There is considerable diversity in the oligomeric state of motors across the myosin superfamily. Some unconventional myosins, e.g. myosin V involved in vesicle transport, are dimeric and processive as individual motors due to the "hand-over-hand" motility of their two motor domains (Yildiz et al., 2004). These processive motors have a high duty ratio, taking many steps before detaching (high mechanical processivity). Other unconventional myosins, such as myosin VI, VII, and X, are monomers and are not processive as individual motors; however, they can work in teams to carry out their cellular functions. Rather than a coiled-coil for dimerization, the neck domain of these motors is followed by a single alpha-helix (SAH) domain that amplifies the power stroke of the lever arm (Knight et al., 2005; Peckham, 2011). These SAH domains have been well-characterized biophysically (Sivaramakrishnan et al., 2008, 2009) and will be used as an important tool in Chapters 2 and 3. On the other hand, Myosin VI is a monomer in solution but has been shown to undergo cargo-mediated dimerization, an important regulatory mechanism (Yu et al., 2009; Phichith et al., 2009; Mukherjea et al., 2014).

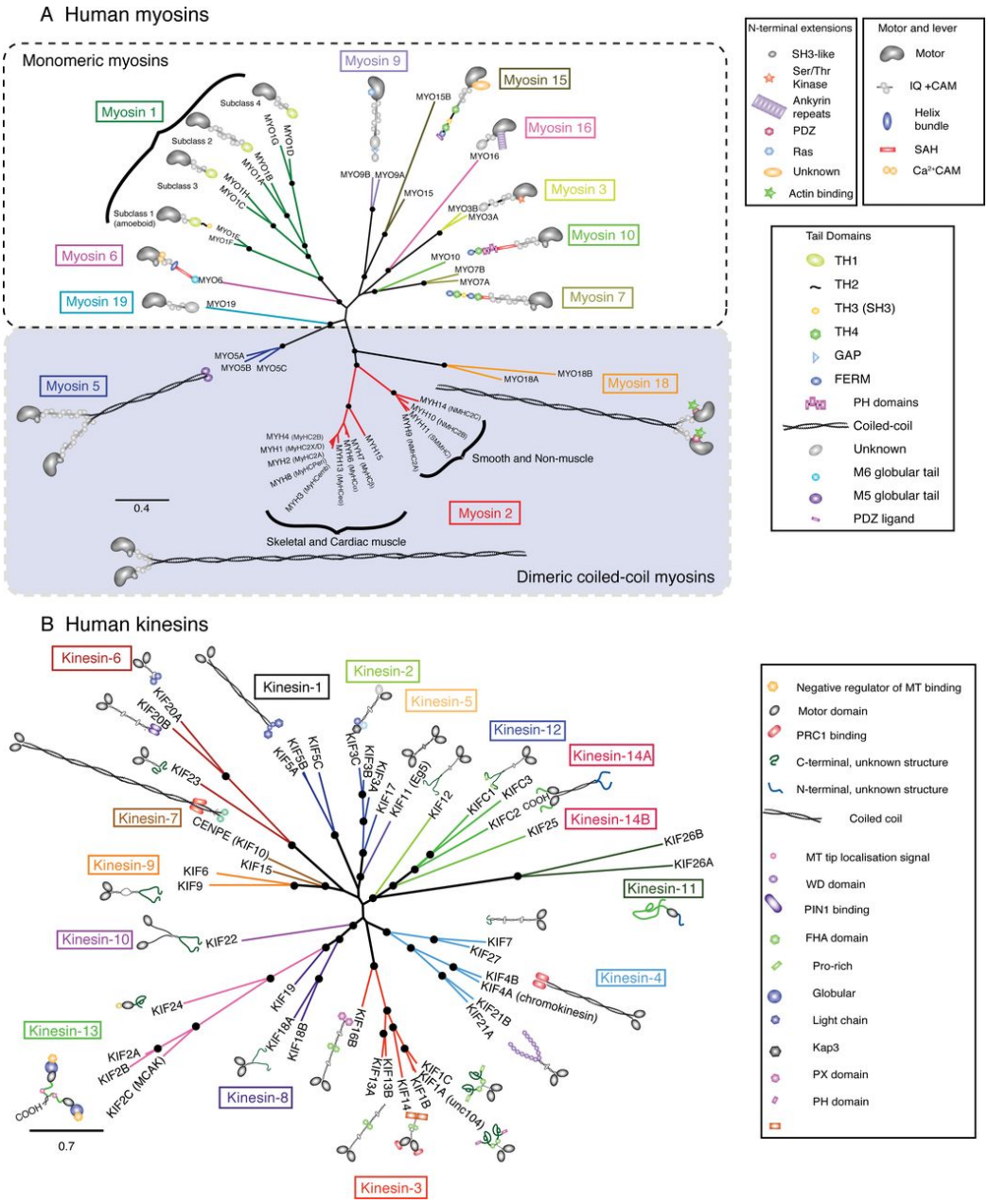

Figure 1.4: **The myosin and kinesin family trees for humans.**
Reprinted from Peckham, 2011, with permission.

1.4 Kinesins

A large number of kinesin motors are involved in anterograde transport of cargoes to the plus ends of microtubules in the cell periphery (Hirokawa et al., 1991). Transport kinesins carry diverse cargoes such as vesicles, mRNA, proteins, organelles,

and viruses. Other kinesins are involved in mitosis or walk in the opposite direction, but these will not be covered here. Owing to their critical cargoes, defects in kinesin function cause neurodegenerative diseases, developmental defects, and cancers.

The kinesin superfamily is shown in Figure 1.5 and is subdivided into fifteen different kinesin families (KIFs) based on phylogenetic analysis (Verhey and Hammond, 2009; Hirokawa et al., 2009). All members share a highly conserved motor domain (∼30-60% amino acid sequence homology), with greater variation in other regions (Hirokawa and Noda, 2008). Kinesins differ in their biophysical/biochemical motility properties as well as in their cellular functions; many studies seek to link these and demonstrate how a specific motor is optimized for its function. Much work remains to be done in this area.

At one end of kinesin, the motor domain or "head" binds to the microtubule track and hydrolyzes ATP, generating directional force. At the other end, the tail binds to cargo. The two ends are connected via a stalk formed by coiled-coils and flexible hinge regions. The stalk allows oligomerization of two motor domains and any adapter proteins for cargo binding. Between the motor domain and the stalk is the neck linker, which is the force-generating segment of kinesins (analogous to the lever arm of the myosins) (Rice et al., 1999; Hwang et al., 2008). A schematic of the structure of kinesin-1 is shown in Figure 1.7. Notably, most kinesins function as dimers, unlike the oligomeric diversity of myosins (Figure 1.4). It is thought that kinesins carry each cargo alone or in small groups (Miller and Lasek, 1985). In the absence of cargo, they are autoinhibited to prevent microtubule crowding and futile ATP consumption (Verhey and Hammond, 2009).

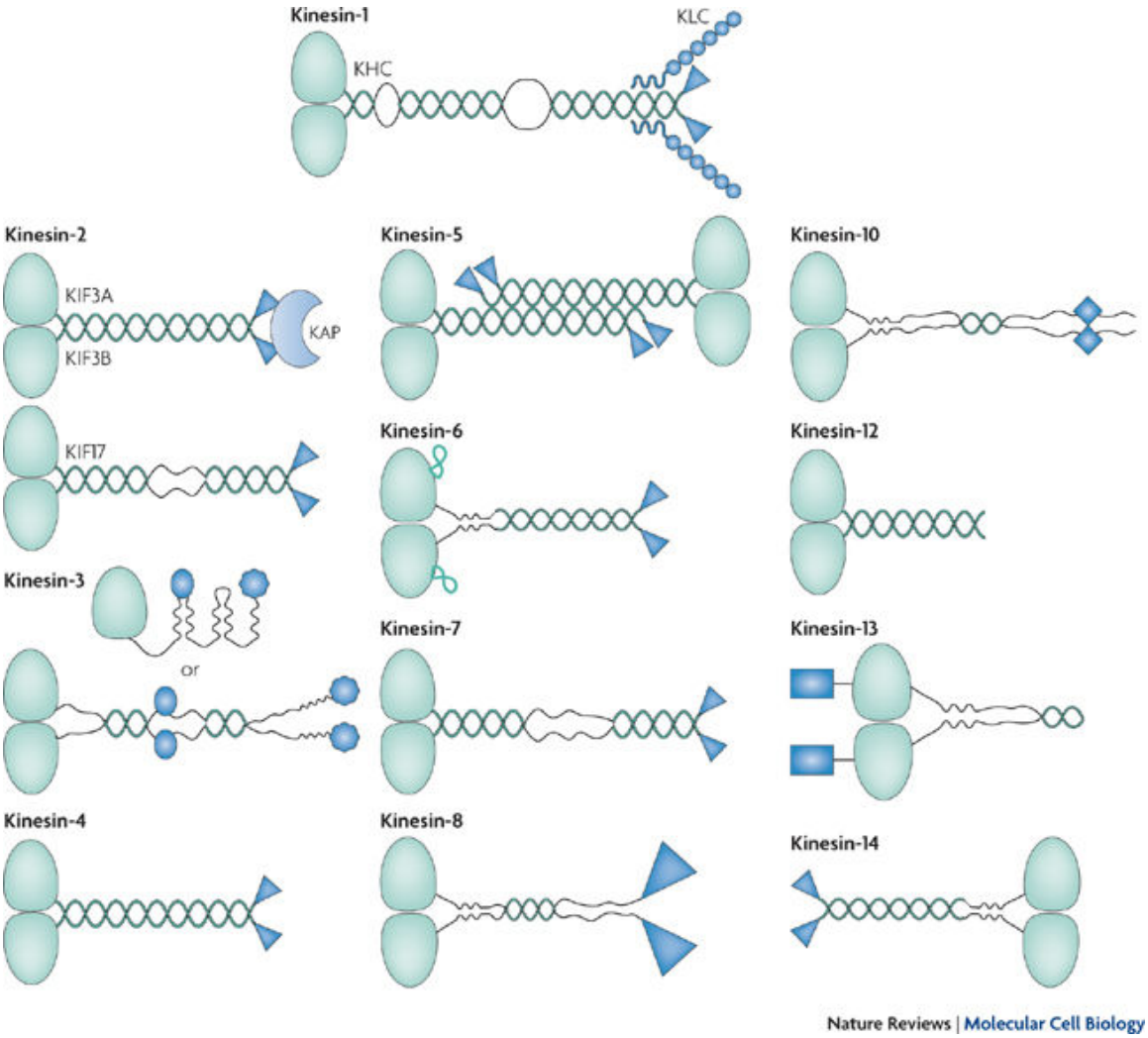

Figure 1.5: **The kinesin superfamily.**
Reprinted from Verhey and Hammond, 2009, with permission.

This dissertation includes studies of the kinesin-1, -2, and -3 families, introduced in the following sections. Figure 1.6 shows their subunit organization.

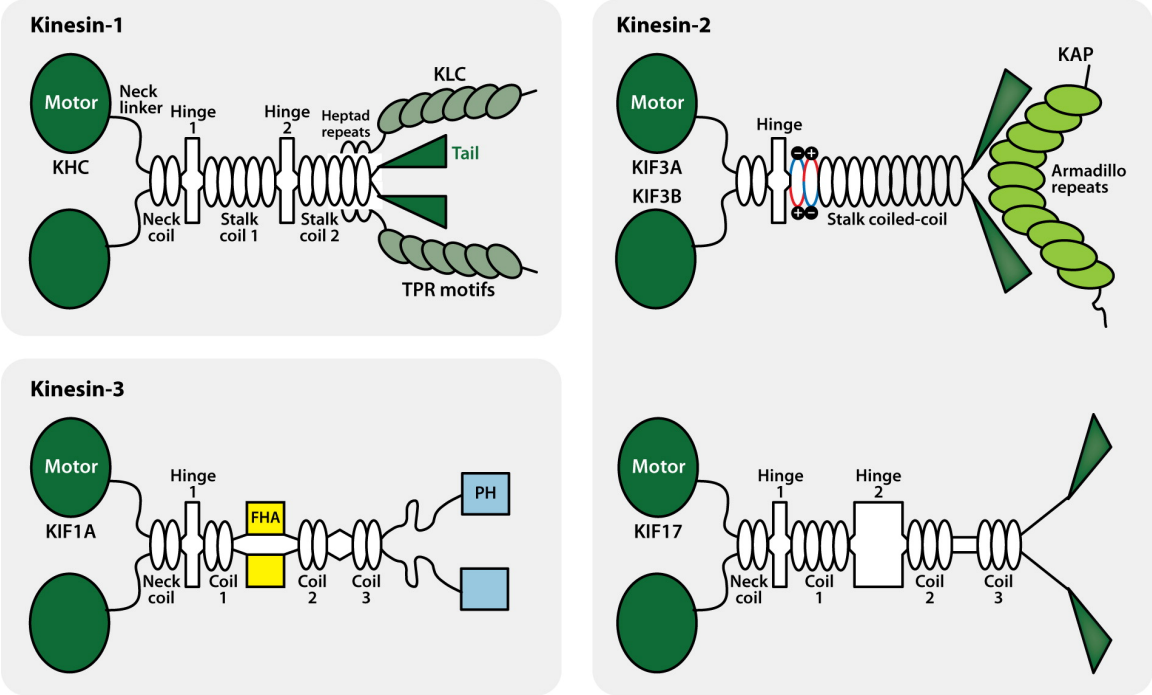

Figure 1.6: **Subunit composition of kinesin motors.** Schematic of the subunit composition and organization of kinesin-1, kinesin-2, and kinesin-3 motors. All these kinesins contain a kinesin motor domain (dark green oval) at their N terminus for ATP-dependent processive motion toward the plus ends of microtubules. These kinesins also have a neck domain (neck linker and neck coil) and varying amounts of coiled-coil stalk regions for oligomerization. Several of these kinesins have protein-protein or protein-lipid interaction domains such as TPR, Armadillo, FHA, and PH domains. Note that the kinesin-3 motor KIF1A is depicted as a dimeric molecule as this appears to be the state of the processive motor, although it is still unclear whether KIF1A motors are monomeric or dimeric in solution. Abbreviations: FHA, forkhead associated; KAP, kinesin-associated protein; KHC, kinesin heavy chain; KIF, kinesin family; KLC, kinesin light chain; PH, pleckstrin homology; TPR, tetratricopeptide repeat.
Reprinted from Verhey et al., 2011, with permission.

1.4.1 Kinesin-1 family

Kinesin-1, or conventional kinesin, is the founding member of the kinesin superfamily and the canonical transport kinesin. Much of what we know about kinesins comes from this family, which was first discovered in giant squid axoplasm (Vale et al., 1985). Kinesin-1 is highly expressed in the nervous system and is critical for vesicle and organelle transport.

Kinesin-1 is a heterotetramer composed of two kinesin heavy chains (KHC) and two kinesin light chains (KLC) (Figure 1.6). KHC consists of an N-terminal motor domain for ATP hydrolysis and microtubule binding, a neck domain (neck linker for processivity plus neck coil for homodimerization), a coiled-coil stalk with hinges for flexibility, and a tail domain for regulation of motor activity and cargo binding. Three genes encode for KHC subunit proteins in mammals: *KIF5A, KIF5B, and KIF5C*. Four genes encode for the KLC subunit, *KLC1-4*, which contains six tetratricopeptide repeat motifs for cargo binding. The KHC subunits homodimerize and can additionally assemble with any of the four KLC homodimers, allowing for distinct combinations with specific roles in cells (DeBoer et al., 2008). Physical dimensions are shown in Figure 1.7.

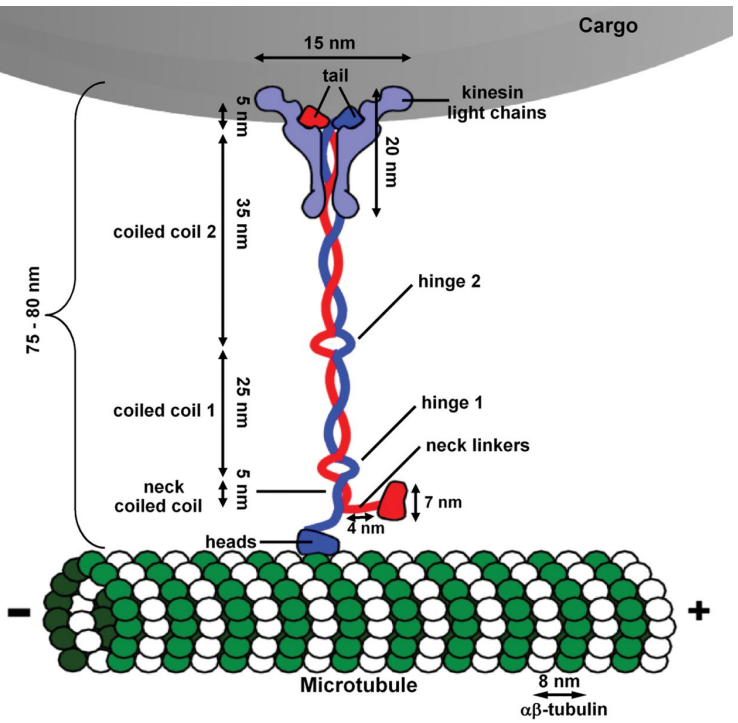

Figure 1.7: **A schematic diagram of the kinesin-1 structure bound to a microtubule with associated light chains.**
Dimensions are approximate and the diagram is based on information in the literature. Reprinted from Jeppesen and Hoerber, 2012, with permission.

A seminal study found that a single kinesins can move a microtubule several

microns (Howard et al., 1989). Later, Svodoba et al. optically trapped single beads attached to single kinesin-1 molecules and showed that kinesin-1 takes 8-nm center-of-mass steps along the microtubule and can transport against loads of ∼5 pN (Svodoba et al., 1993). Kinesin-1 is a microtubule protofilament tracer and walks parallel to the microtubule long axis (Ray et al., 1993). Indeed, tubulin dimers also have an 8 nm periodicity in a microtubule protofilament. A later study used interferometry to track beads coupled to single kinesin molecules with high spatial and temporal resolution. By examining the dwell time between steps at limiting ATP and the motor speed as a function of ATP, the authors showed that kinesin hydrolyzes one molecule of ATP per 8 nm center-of-mass step (Schnitzer and Block, 1997).

However, whether the two motor heads moved in an inchworm-like manner, with one head always in front of the other, or alternated positions in a hand-over-hand manner, remained unclear and was a controversial topic in the field for years. Elegant high-resolution tracking of kinesin motor heads revealed that kinesin walks hand-over-hand (Yildiz et al., 2004). The coordination of the two motor domains is maintained by alternating ATPase cycles, ensuring that one head remains bound to the microtubule as the other head takes a step forward (Hackney, 1994; Rosenfeld et al., 2003). Thus, kinesin-1 motors are processive as single motors and maintain their interaction with the microtubule track for hundreds of catalytic cycles.

Specific roles for individual members of the kinesin-1 family have also been identified. KIF5A is neuron-specific and has similar expression level in various types of neurons, but lower expression than KIF5C (Kanai et al., 2000). A study of *Kif5a*-knockout mice revealed reduced $GABA_A$ receptor-mediated synaptic transmission (Nakajima et al., 2012). Impaired inhibitory neural transmission resulted in mice with epileptic phenotypes (Nakajima et al., 2012; Xia et al., 2003).

KIF5B is ubiquitously expressed. *Kif5b*-knockout mice are embryonic lethal, and analysis of abnormal organelle distribution in extraembryonic cells revealed that

KIF5B is essential for proper mitochondrial and lysosomal localization (Tanaka et al., 1998). In the nervous system, KIF5B is expressed in glial cells and strongly upregulated in axon-elongating neurons, such as olfactory primary neurons and mossy fibers (Kanai et al., 2000).

KIF5C is also neuron-specific, and its strong enrichment in lower motor neurons in mice 2 weeks or older suggests that it is important for motor neuron maintenance rather than axonal formation (Kanai et al., 2000). Surprisingly, *Kif5c*-knockout mice were viable with intact nervous systems. They did, however, have smaller brain size and relative loss of motor neurons to sensory neurons (Kanai et al., 2000). KIF5A and KIF5B expression level remained unchanged in these mutants. Their viability suggests that other proteins might compensate for the lack of KIF5C.

Thus, the same study investigated functional redundancy between the three kinesin-1 motors (Kanai et al., 2000). KIF5A, KIF5B, and KIF5C are highly similar, with 60% sequence identity (80% identical in the motor domain and 90% identical in the C-terminal coiled-coil region) (Kanai et al., 2000). A rescue study used cultured *Kif5b*-knockout cells with abnormal perinuclear aggregation of mitochondria from mice that were embryonic lethal (Kanai et al., 2000). However, transfection of KIF5A, KIF5B, and KIF5C resulted in dispersion of mitochondria, recovering the phenotype of wild-type control cells. This provided strong evidence for functional redundancy among the three kinesin-1 motors, at least in organelle localization.

Numerous cargo and adapter protein binding partners have been identified, with disease-related proteins being subjects of particular focus. Because kinesin-1 motors are so abundant in the nervous system, they are involved in many neurological disorders. Huntingtin-associated protein-1 interacts with KLC (McGuire et al., 2006); early-onset dystonia protein TorsinA binds to KLC (Kamm et al., 2004); and KIF5B stably associates with two proteins, neurofibromin and merlin, involved in Neurofibromatosis (Hakimi et al., 2002). Kinesin-1 motors have also been identified

on vesicles containing mammalian prion protein, which can convert to a pathogenic form involved in Creutzfeldt-Jakob disease (Encalada et al., 2011).

Beyond the role of simply transporting pathological cargoes, kinesin mutations themselves have been implicated in human neurodegenerative diseases. For example, mutations in KIF5A, mostly in the motor domain, have been identified in patients with hereditary spastic paraplegia (Reid et al., 2002; Blair et al., 2006; Crimella et al., 2012) and in axonal Charcot-Marie-Tooth type 2 (Crimella et al., 2012).

1.4.2 Kinesin-2 family

First discovered in sea urchin eggs (Cole et al., 1992, 1993), the kinesin-2 family contains two subfamilies, both of which are involved in multiple types of intracellular transport. Kinesin-2 family motors walk along axonemal microtubules and carry out intraflagellar transport (IFT) to build and maintain cilia and flagella (Scholey, 2008). They also walk along cytoplasmic microtubules to transport organelles, melanosomes, and membrane-bound vesicles (Yamazaki et al., 1995; Tuma et al., 1998; Scholey, 2013).

There are four kinesin-2 genes in mammals: *Kif3A, Kif3B, Kif3C,* and *Kif17*. The two kinesin-2 subfamilies have distinct structures (Figure 1.6). Motors in one subfamily are heterotrimeric, composed of two different motor polypeptides plus a globular, non-motor accessory protein, kinesin-associated polypeptide (KAP). KIF3A associates with KIF3B or KIF3C, but KIF3B and KIF3C do not associate (Cole, 1999). Interestingly, this heterodimeric oligomerization is unique within the kinesin superfamily. KIF3AB further associates with KAP to form a heterotrimeric complex, but KIF3AC does not. The other subfamily, KIF17 in mammals, is composed of two identical motor polypeptides (Verhey et al., 2011).

Although optical trapping studies measuring 8 nm steps under a variety of forces and ATP concentrations suggest that KIF3AB motors also take 8 nm hand-

over-hand steps along the microtubule lattice (Andreasson et al., 2015), KIF3AB motors have distinct catalytic properties from kinesin-1 motors (Albracht et al., 2014). KIF3AB motors also exhibit distinct behavior against opposing force; rather than stalling like kinesin-1, they rapidly unbind and rebind to the microtubule (Andreasson et al., 2015). In contrast to KIF3AB, homodimeric KIF17 is fast, highly processive (Hammond et al., 2010), and continues stepping against 6 pN hindering load (Milic et al., 2017). These behaviors have implications for how well these motors cooperate in teams and will be discussed in more detail later.

Kinesin-2 motors are ubiquitous and have many critical functions. *In vitro* experiments with purified vesicles containing *N*-methyl-D-aspartate (NMDA) receptors suggested that KIF17 transports these vesicles in dendrites (Setou et al., 2000). The significance of this role was revealed later, when interestingly, overexpression of KIF17 in transgenic mice led to improved spatial learning and working memory in behavioral tasks (Wong et al., 2002). KIF3AB disperses pigment in *Xenopus laevis* melanophores (Tuma et al., 1998), transports N-cadherin and organizes the developing neuroepithelium (Teng et al., 2005), and is involved in COPI-dependent retrograde transport from the Golgi to the endoplasmic reticulum (Stauber et al., 2006). Furthermore, *Kif3A*-knockout mice are embryonic lethal, show ciliary morphogenesis defects, and suggest the motor's involvement in mesodermal patterning and neurogenesis (Takeda et al., 1999; Marszalek et al., 1999). Disruption of IFT leads to developmental defects and ciliopathies such as polycystic kidney disease (Lin et al., 2003).

Why KIF3AB and KIF3AC are heterodimers has puzzled the field for years. Other kinesins carry out their functions effectively as homodimers, so what drove kinesin-2 motors to evolve with two different motor domains? Several studies have revealed differences in the kinetic and motile properties of the two subunits (Zhang and Hancock, 2004; Zhang et al., 2016; Gilbert et al., 2018), but their significance *in vivo* remains unclear.

One important aspect to note is the diversity in heteromeric kinesin-2 motility among species. Brunnbauer et al. investigated the trajectories of full-length, heterodimeric kinesin-2 motors from several species on freely suspended microtubules using a laser trap assay (Brunnbauer et al., 2012). They found that mouse *Mm*KIF3AB was the only kinesin-2 motor they tested that tracked protofilaments like kinesin-1 (Ray et al., 1993), walking parallel to the microtubule long axis. In contrast, *Sp*KRP85/95, *Xl*KLP3a/3b, and *Ce*KLP11/20 (which contains one processive and one non-processive subunit) exhibited left-handed spiraling around the microtubule with a range of pitches (Brunnbauer et al., 2012). Through a series of chimeric constructs, the authors demonstrated that torque generation is not linked to processivity, as previous studies suggested; instead, it is dictated by the stability of the neck domain. Adding flexible peptides after the neck linker to destabilize the neck allowed motors to side-step and spiral around microtubules; conversely, crosslinking to stabilize the neck reduced spiraling (Brunnbauer et al., 2012). The functional implications of these results *in vivo* will be the topic of future investigations. Beyond their scientific interest, these findings underscore the danger of assuming that the properties of motors from one species can be generalized to others.

1.4.3 Kinesin-3 family

The kinesin-3 family has five subfamilies: KIF1, KIF13, KIF14, KIF16, and KIF28. Kinesin-3 motors transport presynaptic vesicles and other membrane-bound organelles in neurons. They were first identified in *C. elegans* because mutations in the *unc-104* gene caused defects in synaptic vesicle transport in axons, resulting in slow and uncoordinated movement (Otsuka et al., 1991).

Compared with other kinesin families, the most notable features of kinesin-3 motors are their high processivity, allowing them to travel the long length of the axon, and their controversial oligomeric state. There has been differing evidence on

the oligomeric state of KIF1A in solution and as a functional motor. Several studies provided evidence that truncated KIF1A motors are processive as monomers, undergoing biased Brownian diffusion (Okada and Hirokawa, 1999; Okada et al., 2003). Optical trapping experiments with single KIF1A motors showed that one ATP hydrolysis event leads to one step, with step sizes distributed around multiples of 8 nm (Okada et al., 2003). Kinesin-1 requires two motor heads to be processive, so this raised the question of how a single motor domain could maintain microtubule interaction for multiple steps. The mechanism was thought to be a nucleotide-dependent interaction between a positively charged region in loop 12 of the motor domain known as the K-loop with the negatively charged E-hook at the C-terminal region of tubulin (Okada and Hirokawa, 2000).

However, the speed of KIF1A monomers was ∼8-fold lower than that observed for full-length motors. Another model emerged in which cargo-dependent dimerization was proposed to occur when Unc104/KIF1A clusters within lipid rafts, and single motors only reached maximal speeds as a dimer, suggesting that this is their functional form (Klopfenstein et al., 2002; Tomishige et al., 2002). Later studies showed that expressed and endogenous mammalian KIF1A motors are dimeric *in vivo* using crosslinking analysis, Förster resonance transfer (FRET), and sucrose gradient sedimentation. This work also suggested that KIF1A motors are also regulated by autoinhibition and are activated by cargo binding (Hammond et al., 2009). Thus, it remained controversial how KIF1A motors assemble and are regulated.

Although the kinesin-3 family is one of the largest in the superfamily, the molecular mechanisms underlying its cargo transport remained unknown until recently. A series of papers from the Verhey lab elucidated several critical findings. They showed that full-length kinesin-3 motors KIF1A, KIF13A, KIF13B, and KIF16B are monomeric and inactive when not bound to cargo. Upon cargo binding, they undergo a monomer-to-dimer transition and become highly processive, with run lengths

$\sim$10 um (Soppina et al., 2014). They also investigated the role of the conserved, positively charged K-loop in loop 12 of the kinesin-3 motor domain. They found that the K-loop promotes the motor's initial interaction with the microtubule and facilitates its diffusive motion, likely due to electrostatics. However, surprisingly, they found that the K-loop does not affect the superprocessive motion of kinesin-3 motors (Soppina and Verhey, 2014). Therefore, the structural features that cause kinesin-3's superprocessive motility remain unknown.

Specific roles have been identified for several kinesin-3 family members. KIF16B is involved in trafficking of early endosomes (Hoepfner et al., 2005). KIF13A associates with recycling endosomes and initiates their tubulation (Delevoye et al., 2014). Motors are also involved in more nefarious processes. Various viruses hijack kinesin motors during their replication cycles. For example, KIF13A transports influenza A virus ribonucleoproteins (Ramos-Nascimento et al., 2017). Defects in kinesin-3 transport are thought to cause various neurodegenerative and developmental defects (Li and DiFiglia, 2012). A mutation in the motor domain of KIF1B was associated with Charcot-Marie-Tooth type 2A disease (Zhao et al., 2001).

Overall, although it is now clear that motors within each of the kinesin-1, -2, and -3 families have distinct roles in cells, there remain many gaps in knowledge of single-molecule motility properties because of the assumption that motors in the same family should have similar properties. For example, members of the kinesin-1 family clearly have different tissue expression and functions, yet many researchers treat the family members interchangeably. This is equally true for motors of the same type from different species. A major challenge in the field will be to investigate motors within families and across species that have previously been assumed to be biophysically similar and attempt to understand what drove the evolution of such diverse motors that still contain high sequence and structural similarity.

Despite the large body of research on transport kinesins, much remains un-

known about their function in cells. Topics such as regulation, binding partners, cargo specificity, and multi-motor behavior will remain active topics of research for years to come.

1.5 Motors working in teams

Numerous studies have demonstrated that multiple motor proteins are present on an individual cargo undergoing intracellular transport. Early hints in this direction came from electron microscopy studies showing multiple cross-bridges connecting membrane-bound cargoes to the microtubule track (Miller and Lasek, 1985; Ashkin et al., 1990), as shown in Figure 1.8. Since then, analysis of purified mouse neuronal transport vesicles (Hendricks et al., 2010) and measurements of endosomes (Soppina et al., 2009) and peroxisomes (Kural et al., 2005; Ally et al., 2009) inside live cells have identified motor identity and number in greater detail. These can be multiple motors of different classes (e.g. a kinesin and a dynein) or multiple motors of the same class (e.g. kinesin-1 and kinesin-3 motors) on the same cargo. Thus, there has been a great deal of interest in understanding how multiple motors work together and coordinate their motility.

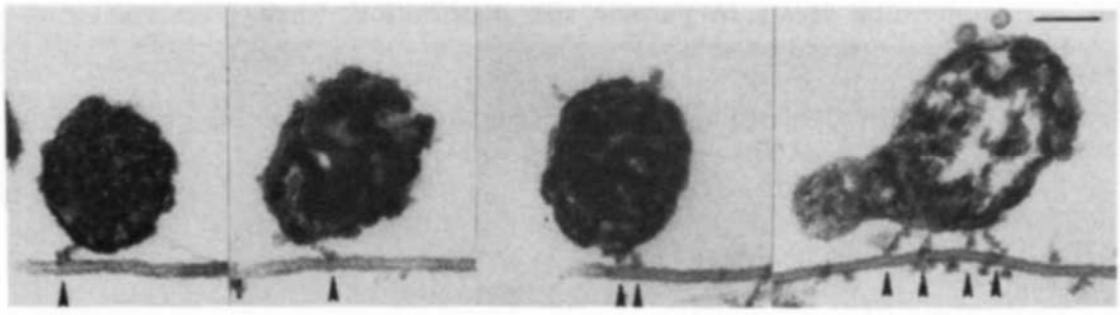

Figure 1.8: **Examples of mitochondria from *Reticulomyxa* with 1, 2, and 4 crossbridges to a microtubule, as seen by electron microscopy.** Bar, 0.1 um. Reprinted from Ashkin et al., 1990, with permission.

An interesting question is how these motors coordinate their activities to avoid

interfering with each other. For cargoes with a kinesin and a dynein, several systems have observed that the presence of kinesin and dynein motors results in a tug-of-war (Soppina et al., 2009; Hendricks et al., 2010). In other systems, the motors appear to be regulated so that only one type of motor is active at a time (Kural et al., 2005; Laib et al., 2009). However, the specific regulatory mechanisms that determine which motors dominate at which times and locations for different cargoes is largely unknown and remain a formidable experimental challenge for the future.

Dimeric kinesin motor proteins are capable of high speeds, long run lengths, and high force generation as individual motors. What then is the advantage of having multiple motors on a cargo? One advantage is that if a motor disengages from the track, other motors present on the cargo can engage and continue the journey. An added advantage would be the ability to dodge a microtubule-associated protein that is blocking the path and avoid a traffic jam (Lakadamyali, 2014). Cytoplasmic crowding and roadblocks on microtubules make this especially important for sustained track interaction. A third advantage may be the ability of multiple motors to generate higher forces than a single motor is capable of. At least *in vitro*, stall forces for kinesin-1 are additive (Vershinin et al., 2007). One major goal in the field is to understand the dynamics of individual motors in a team and reveal how they are related to isolated motor properties. Many theoretical studies have explored this, but experimental limitations have stalled progress. Thus, new tools are required that offer spatial and temporal control over components.

In Chapter 2, I describe the development of a protein-based system to assemble motors in defined numbers in order to observe their coordination both in *in vitro* assays and in specific locations in cells. This modular technique will allow future exploration of a variety of questions on multi-motor transport in cells.

1.5.1 Monomeric motors working in teams

Although most, if not all, kinesins function as dimers, it is theoretically possible that monomeric kinesins can work in teams to drive cargo transport. Leibler and Huse provided a theoretical framework for how monomeric motors could work in teams to drive cargo transport (Leibler and Huse, 1993). This work classified motor proteins as either "porters" or "rowers." Porters work effectively as individual motors because they spend a large fraction of their catalytic cycle engaged with the track (high duty ratio), allowing them to take many successive steps without detaching (Leibler and Huse, 1993; Hackney, 1996). On the other hand, rowers are ineffective as individuals because they spend most of their ATPase cycle off the track (low duty ratio); however, when they are combined in large ensembles, the reduced interference and friction from other members of the ensemble allow them to collectively produce large forces. This framework has never been tested in cells for monomeric kinesins.

To better understand the functional significance of kinesin's well-conserved dimeric structure, several groups have studied the *in vitro* motility of single-headed kinesin-1 motors, both truncated (Berliner et al., 1995; Young et al., 1998; Kamei et al., 2005; Inoue et al., 1997) and full-length (Hancock and Howard, 1998). Most have shown that single kinesin monomers are non-processive, but groups of monomers can glide a microtubule (Hancock and Howard, 1998) or transport a bead (Kamei et al., 2005), albeit at lower speeds and forces than their dimeric forms (Berliner et al., 1995; Kamei et al., 2005; Inoue et al., 1997).

Other studies have shown that KIF1A (kinesin-3 family) monomers can move processively on microtubules (Okada and Hirokawa, 1999; Okada et al., 2003) via biased Brownian diffusion but do not recover their *in vivo* speed until they dimerize on cargo (Tomishige et al., 2002). These observations suggest that kinesin monomers may be able to function as rowers, despite their canonical behavior as dimeric porters.

There is ample evidence that members of both the myosin and dynein families

are monomeric and work in teams to produce motion. The best-studied examples are muscle myosin and flagellar dynein, which work in large ensembles and spend most of their time detached from the track. Myosin VI monomers are nonprocessive in single-molecule assays but can work in teams to transport cargoes with similar speeds as dimers (Sivaramakrishnan and Spudich, 2009). Individual monomers interact only transiently with the track but collectively can generate force and large movements.

Whether monomeric versions of kinesin motors are capable of working in teams to drive transport or whether there is something about the catalytic or mechanical properties of kinesins that prevents them from functioning in this manner is not known. Also unknown is whether monomers are able to collectively transport cargoes when attached to a lipid bilayer and moving through the crowded cellular environment. In Chapter 3, I describe experiments aimed at resolving whether dimerization is required for kinesins to carry out intracellular transport.

1.5.2 Overview of dissertation

Overall, this dissertation focuses on the collective behavior of groups of kinesin motors transporting membrane-bound cargoes along microtubules in mammalian cells.

In Chapter 2, I describe the development of a protein-based system for assembly of defined multi-protein assemblies on a scaffold. This system can be used to probe multi-motor behavior both *in vitro* and in cells.

In Chapter 3, I describe the investigation of the minimal structural requirements for kinesins to carry out transport in cells. I show results from experiments both *in vitro* and in cells that address the question of whether nonprocessive kinesins can act as rowers to collectively carry out cargo transport.

CHAPTER II

Assembly of protein complexes at defined subcellular locations

Portions of this chapter have been adapted from:
Norris, S.R., V. Soppina, A.S. Dizaji, **K.I. Schimert**, D. Sept, D. Cai, S. Sivaramakrishnan, and K.J. Verhey. 2014. A method for multiprotein assembly in cells reveals independent action of kinesins in complex. J. Cell Biol. 207:393-406. doi:10.1083/jcb.201407086.

Author contributions: S.R.N., V.S., D.C., and K.J.V. designed research. S.R.N., V.S., A.S.D., and **K.S.** performed research. A.S.D., D.S., and S.S. contributed new reagents or analytic tools. S.R.N. and A.S.D. analyzed data. S.R.N. and K.J.V. wrote the p aper with input from all authors.

K.S. wrote the text in this chapter.

2.1 Introduction

Thanks to remarkable technological advances, the biophysical and biochemical properties of cytoskeletal motor proteins have been studied in great detail at the single-molecule level. However, in cells, there are multiple motors on a single cargo, rendering it critical to study motor coordination in teams.

Several studies have used DNA origami as scaffolds to group motors together and investigate their motility. DNA scaffolds allow for control over motor number and spacing, and several groups have successfully used them to study multi-motor behavior (Rogers et al., 2009; Derr et al., 2012; Furuta et al., 2013). However, cooperation among kinesin motors remains poorly understood. Furthermore, DNA scaffolds cannot be used in cells, which is a major limitation and prevents the correlation of *in vitro* and *in vivo* behavior.

DNA scaffolds also do not recapitulate physiological motor-cargo linkages. Motors are recruited to their intracellular cargoes via various mechanisms (Akhmanova and Hammer, 2010). Some motors bind directly to transmembrane cargo proteins on transport vesicles or organelles. For example, kinesin-1 light chain is thought to bind directly to amyloid precursor protein, a major player in the development of Alzheimer's disease, on axonal vesicles (Kamal et al., 2000). Other motors dock onto cargoes via lipid binding domains. For example, kinesin-3 motor Unc-104 contains a pleckstrin homology domain that can bind to phosphatidylinositol(4,5)bisphosphate (PIP2) on synaptic vesicles (Klopfenstein et al., 2002), and kinesin-3 motor KIF16B contains a PX domain that can bind to phosphatidylinositol-3-phosphate (PI(3)P) on early endosomes (Hoepfner et al., 2005). However, as more cargo assemblies are identified, these direct binding modes appear to be the exception rather than the rule.

Many motors bind to their cargoes via multi-protein complexes (for reviews, see Akhmanova and Hammer (2010); meng Fu and Holzbaur (2014)). Association with scaffold or adaptor proteins can significantly affect motor properties. Belyy et al. showed that when mammalian dynein associates with dynactin and Bicaudal-D2, its force production increases from 0.5-1.5 pN to 4.3 pN (Belyy et al., 2016). This work illustrated that it is critical to study motor properties in their native context, with the binding partners that link them to their cargo.

This motivated the development of a multi-protein scaffold system to group

multiple motors with defined separation distance that can be used to study motility *in vitro* and in cells.

2.2 Results

We set out to assemble defined, multi-protein complexes in mammalian cells. The goal was to use self-associating protein linkers to attach motors to a protein scaffold. For the scaffold backbone, we opted to use single alpha helix (SAH) domains that are recurrent in nature (Knight et al., 2005) (Figure 2.1 A). These are also called ER/K helices because they are stabilized by ionic interactions between the side chains of alternating glutamate (E) and arginine (R) or lysine (K) residues (Knight et al., 2005). A BLAST search on PubMed from a previous study revealed that this ER/K motif is present in at least 123 distinct proteins in 137 organisms (Sivaramakrishnan et al., 2008). SAHs are stable in solution and act as a bridge between protein subdomains in myosin VI and myosin X, making them an ideal scaffold for our system. We selected helices of 5, 10, 20, and 30 nm.

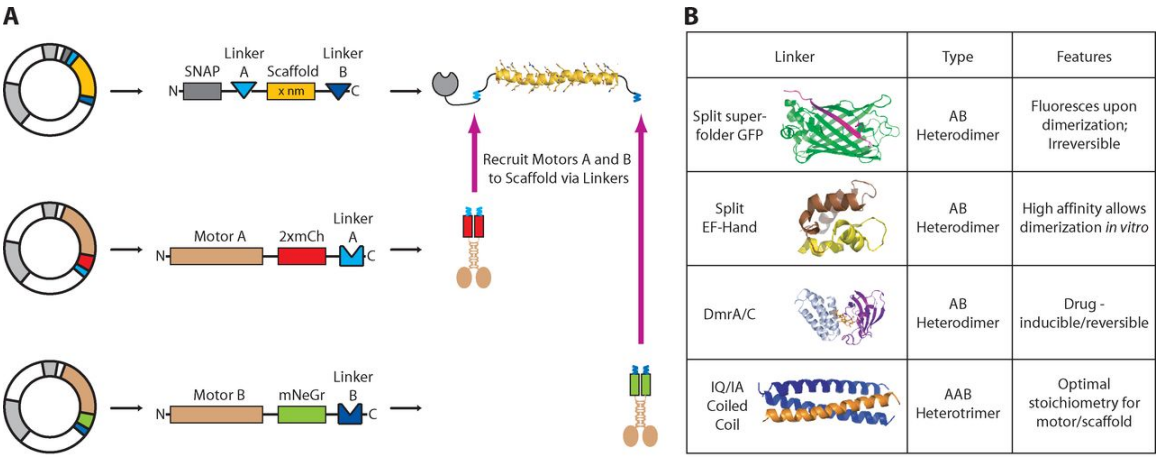

Figure 2.1: **A protein-based system for assembly of defined multi-protein complexes.**
(A) Plasmids for expression of scaffold (top) and motor components (middle and bottom) are cotransfected into mammalian cells, and the protein components are allowed to self-assemble. The scaffold (yellow) is a SAH with linkers (blue) attached at each end. (B) Summary of the four linker components and their features. Reprinted from Norris et al., 2014, with permission.

Next, we cloned and screened linker proteins to attach to the scaffold, basing our selection on several criteria: 1) They had to self-associate. 2) They had to have well-characterized structural and assembly properties. We selected alpha-helical protein segments known to form coiled-coils of a certain orientation and oligomeric state. In order to assemble dimeric kinesin motors on a monomeric scaffold, we predicted that a trimeric coiled-coil would be optimal. Using single-molecule motility assays and coimmunoprecipitation (summarized in Figure 2.2 A), we tested the following coiled-coil structures for their ability to connect motors to the scaffold: a homotrimeric variant of the leucine zipper from *Saccharomyces cerevisiae* GCN4 (Holton and Alber, 2004); the homotrimeric coiled-coil domain of mammalian coronin 1 (Kammerer et al., 2005); and de-novo designed coiled-coils of homotrimeric (Burkhard et al., 2002), homodimeric (Litowski and Hodges, 2002), or heterotrimeric (IA/IQ) (Kiyokawa et al., 2004) form. The heterotrimeric IA/IQ coiled-coil was the best for our geometry. The others exhibited no or very limited motility in the screen

or had other complications.

A

Schematic	Linker	Type	Notes	Reference
	IQ/IA	Antiparallel heterotrimeric coiled-coil (AAB-type)	Worked well in motility and Co-IP screen (Fig. 2, S1)	Kiyokawa et al., 2004
	GCN4 Trimer	Antiparallel homotrimeric coiled-coil; mutant version (N16A) of leucine zipper of yeast transcriptional activator GCN4 (AAA-type)	Very limited motility in screen	Holton and Alber, 2004
	ccCor1	Homotrimeric coiled-coil domain of mammalian actin-associated protein coronin 1 (parallel, AAA-type)	Worked well in screen; Abandoned due to complications from homotrimeric form and interactions with actin	Kammerer et al., 2005
	p4	Antiparallel coiled-coil designed de novo; forms homotrimer (AAA-type)	No motility in screen	Burkhard et al., 2002
	EK Coil	Heterodimeric coiled-coil designed de novo (AB-type)	Very limited motility in screen	Litowski and Hodges, 2002

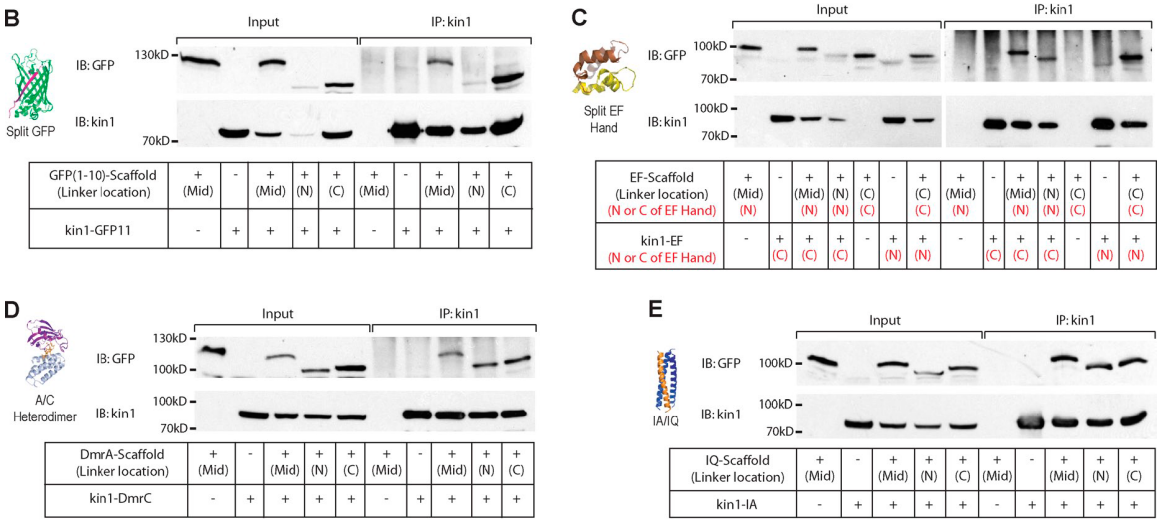

Figure 2.2: **Characterization of self-assembling linkers.**
(A) Several potential coiled-coil linkers were screened via single molecule motility assays to determine their suitability for assembling kin1 motors and SAH scaffolds. The heterotrimeric IA/IQ sequences were most efficient at recruiting dimeric kin1 motors to monomeric SAH scaffolds. (B-E) Coimmunoprecipitation assays. Motor-linker and linker-scaffold-GFP components were coexpressed in COS7 cells and immunoprecipitated (IP) from cell lysates with a monoclonal antibody to kin1 (IP:kin1 lanes), and the presence of scaffold was detected by immunoblotting (IB) for the GFP tag (IB:GFP). Input = 1/4 of lysate compared with IP lanes. ± indicates the presence of the plasmid in transfection. The position of the linker with respect to the scaffold is indicated in black text as N terminus (N), middle (Mid), or C terminus (C). For the split GFP linker (B), the first 10 strands of the barrel (GFP(1-10)) were attached to the scaffold and the last strand (GFP11) was attached to kin1. For the split EF Hand linker (C), the red text indicates whether the N-terminal half (N) or C-terminal half (C) of the EF Hand domain was attached to the scaffold or motor components. The opposite configurations showed no assembly. These experiments were performed by Stephen R. Norris. Reprinted from Norris et al., 2014, with permission.

In addition to the alpha-helical protein segments, we also tested protein-protein linkers for their efficacy at connecting motors to scaffolds (Figure 2.1 B). They all offer specific benefits in assembling multi-protein complexes. We tested: 1) A split superfolder GFP that provides a green fluorescent signal upon assembly, which is almost irreversible (Pinaud and Dahan, 2011). 2) The split EF Hand domain from calbindin that assembles with high affinity ($K_d \sim 1$ nM) that can be increased ($K_d \sim 1$ pM) in the presence of calcium (Lindman et al., 2009). 3) The drug-inducible dimerization of DmrA (FKBP) and DmrC (FRB domain) upon addition of A/C Heterodimerizer (Rapalog-1, AP21967) that has been used in cells to induce dimerization of proteins (DeRose et al., 2013).

Linkers were tested at the N terminus, middle, and C terminus of a 30 nm SAH scaffold. Coimmunoprecipitation demonstrated protein expression, solubility, and interaction with the motor (Figure 2.2 B-E). We also tested the linkers and arrangements in single-molecule assays with a truncated, constitutively active version of kinesin-1, KIF5C(1-560), or kin1. For these data, see Figure 2 of Norris et al. (2014). The motor-linker-scaffold complexes had similar run length and velocity distributions to kin1 without a scaffold, suggesting that we can assemble and use scaffold-linker-motor complexes in *in vitro* motility assays by expressing constituent proteins in mammalian cells and collecting them in cell lysates. Therefore, we decided to move forward with the four protein-protein linkers and the de-novo designed IA/IQ peptides (two IA peptides attached to a dimeric kinesin assemble with one IQ peptide attached to a scaffold, forming an AAB-type heterotrimeric coiled-coil) (Kiyokawa et al., 2004).

Verifying multiple protein assembly in live cells

After characterizing the protein linkers *in vitro*, we next tested whether we could use them to recruit two proteins to the same scaffold in live cells. We did this

by utilizing Förster resonance transfer (FRET) and making use of SAH domains of known length for the scaffold (Knight et al., 2005; Sivaramakrishnan et al., 2008, 2009; Baboolal et al., 2009). We used the split superfolder GFP as the FRET donor and mCherry as the acceptor. The scaffold had half of the split superfolder GFP on one end and the DmrA domain on the other end (Figure 2.3 A). Therefore, for FRET to occur, the other half of the split GFP should bind to the scaffold and produce green signal, and addition of A/C homodimerizer should recruit the mCherry-tagged DmrC domain to the opposite end of the scaffold. In the absence of A/C heterodimerizer, mCherry remained cytosolic and low/now FRET was observed from the scaffold-associated GFP complex, as expected. Consistent with expectations, addition of A/C heterodimerizer induced recruitment of mCherry to the scaffold-GFP complex, causing a FRET signal that varied with scaffold length; high FRET occurred at a short separation distance (GSG peptide as the scaffold), and no FRET occurred for a 10-nm scaffold (Figure 2.3 B-C). These results demonstrate that our scaffolds and linkers can assemble into defined, multi-protein complexes in live cells.

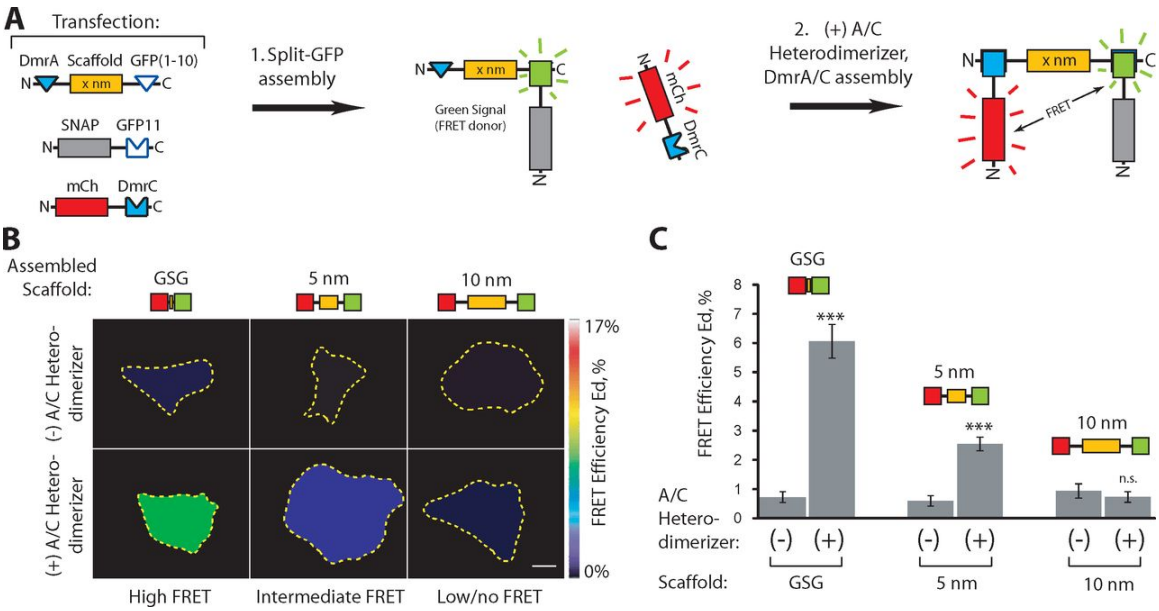

Figure 2.3: **Assembly of two proteins on a scaffold in live cells.**
(A) Schematic of multi-protein assembly. Plasmids encoding the indicated components were expressed in COS7 cells (Transfection). Self-assembly of the split GFP linker (step 1) recruits the SNAP-GFP11 component to the DmrA-scaffold-GFP(110), resulting in green fluorescence. Addition of A/C heterodimerizer (step 2) recruits the mCherry-DmrC component, resulting in FRET. (B and C) FRET donor (split GFP) and FRET acceptor (mCherry) components were recruited to scaffolds of 0 nm (GSG peptide), 5 nm SAH, or 10 nm SAH by the addition of A/C heterodimerizer for 1 h, and FRET was determined in live cells. (B) Representative calculated FRET efficiency (Ed) images. Yellow dotted lines indicate the outline of each cell. Bar, 10 μm. (C) Calculated FRET efficiencies (Ed). n $\geq$ 31 cells in three independent experiments for each condition. ***, P $<$ 0.0001; n.s., not significant as compared with the (-) A/C heterodimerizer condition. Data are presented as the average $\pm$ SEM (error bars). These experiments were performed by Stephen R. Norris (with constructs cloned by Kristin Schimert). Reprinted from Norris et al., 2014, with permission.

Assembling multi-protein complexes at specific subcellular locations

Future multi-motor studies could benefit from complexes being targeted to certain areas of the cell. Thus, we next tested whether we could assemble multi-protein complexes of our characterized scaffolds and linkers at specific subcellular locations. We targeted mCherry-DmrC to the plasma membrane by fusing it to a myristoylation-palmitoylation signal sequence (Figure 2.4 A). We also constructed a lysosome-targeted scaffold by fusing it to a lysosomal membrane protein, Lamp1

(Figure 2.5 A). In the absence of A/C heterodimerizer, DmrA-scaffold-split GFP complexes were cytosolic (Figures 2.4 B and 2.5 B, bottom panels). However, upon addition of A/C heterodimerizer, DmrA-scaffold-split GFP complexes were rapidly recruited to the plasma membrane, colocalizing with the mCherry-DmrC. This was a robust effect for both the plasma membrane-targeted (Figure 2.4 B) and the lysosome-targeted (Figure 2.5 B) mCherry-DmrC components. Thus, we have demonstrated that complexes comprised of multiple proteins can be assembled sequentially at defined locations in live cells.

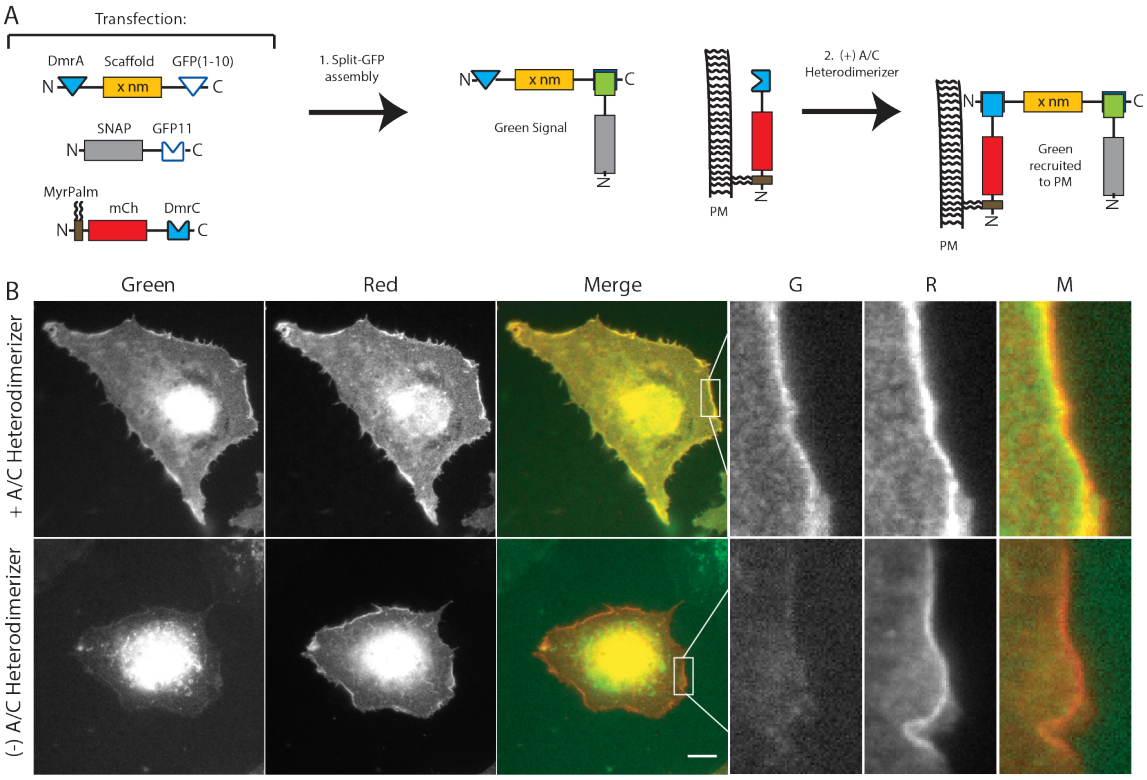

Figure 2.4: **Assembly of multi-protein complexes at the plasma membrane.** (A and B) Step-wise assembly of a multi-protein complex at the plasma membrane in live cells. (A) Schematic of the experimental setup. COS7 cells were transfected with plasmids for expression of the indicated components. The split GFP self-assembles (step 1) and is recruited to the MyrPalm-mCherry component on the plasma membrane by addition of A/C heterodimerizer (step 2). (B) Representative images of cells incubated in the absence or presence of A/C heterodimerizer for 1 h. The three panels on the far right display magnified views of the boxed region in the Merge channel. Bar, 10 μm. The three panels on the far right display magnified views of the boxed region in the Merge channel. Bar, 10 μm. Reprinted from Norris et al., 2014, with permission.

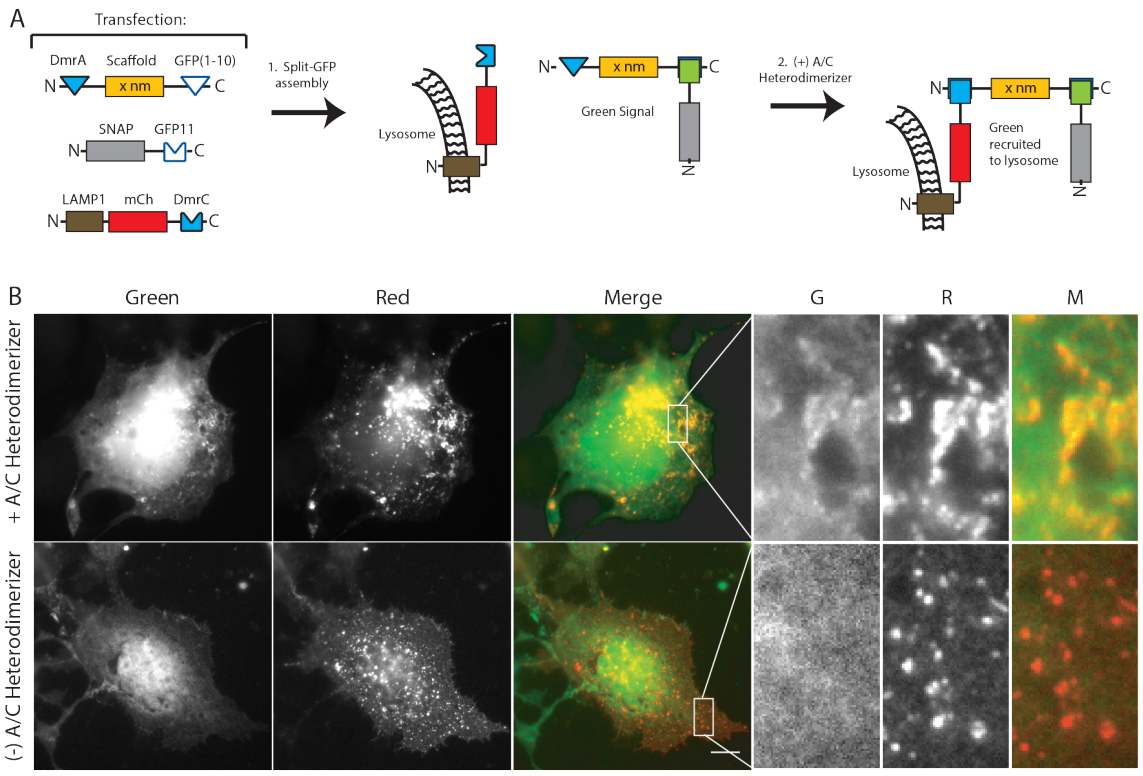

Figure 2.5: **Assembly of multi-protein complexes on the lysosome.** (A and B) Step-wise assembly of a multi-protein complex on the lysosome in live cells. (A) Schematic of experimental setup. COS7 cells were transfected with plasmids for expression of the indicated components. The split GFP self-assembles (step 1) and is recruited to the LAMP1-mCherry component on the lysosome by addition of A/C heterodimerizer (step 2). (B) Images of cells incubated in the absence or presence of A/C heterodimerizer for 1 h. The three panels on the far right display magnified views of the boxed region in the Merge channel. Bar, 10 μm. Reprinted from Norris et al., 2014, with permission.

2.3 Discussion

Many questions in cell biology would benefit from having a well-characterized system to assemble multiple proteins into defined complexes at relevant locations in the cell. To this end, we describe a new method that is broadly applicable to questions in signaling, motility, and organization. This system can be easily generalized and used with other organelle localization signals to facilitate location-specific experiments in live cells.

We opted to utilize FRB-rapalog-FKBP dimerization in order to induce rapid recruitment of components, allowing for studies in live cells. The use of this system demonstrates the feasibility of inducible, sequential complex assembly. A related idea is used to assemble kinesin motors on artificial cargoes in Chapter 3. In the future, it would be possible to use one set of protein linkers to assemble a complex with multiple kinesin-1 motors and then induce the recruitment of another type of motor, observing how the dynamics of that specific complex change with addition of more motors.

This work demonstrates the assembly of multiple protein components into a defined geometry at a specific location in live cells. It was used by Stephen Norris in the Verhey lab to study coordination of kinesin motors coupled on a protein scaffold in COS-7 cells (Norris et al., 2014). He applied this method to directly compare the cooperative behavior of two-kinesin complexes *in vitro* to that in live cells. Taken together, his results suggest that kinesins on a shared cargo act independently and can alternate their activity, but they do not cooperate. This suggests that the presence of multiple motors on a cellular cargo has functional importance beyond what can be deduced by motility properties; for example, having multiple motors probably enables the cargo to navigate around obstacles on the microtubule (Ross et al., 2008).

The tools developed here open up many questions for future investigation. For example, one interesting question is how the emergent behavior of assemblies of different motors is regulated in different areas of the cell. Further work is also required to elucidate how the compliance of the cargo effects motor cooperation. This is possible using this method with protein scaffolds of different stiffness.

2.4 Materials and methods

Adapted from Norris et al. (2014).

Plasmids

Constitutively active versions of the kinesin-1 motor rat KIF5C (aa 1-560) and the kinesin-3 motor rat KIF1A (aa 1-393 with the leucine zipper dimerizing segment of GCN4) have been described previously (Cai et al., 2007,2009; Soppina et al., 2014). DNA fragments encoding SAH domains of various lengths were generated by PCR cloning of the relevant sequences: a 5-nm helix from *Homo sapiens* translation initiation factor IF-2; a 10-nm helix from *Sus scrofa* Myosin VI medial tail; a 20-nm helix from *S. cerevisiae* mannosyltransferase MNN4; and a 30-nm helix from *Trichomonas vaginalis* Kelch-motif family protein (Sivaramakrishnan et al., 2008, 2009). The 60-nm helix is a tandem repeat of 30-nm helices separated by four tandem Gly-Ser-Gly (GSG) sequences. Multiple GSG repeats were also included between all scaffold and linker components to ensure flexibility and rotational freedom of each component. IA/IQ fusions were generated by insertion of oligonucleotides encoding the peptides. Plasmids encoding FKBP and FRB were obtained from ARIAD Pharmaceuticals and are now available from Takara Bio Inc. as DmrA and DmrC, respectively. Plasmids encoding mNeonGreen were obtained from Allele Biotechnology. EF Hand and tandem mCherry sequences were synthesized (DNA 2.0). Plasmids encoding split superfolder GFP components were a gift from F. Pinaud (University of Southern California, Los Angeles, CA). Each component was subcloned behind the cytomegalovirus promoter in the EGFP-N1 vector (Takara Bio Inc.); this vector also contains an SV40 origin for replication in mammalian cells and a kanamycin resistance cassette for amplification in Escherichia coli. All plasmids were verified by DNA sequencing.

Cell culture, transfection, and immunofluorescence

COS cells were cultured, transfected, and lysed as described previously (Cai et al., 2007; Soppina et al., 2014). For immunoprecipitation, lysates were incubated

with antibodies for 3 h at 4°C, Protein A agarose beads were added for an additional 30 min at 4°C, and the immunoprecipitates were analyzed by blotting with a monoclonal antibody to bovine brain kinesin-1 (Mouse MAb1614; EMD Millipore) or a polyclonal antibody raised in rabbits against a GFP peptide (antigen sequence CFKEDGNILGHKLE). For immunoprecipitation experiments using DmrA/C linkers, 20 ng/ml rapamycin (EMD Millipore) was added 1 h before lysis and maintained throughout lysis and immunoprecipitation. For immunofluorescence, monoclonal antibodies to total β tubulin (Mouse E7; Developmental Studies Hybridoma Bank) and acetylated α-tubulin (Mouse 6-11B-1, #T7451; Sigma-Aldrich) were used.

Live-cell imaging

Fluorescence images of live COS7 cells were collected at 37°C in Leibovitzs L-15 medium without phenol red (Life Technologies) using an inverted microscope (IX70; Olympus) with a 40x objective lens (LCPlan Fl, NA 0.6, 1.5x tube lens) and an X-Cite 120 metal halide light source (EXFO). For DmrA/C FRET experiments, A/C heterodimerizer (Takara Bio Inc.), equivalent to Rapalog-1 AP21967 (ARIAD Pharmaceuticals) was added at 500 nM for 60 min unless otherwise noted. Fluorescence excitation and emission wavelengths were selected using a DAPI/FITC/Tx Red filter set (Chroma Technology Corp.) and a Lambda 10-3 filter wheel controller (Sutter Instrument) equipped with a shutter for epifluorescence illumination control. Images were recorded with a CoolSNAP HQ2 14-bit charge-coupled device (CCD) camera (Photometrics).

CHAPTER III

Monomeric kinesin cooperativity in intracellular transport

3.1 Introduction

Cytoskeletal motor proteins transport cargoes directionally along actin or microtubule filaments in eukaryotic cells. Defects in motor protein function impair this transport and are linked to numerous diseases including neurodegeneration and cancers. A large number of kinesin motors are involved in transport of cargoes to the plus end of microtubules in the cell periphery. Transport kinesins such as kinesin-1, the founding member of the kinesin superfamily, are dimerized through a coiled-coil stalk and thus have two motor domains for ATP hydrolysis and microtubule binding. The coordination of the two motor domains in kinesin-1 is maintained by alternating (out-of-phase) ATPase cycles, ensuring that one domain remains bound to the microtubule as the other takes a step forward (Hackney, 1994; Rosenfeld et al., 2003; Yildiz et al., 2004). Thus, kinesin-1 motors are processive as single motors and maintain their interaction with the microtubule track for hundreds of catalytic cycles.

Several studies have investigated the *in vitro* motility of single-headed kinesin-1 motors, both monomeric motors generated by truncation of the coiled-coil stalk (Berliner et al., 1995; Young et al., 1998; Kamei et al., 2005; Inoue et al., 1997)

and full-length molecules lacking one of the motor domains (Hancock and Howard, 1998). These studies demonstrated that single kinesin monomers are not processive, providing strong support for the model that dimerization is required for processive motion.

Yet groups of kinesin monomers can glide a microtubule or transport a bead, albeit at lower speeds and forces than their dimeric forms (Berliner et al., 1995; Kamei et al., 2005; Inoue et al., 1997), suggesting that monomeric motors could work cooperatively in teams to drive cargo transport. Indeed, a recent study showing that single-headed KIF1A motors are able to extract membrane tubes from giant vesicles proposed that the presence of a diffusive state in KIF1A's mechanochemical cycle may facilitate its cooperative force generation in groups (Roth et al., 2015). In addition, several members of the myosin family are known to exist as monomers but can drive processive cargo transport in cells (Pyrpassopoulos et al., 2016; Dunn et al., 2007).

A theoretical framework for how dimeric and monomeric motors function to drive processive cargo transport was proposed by Leibler and Huse (Leibler and Huse, 1993). Dimeric motors such as kinesin-1 work as "porters" and can drive long-range transport alone or in small groups because they spend most of their ATPase cycle bound to their track (high duty ratio). Monomeric motors, such as myosin-2 and flagellar dynein, work in large ensembles and spend most of their time detached from the track. Like "rowers" in a boat, individual monomers interact only transiently with the track but collectively can generate force and large movements. While this model is consistent with the ability of ensembles of kinesin monomers to drive processive transport in bead transport or gliding assays, it is not clear whether monomers are able to collectively transport cargoes when attached to a lipid bilayer and moving through the crowded cellular environment.

To test whether kinesin monomers can work collectively to drive cargo transport in cells, we directly compared dimeric motors to artificial monomeric motors

across the kinesin-1, -2, and -3 families in both *in vitro* and cellular assays. We find that surprisingly, the monomeric motors are able to drive the dispersion of peroxisomes to the cell periphery, suggesting that dimerization and processive motility at the single-molecule level are not required for cargo transport by teams of motors. We further explore the mechanics of this cooperativity and find that in general, kinesin monomers are efficient transporters if the motor-to-cargo distance is short and the cargo imposes minimal load on the motors. As the length of the stalk increases, monomers become less efficient, and dimerization becomes necessary to pull against load. Together, these results lend insight into the minimal requirements and mechanical modulators of collective kinesin cargo transport. They may also shed light on why most kinesins evolved to function as dimers.

3.2 Results

3.2.1 Single-headed KIF1A motors can transport membrane-bound cargo in cells

Can monomeric kinesin motors work in teams to transport a cargo in cells? To investigate this, we focused on the kinesin-3 motor KIF1A based on its ability to diffuse along the microtubule lattice as a monomer (Okada and Hirokawa, 1999; Okada et al., 2003) and to extract membrane tubes from giant vesicles (Roth et al., 2015). We utilized a constitutively active, truncated version of KIF1A that contains the motor domain, neck linker, neck coil, and the GCN4 leucine zipper [KIF1A(1-393)-LZ)] and is known to exist as a dimer, along with a monomeric version containing only the motor domain and neck linker [KIF1A(1-369)] based on our previous work (Hammond et al., 2009; Soppina and Verhey, 2014). We first verified their motility properties as individual motors by imaging 3xmCit-tagged motors with total internal reflection fluorescence (TIRF) microscopy (Norris et al., 2015). Dimeric KIF1A motors display

long, processive, uni-directional runs at fast speeds (Figure 3.1 A, left), consistent with previous studies (Soppina et al., 2014), whereas monomeric KIF1A motors show only transient interactions with the microtubule and diffusive motion in both directions (Figure 3.1 A, right), consistent with previous work (Okada and Hirokawa, 1999; Okada et al., 2003; Soppina and Verhey, 2014). Thus, dimerization is required for individual KIF1A motors to undergo robust processive motility along microtubules.

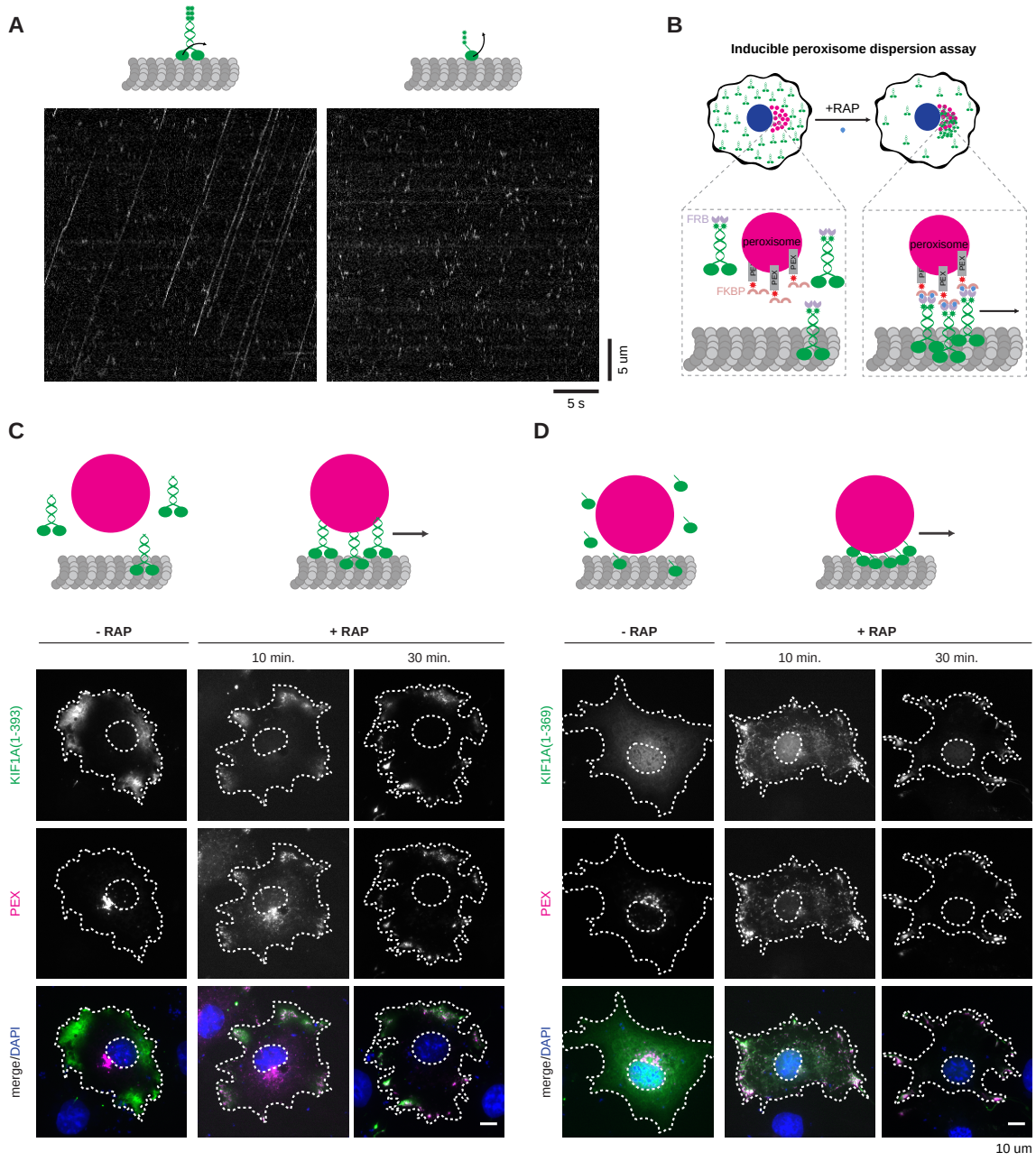

Figure 3.1: **Single-headed KIF1A motors can cooperatively transport cargo in cells despite lacking single-molecule processivity.**
(A) The single-molecule motility of 3xmCit-tagged KIF1A motors was imaged with TIRF microscopy at saturating ATP (2 mM). Representative kymographs of single-motor tracks are shown for dimers (left) and monomers (right). Time is on the x-axis (bar: 5 s) and distance is on the y-axis (bar: 5 um). (B) Schematic of the inducible peroxisome dispersion assay. Motor-mNG-FRB was co-expressed in COS-7 cells with PEX-mRFP-FKBP. Motors were recruited to peroxisomes via rapamycin (RAP) addition and cells were fixed after 0, 10, or 30 min. Representative images at each time point after RAP addition are shown for targeted (C) dimeric KIF1A and (D) monomeric KIF1A motors. Merged images are shown again in Fig. 2 for comparison with other motors. Bar: 10 um.

To test whether dimeric and monomeric KIF1A motors can work effectively in teams for cargo transport in cells, we utilized an artificial cargo trafficking assay where the kinesin of interest is targeted to the peroxisome, and the subsequent redistribution of the peroxisome can be attributed to the transport capacity of the motor (Kapitein et al., 2010a). Peroxisomes are relatively immotile and are localized in the perinuclear region in COS-7 cells. Their dispersion requires <15 pN force generation by the recruited kinesin motors (Efremov et al., 2014; Wiemer et al., 1997). This assay enables the analysis of motor behavior in a physiological environment where motors work in teams to transport membrane-enclosed cargoes.

We fused mNeonGreen-FRB to the C-terminus of our dimeric or monomeric KIF1A motors and co-expressed the tagged motors with a PEX3-mRFP-2xFKBP targeting sequence in COS-7 cells. Rapamycin addition induces the dimerization of FRB and FKBP (Clackson et al., 1998), thereby rapidly recruiting the motor to the peroxisome surface (Figure 3.1 B). The cells were fixed after 0, 10, or 30 minutes of rapamycin treatment and the motor/cargo dispersion was observed by fluorescence microscopy (Figure 3.1 C-D). As expected, recruitment of dimeric KIF1A results in rapid redistribution of the peroxisomes to the cell periphery (Figure 3.1 C). To our surprise, we found that monomeric KIF1A motors are also able to transport peroxisomes as well as the dimeric motor (Figure 3.1 D), despite lacking the single-motor processivity of the dimer form. These results suggest that groups of monomeric KIF1A motors are able to work cooperatively while attached to a lipid bilayer to drive transport in a cellular environment. They also demonstrate that dimerization of kinesin motors is not required for cargo transport in cells.

3.2.2 Single-headed motors from the kinesin-1, -2, and -3 families can transport membrane-bound cargo in cells

We next asked whether other monomeric kinesin motors can work in teams to drive cargo transport in cells or whether this property is unique to KIF1A. To test this, we compared the ability of dimers and monomers across the kinesin-1, kinesin-2, and kinesin-3 families for their ability to drive peroxisome dispersion in cells. We constructed artificial monomeric motors containing only the motor domain and neck linker for members of kinesin-1 (KIF5A, KIF5B, KIF5C), kinesin-2 (KIF3AB, KIF17), and kinesin-3 (KIF13B, KIF16B) families based on coiled-coil predictions and previous work (Hariharan and Hancock, 2009; Phillips et al., 2016). The amino acid composition of each construct is indicated in Figure 3.2. We first verified that all monomeric motors are able to interact with microtubules as single molecules. Indeed, the monomeric kinesin-1 and kinesin-2 motors display rapid binding and unbinding events with little to no diffusive motion, whereas the transient interactions of monomeric kinesin-3 motors consist of short periods of diffusive motion (Figure 3.3).

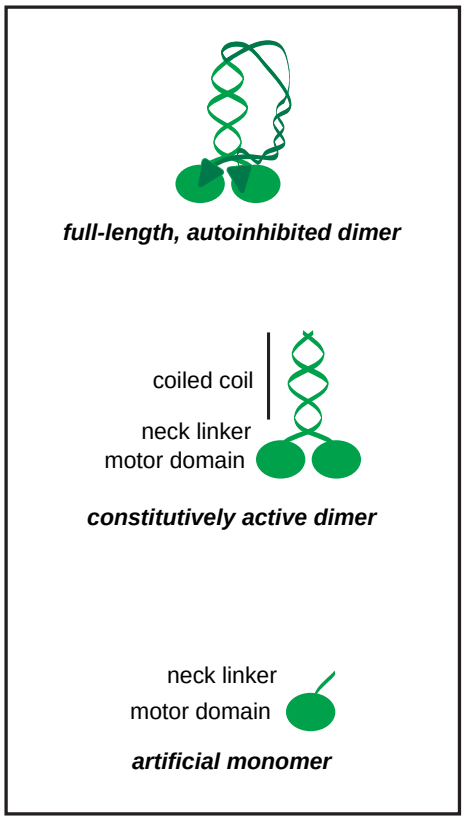

		Dimer	Monomer
Kinesin-1	KIF5A	(1-560)	(1-338)
	KIF5B	(1-560)	(1-336)
	KIF5C	(1-559)	(1-339)
Kinesin-2	KIF3A	(1-419)	(1-355)
	KIF3B	(1-414)	(1-350)
	KIF17	(1-738)	(1-349)
Kinesin-3	KIF1A	(1-393)	(1-369)
	KIF13B	(1-412)	(1-367)
	KIF16B	(1-398)	(1-372)

Figure 3.2: **Design of constructs for comparing kinesin dimers to monomers.** Artificial monomeric kinesins containing the motor domain and neck linker were constructed based on coiled-coil predictions and previous work. Amino acids are indicated.

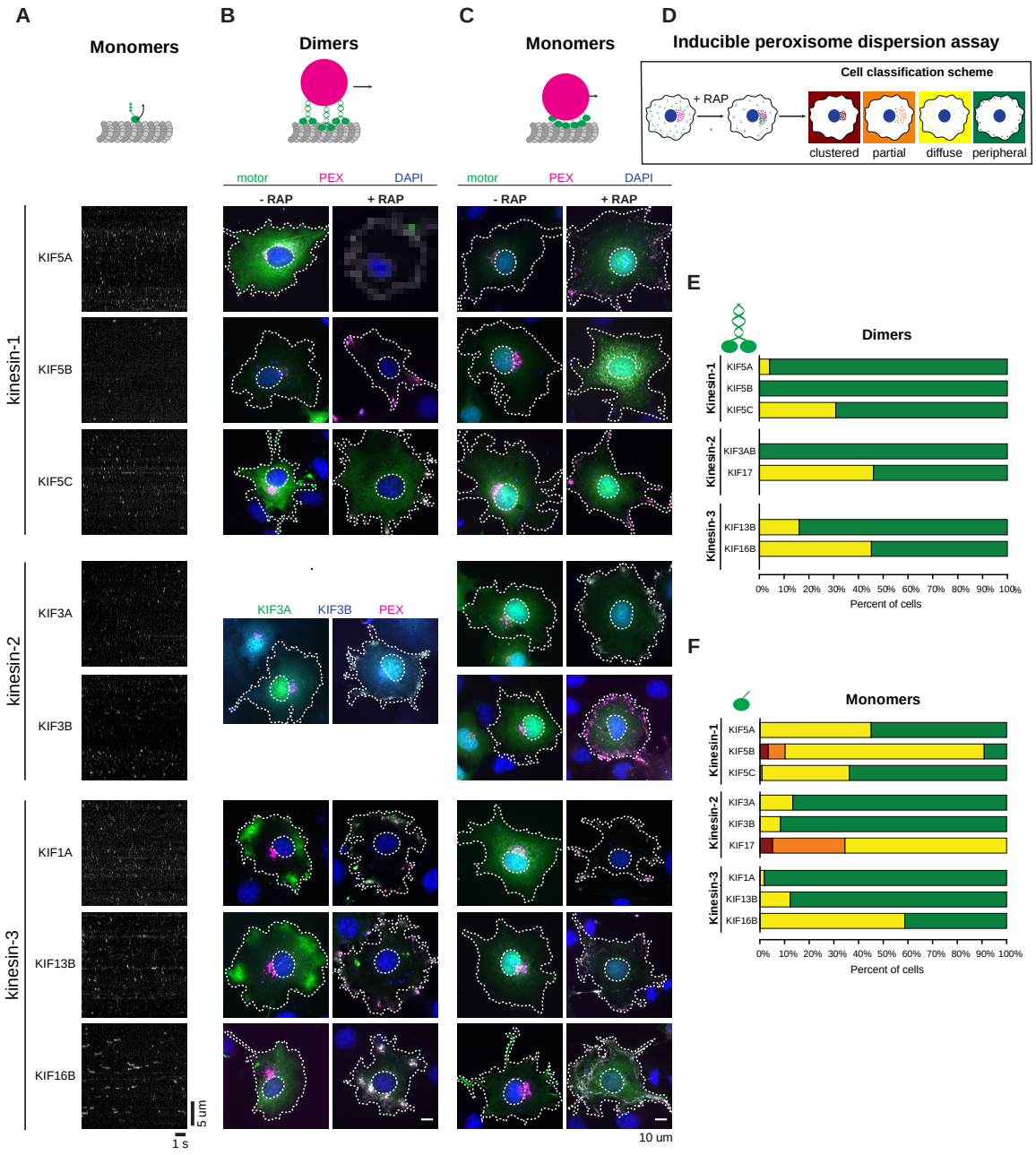

Figure 3.3: **Minimal kinesins containing a single motor domain and neck linker can collectively transport peroxisomes to the cell periphery.**
(A) Monomers from the kinesin-1, -2, and -3 families were tagged with 3xmCit and imaged with TIRF microscopy at saturating ATP. Representative kymographs are shown. Time is on the x-axis (bar: 1 s); distance is on the y-axis (bar: 5 um). (B, C) Representative images of fixed COS-7 cells co-expressing PEX3-mRFP-FKBP (magenta) and (B) dimeric or (C) monomeric motor-mNG-FRB (green). Left column: no RAP; right column: 30 min. after RAP addition. Only merged images are shown for clarity. Figures 3.4, 3.5, and 3.6 contain individual fluorescence channels. Bar: 10 um. (D) Cells were classified into 4 categories based on peroxisome localization: clustered (red), partially dispersed (orange), diffuse (yellow), or peripheral (green). Quantification of the proportion of cells in each category with targeted (E) dimers and (F) monomers. Motility assays in (A) were performed by Breane Budaitis in the Verhey laboratory.

We then examined the ability of the dimeric and monomeric motors to drive peroxisome dispersion in cells. The dimeric and monomeric versions of each motor were tagged with mNG-FRB and co-expressed in COS-7 cells with the PEX3-mRFP-FKBP construct and motor recruitment to the peroxisome surface was induced with rapamycin. For KIF3AB, only the 3A subunit was tagged with mNG-FRB, and the 3B subunit was fused to TagBFP to encourage the binding of heterodimers. The cells were fixed after 0, 10, or 30 min of rapamycin treatment and peroxisome dispersion was examined by fluorescence microscopy. For clarity, representative images before and after 30 minutes of rapamycin treatment are shown in Figure 3.3 B-C, with individual channels in Figures 3.4, 3.5, and 3.6. Control experiments in the absence of RAP, absence of motor expression, and presence of ethanol vehicle show no peroxisome dispersion. Data are pooled from at least three independent experiments. As expected, dimeric versions of each kinesin motor are able to drive peroxisome dispersion (Figure 3.3 B). Surprisingly, the monomeric motors are also able to drive peroxisome dispersion (Figure 3.3 C). These experiments indicate that the ability of kinesin motors to generate motion in cells requires only the catalytic core and the neck linker.

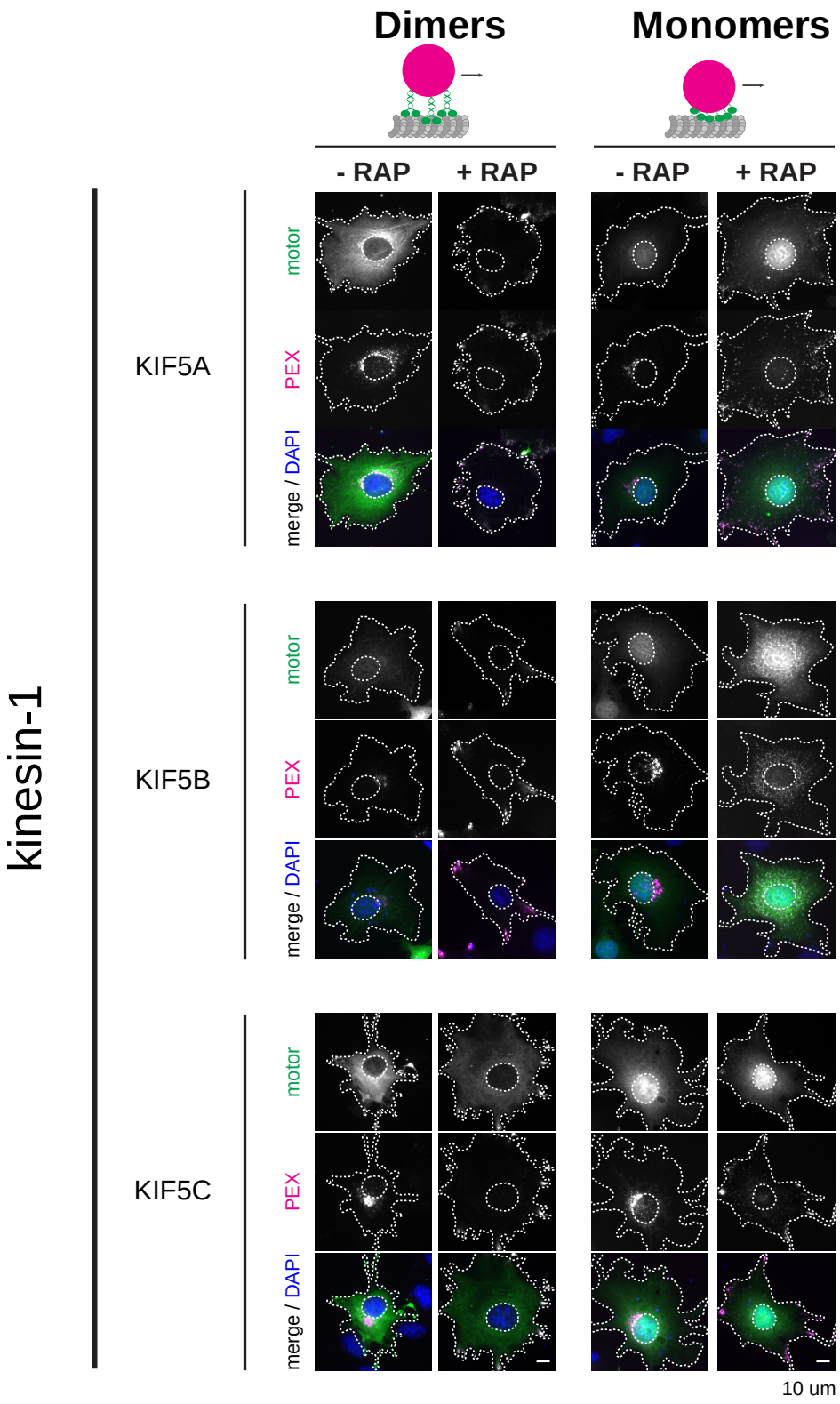

Figure 3.4: **Individual fluorescence channels in peroxisome dispersion assay with kinesin-1 family motors (from merged images in Figure 3.3 B-C).** Representative images of fixed COS-7 cells co-expressing PEX3-mRFP-FKBP (magenta) and dimeric (left panel) or monomeric (right panel) motor-mNG-FRB (green). In each panel, left column: no RAP; right column: 30 min. after RAP addition. Bar: 10 um.

To quantify these results, we classified the peroxisome localization into 4 categories: clustered, partially dispersed, diffuse, or peripherally dispersed (Figure 3.3 D). For the kinesin-1 motors, it is interesting that a dimeric KIF5B motor is most effective at full dispersion of the peroxisomes, whereas the monomeric KIF5B is the least effective (Figure 3.3 E-F). For the kinesin-2 motors, KIF17 is a less effective motor than KIF3AB in both the dimeric and monomeric states. For the kinesin-3 motors, all motors are effective at peroxisome transport, although KIF16B appears less effective in both the dimeric and monomeric states (Figure 3.3 E-F). Thus, despite the importance of dimerization for processive motion at the single-molecule level, dimerization is not required for kinesin motors to work effectively in teams to drive transport in cells.

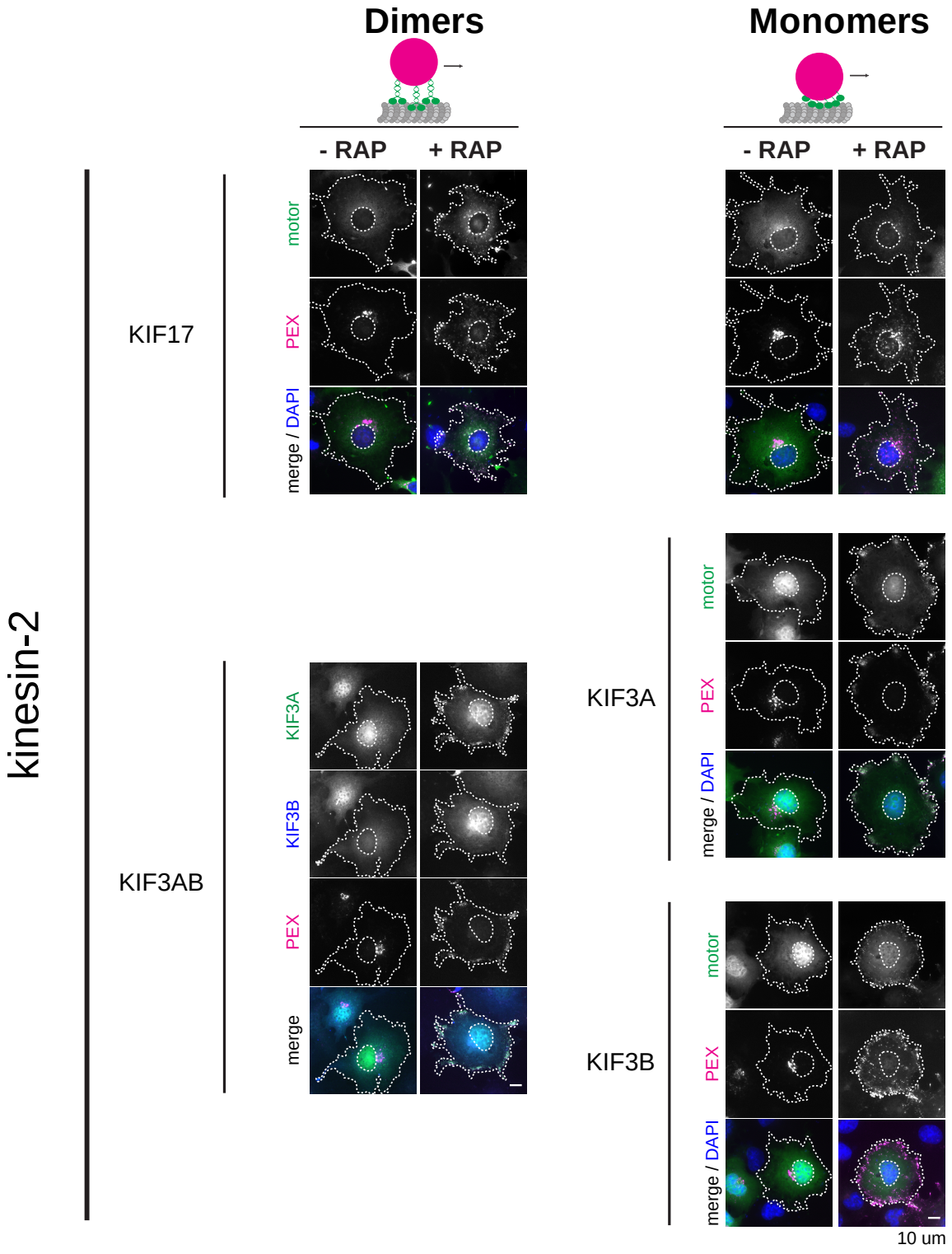

Figure 3.5: **Individual fluorescence channels in peroxisome dispersion assay with kinesin-2 family motors (from merged images in Figure 3.3 B-C).** Representative images of fixed COS-7 cells co-expressing PEX3-mRFP-FKBP (magenta) and dimeric (left panel) or monomeric (right panel) motor-mNG-FRB (green). In each panel, left column: no RAP; right column: 30 min. after RAP addition. Bar: 10 um.

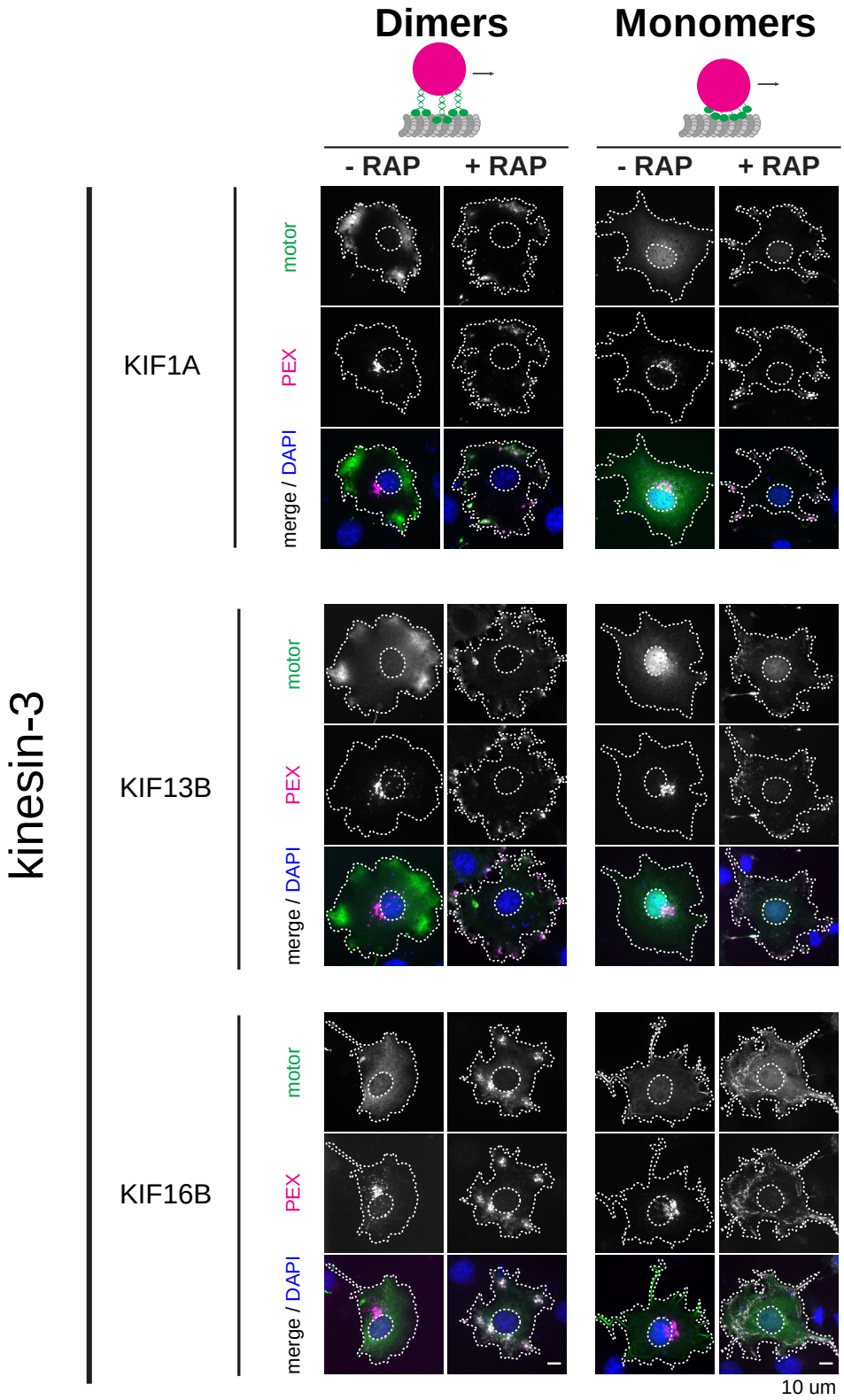

Figure 3.6: **Individual fluorescence channels in peroxisome dispersion assay with kinesin-3 family motors (from merged images in Figure 3.3 B-C).** Representative images of fixed COS-7 cells co-expressing PEX3-mRFP-FKBP (magenta) and dimeric (left panel) or monomeric (right panel) motor-mNG-FRB (green). In each panel, left column: no RAP; right column: 30 min. after RAP addition. Bar: 10 um.

3.2.3 Monomeric motors are impaired at high-load cargo transport in cells

The fact that kinesin monomers are able to cooperatively transport peroxisomes in cells raises the question of why most kinesins exist as dimers. One potential advantage of being a dimer is that a dimeric motor can generate higher forces than monomeric motors working individually or in teams. We hypothesized that although monomer teams can generate sufficient force for transport of peroxisomes, these motor teams would be ineffective when challenged with a high-load cargo. To test this, we examined the ability of monomeric motors to drive dispersion of the Golgi complex in COS-7 cells. The Golgi is held in a tight cluster in the perinuclear region of COS-7 cells by a combination of cytoplasmic dynein, myosin motors, and linker proteins (Brownhill et al., 2009; Wei and Seemann, 2017). Targeted kinesins must work against this opposing force to disperse the Golgi (Figure 3.7 A), with one study suggesting that movement of the Golgi requires 200 pN force (Guet et al., 2014; Egea and Serra-Peinado, 2014). We thus used the C-terminal region of GMAP210 to target the mRFP-FKBP module to the cis-Golgi membrane (Infante et al., 1999; Nguyen et al., 2014; Engelke et al., 2016). Cells expressing a kinesin-mNG-FRP and the GMAP210-mRFP-2xFKBP were fixed 0, 10, or 30 min after rapamycin treatment and stained with an antibody against the Golgi marker Giantin to probe for dispersion of Golgi components.

We examined the ability of dimers and monomers of the kinesin-1, -2, and -3 families to disperse the Golgi to the cell periphery (Figure 3.7 B-C). Representative images before and after 30 minutes of rapamycin treatment are shown in Figure 3.7 B-C, with individual channels in 3.8. Control experiments demonstrated that no Golgi dispersion occurs in the absence of rapamycin, in the absence of motor-mNG-FRB expression, or upon treatment with ethanol vehicle. To directly compare Golgi and peroxisome dispersion, we used the same cargo dispersion phenotypes to categorize

cellular phenotypes after rapamycin-induced targeting (Figure 3.7 A). Compared to peroxisome dispersion, there is much more variation both across and within families in terms of a motors ability to disperse the Golgi complex. In general, dimeric motors (Figure 3.7 D) are better at dispersing the Golgi than their monomeric versions (Figure 3.7 E). This supports the hypothesis that dimerization enables kinesin motors to generate higher forces necessary for the transport of high-load cargoes in a cellular context.

For kinesin-1 motors, we find that dimeric KIF5B and KIF5C motors are effective at Golgi dispersion (>50% of cells have peripheral dispersion) whereas dimeric KIF5A motors are less effective (<10% of cells have peripheral dispersion) (Figure 3.7 D). Interestingly, the monomeric motors show the opposite trend; monomeric KIF5B and KIF5C cannot disperse the Golgi (>95% remain clustered) and the monomeric KIF5A is relatively effective (<10% remain clustered) (Figure 3.7 E).

For kinesin-2 motors, we find that dimeric KIF3AB is an effective motor for Golgi dispersion (>30% of cells have peripheral dispersion) whereas dimeric KIF17 is completely ineffective (0% of cells have peripheral dispersion (Figure 3.7 D). Indeed, the majority of cells expressing KIF17 still have clustered Golgi, despite the fact that the motor is targeted to the Golgi after rapamycin treatment (Figure 3.7 B,D). For the monomeric kinesin-2 motors, we were surprised to find that monomeric versions of both subunits (KIF3A and KIF3B) of the heterodimeric motor are able to disperse the Golgi. 20% of the cells expressing monomeric KIF3A have a peripheral dispersion phenotype and >50% of cells expressing monomeric KIF3B have this phenotype (Figure 3.7 E). In fact, the KIF3B monomer disperses the Golgi to the cell periphery in a larger percent of cells (55%) than does the KIF3AB dimer (32%).

For kinesin-3 motors, all dimeric motors are capable of Golgi dispersion (15% peripheral dispersion for both KIF13B and KIF16B) (Figure 3.7 D), whereas the monomeric versions are relatively inefficient at Golgi dispersion (30%, 30% and 60%

clustered for KIF1A, KIF13B, and KIF16B, respectively) (Figure 3.7 E). We had expected KIF1A to be effective as a monomer based on the original characterization of this motor as a monomer (Okada et al., 1995; Okada and Hirokawa, 1999; Okada et al., 2003); however, KIF13B is the only monomeric kinesin-3 whose recruitment results in peripheral dispersion of the Golgi complex (10% of cells).

Taken together, these results indicate that monomeric kinesin motors are generally ineffective at transport of a high-load cargo in a cellular environment. Thus, a benefit provided by dimerization is that the motor can generate sufficient forces required for transport of certain cellular cargoes.

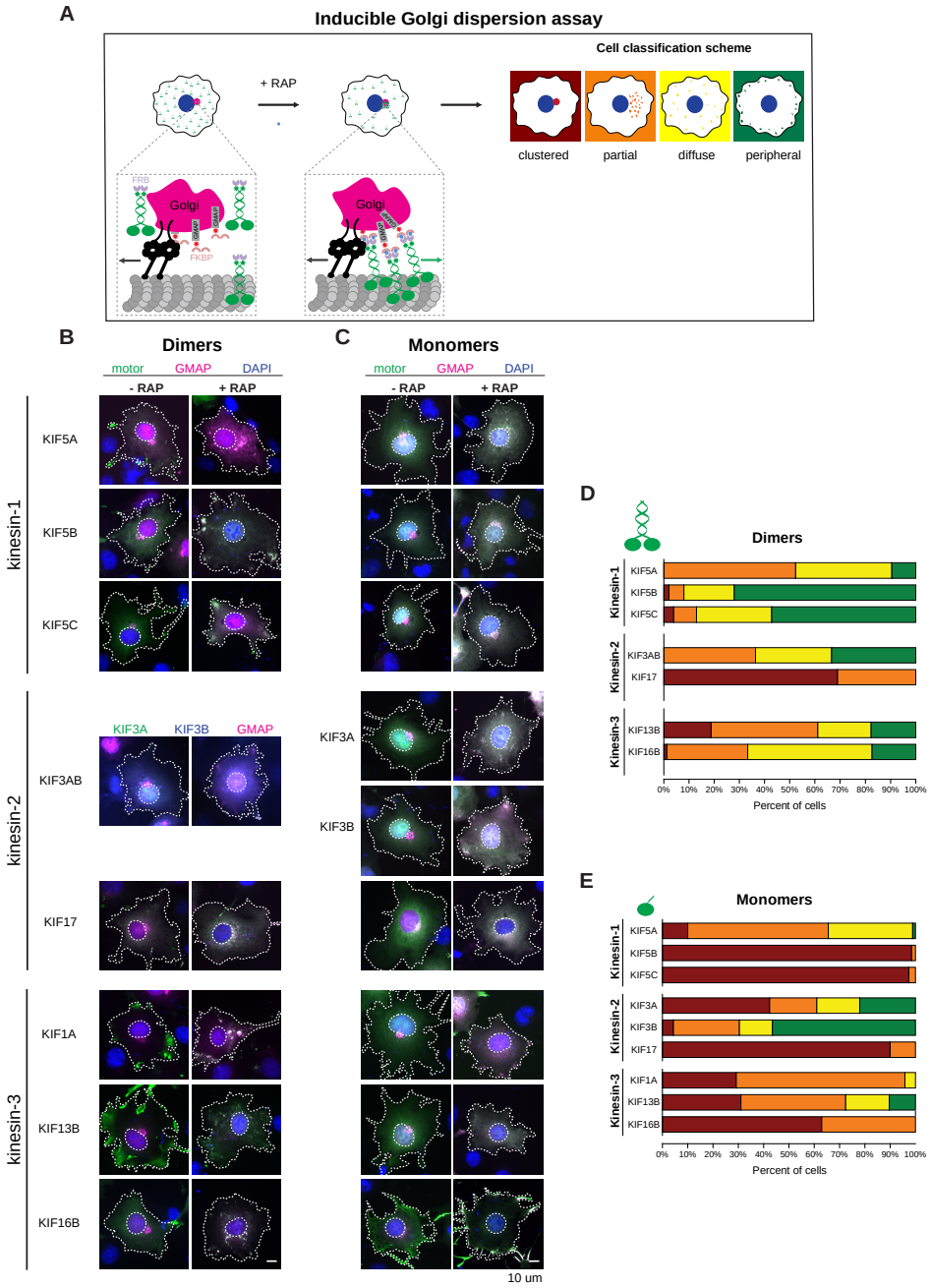

Figure 3.7: **Motor dimerization facilitates transport of high-load cargoes in cells.** (A) Schematic of the inducible Golgi dispersion assay. Targeted kinesins must work against the opposing force of endogenous proteins that hold the Golgi in a cluster in the perinuclear region, making Golgi a high-load cargo. Representative images of fixed COS-7 cells co-expressing (B) dimeric or (C) monomeric motor-mNG-FRB (green) and GMAP-mRFP-FKBP (magenta) before (left column) and 30 min. after (right column) RAP addition. Only merged images are shown for clarity. They are shown again in Figure 3.8 along with individual fluorescence channels. Quantification of the proportion of cells within each category with targeted (D) dimers and (E) monomers shows that Golgi dispersion is more heterogeneous than peroxisome dispersion, and dimerization generally benefits high-load transport. Bar: 10 um. Only quantification at the 30 min. time point is shown for clarity.

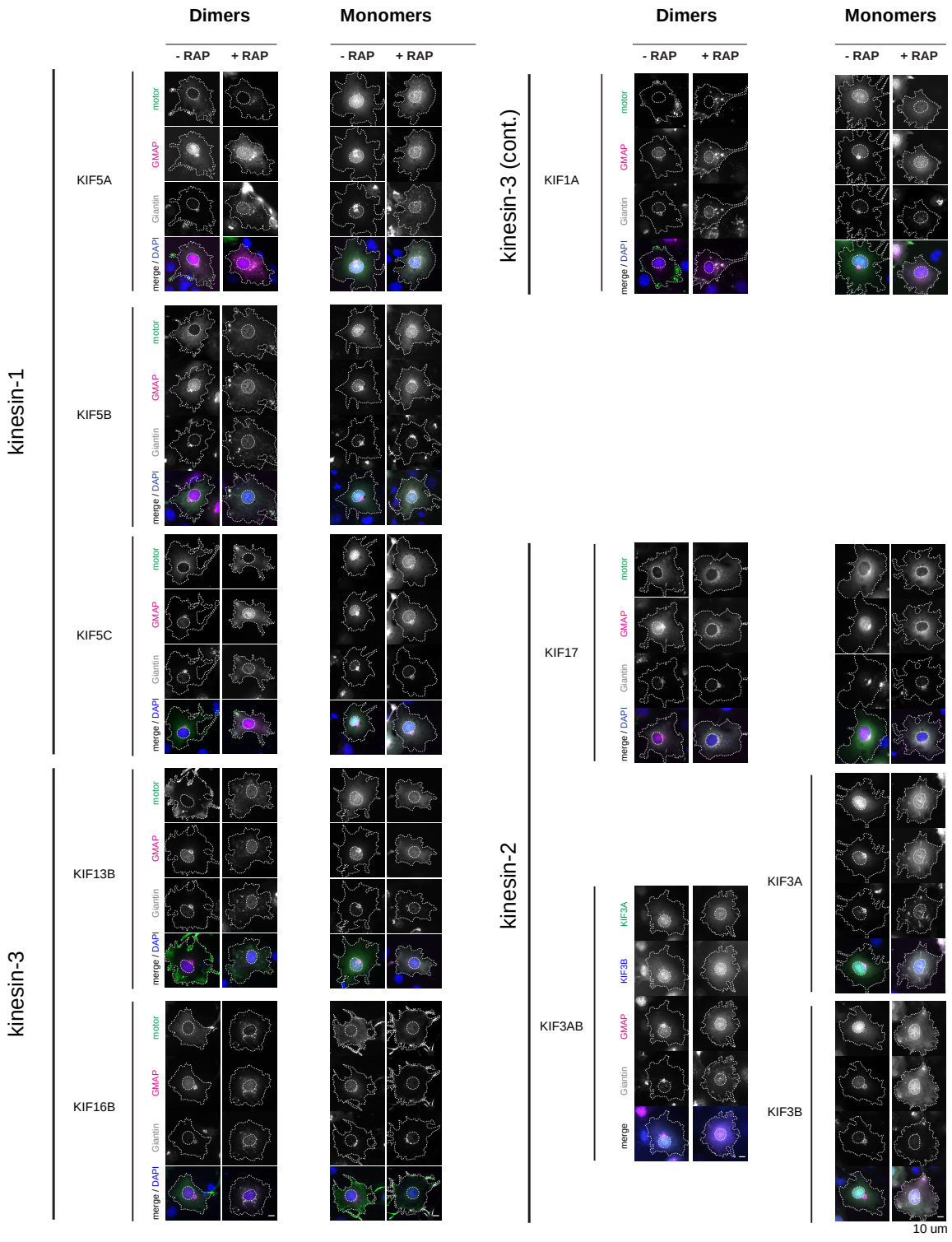

Figure 3.8: **Individual fluorescence channels in Golgi dispersion assay with kinesin-1, -2, and -3 family motors (from merged images in Figure 3.7 B-C).** Representative images of fixed COS-7 cells co-expressing GMAP-mRFP-FKBP (magenta) and dimeric (left panel) or monomeric (right panel) motor-mNG-FRB (green). In each panel, left column: no RAP; right column: 30 min. after RAP addition. Bar: 10 um.

3.2.4 The length of KIF3B monomers modulates their cooperativity in cells and *in vitro*

Kinesins are generally extended molecules containing extensive non-motor segments that contribute to oligomerization, cargo binding, and regulation of motor activity. We thus asked how the addition of non-motor elements would affect the ability of kinesin monomers to cooperate in intracellular cargo transport. We speculated that teams of monomers may only be able to row along the microtubule and generate force if there is a short distance between the motor and the cargo. To test this, we took advantage of the unique ability of KIF3B to function in Golgi dispersion and appended single alpha helix (SAH) domains of varying length (5, 10, 20, or 30 nm) after the neck linker of the KIF3B monomer (Figure 3.9 A). SAHs are stable helical structures found in a number of proteins, including myosins, and have been well-characterized biophysically (Spink et al., 2008; Sivaramakrishnan et al., 2008, 2009). Their defined length and mechanical properties make them ideal for protein engineering applications (Swanson and Sivaramakrishnan, 2014). We tested the functionality of the extended motors in the peroxisome and Golgi dispersion assays. With both cargoes, we observed a robust trend: as the length of the monomer increases, it is less efficient at working in teams to transport both peroxisomes and Golgi in cells (Figure 3.9 B).

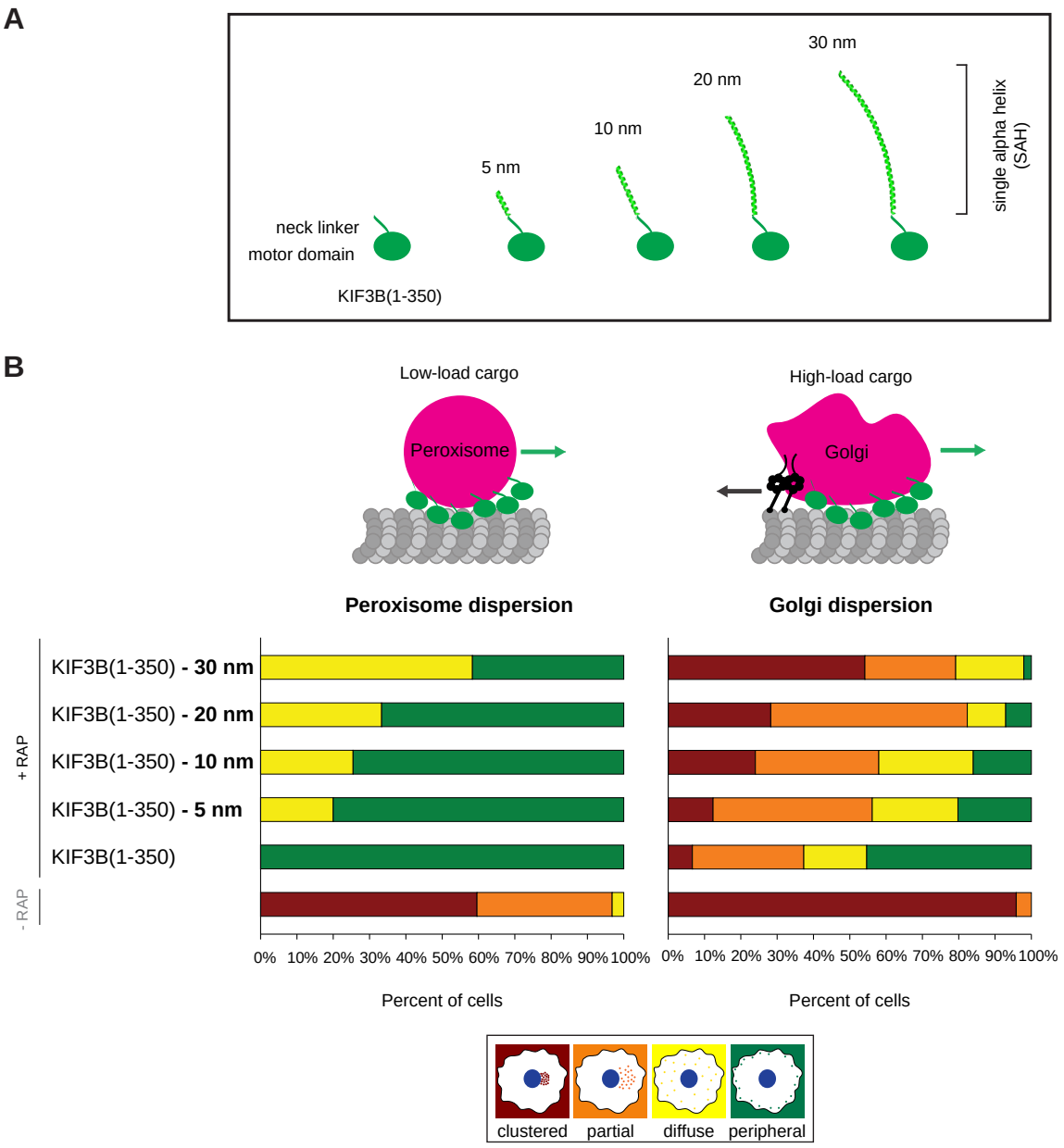

Figure 3.9: **Increasing the extension between KIF3B monomers and cargo reduces transport ability in a length-dependent manner.**
(A) SAH sequences of known length (5, 10, 20, or 30 nm) were inserted after the motor domain and neck linker of KIF3B. (B) Extended motors were tested in the peroxisome (left) and Golgi (right) dispersion assays. Only quantification at the 30 min. time point is shown for clarity. The longer the SAH extension, the worse the motor is at cooperatively dispersing both Golgi and peroxisomes.

To gain a mechanistic understanding of the ability of long and short monomers to cooperate in a multi-motor situation, we immobilized monomeric KIF3B-SAH con-

structs on beads and determined their speed (Figure 3.10 A) and force generation (Figure 3.10 B) in a multi-motor context. For these assays, we compared the minimal KIF3B monomer (no SAH) to the monomer with a 20 nm SAH because these showed significant differences in the peroxisome and Golgi dispersion assays (Figure 3.9 B). Beads coated with multiple KIF3B monomers of both lengths show consistent unidirectional motility along microtubules (Figure 3.10 A). The short monomers drive bead motility with faster speeds (722.8 $\pm$ 482.1 nm/s) than the longer monomers (217.4 $\pm$ 203.9 nm/s) (Figure 3.10 A). To determine the force production of the KIF3B monomers, we used optical trapping and found that the short monomers generate higher forces than the long monomers. Beads coated with short KIF3B monomers move quickly out of the trap and stall at 6-8 pN of force before returning to the center of the trap, whereas beads coated with long KIF3B monomers (KIF3B-20 nm SAH) move more slowly and detach at lower forces before returning to the center of the trap (Figure 3.10 B-C). Quantification of multiple events showed that short monomers detach from the microtubule track at an average of 6 pN, whereas long monomers detach from the microtubule track at an average of 4 pN (Figure 3.10 B). Strikingly, at a lower motor concentration, KIF3B monomers generate up to 11 pN of force (data not shown).

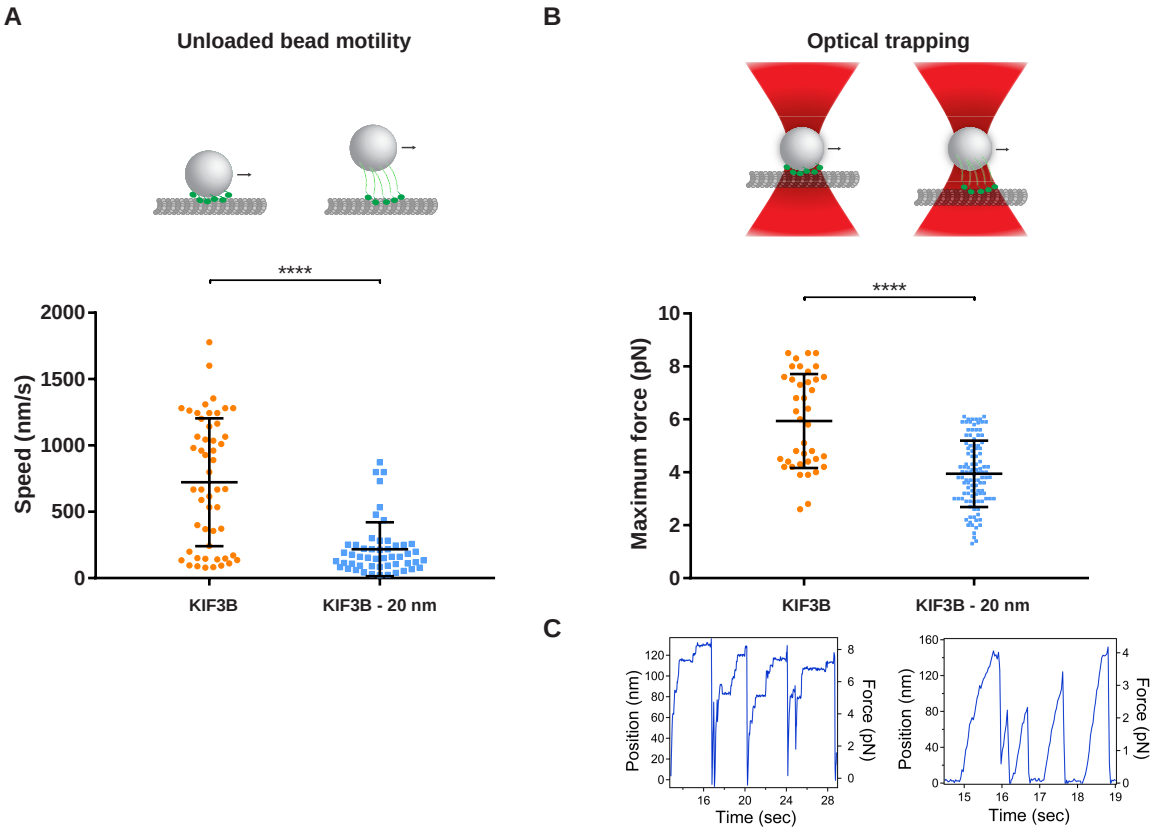

Figure 3.10: **Short KIF3B monomers drive faster unloaded bead motility and generate higher force compared to their elongated forms.**
Monomeric, biotinylated KIF3B motors were bound to 0.4 um streptavidin beads and tested for their ability to cooperate *in vitro* at different lengths. The minimal KIF3B monomer (with no SAH) was compared to an extended KIF3B monomer (with 20 nm SAH) to measure multi-motor motility properties in vitro. Identical bead stocks, motor preparations, and incubation conditions were used for both assays, except the motor concentration, which for had to be altered for feasibility in each assay geometry. (A) Top: schematic of unloaded bead motility assays. Fluorescent, streptavidin-coated polystyrene beads bound to biotinylated motors were imaged with TIRF microscopy and their speeds were measured by kymograph. At equal motor concentration (35 nM), beads bound to minimal KIF3B monomers moved at significantly higher speeds of 723 $\pm$ 482 nm/s (67 nm/s SEM) than beads bound to elongated KIF3B monomers, which move at speeds of 217 $\pm$ 204 nm/s (29 nm/s SEM). n = 52 events for short monomers and 51 events for longer monomers. (B) Top: Schematic of optical trapping assay. At equal motor concentration (7 nM), minimal KIF3B monomers produce significantly higher forces of 5.9 $\pm$ 1.8 pN (0.3 pN SEM) than elongated KIF3B monomers, which produce 3.9 $\pm$ 1.3 pN (0.1 pN SEM). n = 39 events for short monomers and 108 events for long monomers. (C) Example traces of optically trapped beads are shown for each motor. Data are reported as mean $\pm$ standard deviation (error bars). ****, $P < 0.0001$ (two-sample Kolmogorov-Smirnov test).
Optical trapping experiments were performed by Dana N. Reinemann in the laboratory of Matthew Lang at Vanderbilt University.

These results indicate that the impaired ability of the longer KIF3B monomers to drive cargo transport in cells is due, at least in part, to their reduced speed and force generation in a multi-motor context as compared to the short monomers. They also demonstrate that the ability of monomeric kinesins to work effectively in teams and transport cargo depends on the distance between the motor domain and the cargo. For kinesins known to be involved in transport of membrane-bound cargoes in cells, the presence of structural elements involved in oligomerization and/or motor regulation result in an increased motor-to-cargo distance and thereby impose a constraint on motor function that dimerization appears to reduce or solve.

3.3 Discussion

This study provides the first investigation of the effect of dimerization on intracellular transport driven by kinesin motors. We show that non-processive kinesin monomers are able to collectively generate force and drive transport while attached to a membrane-bound cargo. While other studies have demonstrated that monomeric kinesins can be assembled into processive complexes (Berliner et al., 1995; Stewart et al., 1993; Jamison et al., 2012; Schindler et al., 2014), this study is the first to demonstrate cargo transport by nonprocessive motors attached to a membrane and pulling against a load in a cellular environment. We find that transport driven by monomeric kinesins is most efficient a) under low-load conditions, and b) when the motor-to-cargo distance is short.

Numerous studies have sought to explain the ability of KIF1A monomers to undergo processive motion. Theoretical papers have proposed that it is KIF1A's weak binding state that allows it to cooperate as a monomer. However, our results indicate that this is not required. We demonstrate that the ability of kinesins to generate motion requires only the catalytic motor domain and the neck linker. These minimal elements enable the motors to work as rowers; each member of the team briefly binds

to the track, generates an impulse of force, and then releases from the track. However, it is remarkable that despite the ability of all of the monomeric motors we tested to bind to microtubules (Figure 3.3 A), the motors display large differences in their ability to drive processive transport in cells. The sequence similarity among kinesin-1, -2, and -3 motor domains is high, indicating that small sequence changes can lead to large functional consequences.

An important finding is that the motors that are most effective as monomers in teams are not the ones that are most effective as dimers in teams. It is especially surprising that although kinesin-1 dimers, the canonical porters, are able to disperse Golgi better than kinesin-2 dimers, KIF3A and KIF3B (kinesin-2) monomers are significantly stronger in teams than kinesin-1 monomers. One possibility is that the motility parameters that benefit monomers are not the same as the ones that benefit dimers. Indeed, motor parameters such as motor-to-motor gating, load-dependent off-rate, catalytic speed, and rebinding rates are known to impact the transport output of individual dimeric motors and may also be important for multi-motor transport driven by monomeric motors. For example, rapid unbinding of individual motor domains may help a monomer in a team setting but hinder the cooperation of individual motors domains within a dimer. Another possibility is that the stalk plays an important role in force-generating capability. If it were merely an inert linkage that had the same role in all motors, we would expect the strongest dimers to correspond to the strongest monomers, but this is not the case even within families.

The kinesin-3 motor KIF1A was originally described as a monomeric processive motor and we find that monomeric versions are more effective than the other kinesin motors when at working in teams to drive peroxisome transport (98% peripheral dispersion). However, we were surprised to find that monomeric versions of KIF1A are less effective at Golgi dispersion than monomeric versions of other kinesins, in particular the kinesin-1 KIF5A and the kinesin-2s KIF3A and KIF3B.

Further work is needed to decipher the parameters that limit teams of KIF1A motors under high-load conditions, including force generation and rebinding rate.

It is also unclear why the other kinesin-2 motor, KIF17, is ineffective in teams since it is significantly faster than KIF3AB across a wide range of applied forces (3 times faster unloaded than KIF3AB at saturating ATP), highly processive, and continues stepping against 6 pN hindering load (Milic et al., 2014; Hammond et al., 2010). Future work will explore the features of kinesin-2 motors that endow them with surprising multi-motor behavior.

3.3.1 High force generation by monomeric KIF3B motors

The unique ability of KIF3A and KIF3B (kinesin-2) monomers to generate high force *in vivo* is striking. We were also surprised at the magnitude of force production by KIF3B when attached to beads and manipulated in an optical trap *in vitro*. We found that multiple KIF3B monomers with short motor-to-cargo linkers can withstand up to 11 pN of force at a concentration of 7 nM. In contrast, multiple kinesin-1 KIF5B monomers are capable of withstanding an average of only $\sim$2.7 pN at comparable concentrations (Kamei et al., 2005); this is consistent with our observation that monomeric KIF5B motors cannot transport high-load cargo in cells. That KIF3A and KIF3B are uniquely well-suited to transport high-load cargoes even as monomers is especially interesting given their unique assembly as a heterodimeric KIF3AB motor in the native molecule. Insights about these monomeric motors could inform studies seeking to explain the functional significance of the heterodimeric KIF3AB structure.

The structural and mechanical features that enable KIF3A and KIF3B motors to function effectively as monomers, even under high-load conditions, are unclear. Biophysical findings offer some hints. A recent study showed that although kinesin-2 motors are less processive than kinesin-1 at the single-molecule level, KIF3A homod-

imers with a KHC stalk have a reattachment rate is four-fold faster (Feng et al., 2018). The authors propose that this "dynamic tethering" makes kinesin-2 (KIF3AB) an especially helpful team player because its rapid rebinding allows a cargo assembly to dodge obstacles and remain associated with the microtubule (Feng et al., 2018). Furthermore, this rapid reassociation with the microtubule after unbinding may allow groups of KIF3A and KIF3B monomers to function well as rowers because each motor can interact more frequently with the track, increasing the efficiency of the ensemble.

Another distinctive feature of KIF3AB motors is that they rapidly unbind in response to opposing force, in contrast to the stalling behavior of kinesin-1 (Andreasson et al., 2015). Their tendency to dissociate from the microtubule rather than stall under load likely reduces friction and interference and facilitates their cooperative force generation as single-headed rowers.

3.3.2 Features that facilitate the cooperativity of monomers

Muscle myosins function in a confined environment, and despite their frequent unbinding, their spatial proximity to the track allows them to quickly rebind and engage in productive rowing. It is possible that the cargoes in our assays are playing a similar role, spatially confining motors near the microtubule and allowing them to rapidly rebind. This rapid rebinding may be especially beneficial for monomers, whose short length decreases the volume they are able to sample. Thus, rebinding quickly ensures that instead of diffusing away in the membrane from the track or sterically hindering other productive motors, they engage with the track and produce an impulse of force, contributing to the forward motion of the cargo.

Spatial considerations are important when interpreting these assays. One study showed that purified neuronal transport vesicles, primarily late endosomes and lysosomes, had a mean diameter of 90 nm (Hendricks et al., 2010). It is worth noting that in our cellular assays, the extracted Golgi fragments are of unknown size and

are likely not uniform. Peroxisomes are usually spherical and 0.1-1 um in diameter, but they can also change shape (Smith and Aitchison, 2013). The beads we used in our *in vitro* assays are spherical with 0.4 um diameter, so this is a reasonable size for comparison with endogenous cargoes.

A short motor-to-cargo linker is not essential for processive transport in teams, but it enables the monomers to be more effective, particularly in high force situations. Relevant to this is the myosin I family, which contains only a short linker sequence before the cargo binding segment. Recent work showed that these motors can generate collective force when attached to a lipid bilayer on a bead (Pyrpassopoulos et al., 2016). For myosin II motors, each motor in the filament effectively works as a monomer, yet these motors are capable of high force generation because their assembly into bipolar filaments means that the distance separating the motor from the cargo (the filament) is short. Some dimeric kinesin and myosin motors have been shown to be non-processive as single motors yet can drive processive cargo transport when working in teams. This has previously been demonstrated for non-processive kinesin-14 (Case et al., 1997; Furuta et al., 2013; Jonsson et al., 2015; Walter et al., 2015) and kinesin-6 family motors (Tao et al., 2016). Given our results with monomeric KIF3B motors with SAH linker sequences, these non-processive dimeric motors may be capable of cooperating for processive cargo transport as long as high force generation is not required. Future work will investigate the ability of these nonprocessive dimers to transport membrane-bound cargoes in cells.

3.3.3 The advantage of being a dimer

Our data suggest that monomers become less efficient transporters in cells the larger the motor-to-cargo distance. Thus, an advantage to being a dimer is the ability to incorporate non-motor domains for oligomerization and regulation, with a resulting increase in the motor-to-cargo linker distance, and retain the ability to drive high-load

transport in cells. In fact, dimeric motors have been shown to work better when the coiled-coil is extended (Uyeda et al., 1996; Endres et al., 2006; Bieling et al., 2008). Extension of the coiled-coil may merely facilitate multi-motor transport by reducing spatial interference between motors or by increasing the compliance of the system in a manner similar to the increased cooperativity of dimeric kinesins containing breaks in the coiled-coil (Bieling et al., 2008).

Our conclusion with the length-dependence of motor-to-cargo linker for the monomeric motors assumes that the SAH domains are inert spacers of increasing length, but we cannot rule out that the longer SAH domains, which are longer than the SAH persistence length of 15 nm (Sivaramakrishnan et al., 2009), may affect motor cooperation by changing the compliance and/or rigidity of the motor-to-cargo linkage. Future work with additional linkers is needed to address the question of how compliance of the motor-to-cargo linkage affects the ability of motors to work in teams and drive processive cargo transport.

We have shown that although dimerization is required for processive motion of individual kinesin motors, it is not required for teams of motors to effectively transport a membrane-bound cargo in cells. Why then do most, if not all, kinesins exist as dimers? One advantage to being a dimer is likely the ability to generate high force, especially at low motor copy number. Dimerization allows a few motors to effectively transport high-load cargo since each motor can generate force and the forces are additive. Theoretical and experimental studies have suggested that high force generation by dimeric kinesins requires tight coupling between the two motor domains, provided by the neck linker (Yildiz et al., 2008). For monomeric motors, motor-to-motor coupling requires that mechanical interactions between motor domains occur through the cargo itself. For monomeric motors attached to a bead or glass, the rigid cargo can provide this mechanical coupling. However, for monomeric motors attached to a lipid bilayer, motor-to-motor coupling likely requires either high motor numbers

and/or a decrease in the fluidity of the membrane (Nelson et al., 2014; Grover et al., 2016).

CHAPTER IV

Discussion and conclusions

4.1 Discussion

4.1.1 Impact of this work

The kinesin field has long held the belief that to carry out intracellular transport, a kinesin must be both processive and dimeric. Here we have demonstrated that this is not true: kinesin monomers that are nonprocessive as single motors can carry out efficient, long-range transport in cells when grouped on the same cargo. The myosin field has long known that nonprocessive motors can work in teams to generate movement and force. Thus, this work provides a unifying theme for the myosin and kinesin fields: transport ability is not tied to the processive state of individual motors.

In their paper, Leibler and Huse proposed a theoretical framework for classifying motor proteins into porters or rowers based on how they transduce chemical energy into mechanical work (Leibler and Huse, 1993). While subsequent years demonstrated that this classification scheme was applicable to both processive and nonprocessive myosin motors, the absence of monomers in the kinesin superfamily made it unclear whether they also fit into the scheme. The work in this thesis provides experimental evidence that a kinesin can act either as a rower or a porter, both *in vitro* and in cells, depending on its oligomeric state. Thus, kinesins do not have some intrinsic

catalytic property that prevents them from acting as rowers like myosins.

The work in this thesis extends the field's knowledge about commonalities and differences across the kinesin and myosin superfamilies. Kinesins and myosins arose from common ancestor and then evolved in paprallel to form superfamilies (Kull et al., 1996, 1998). Despite a common ancestor, they evolved to associate with different filaments and have different mechanochemical cycles, such that ATP hydrolysis controls different stages of their stepping cycles. They also have almost no sequence identity. Yet the motors can have similar mechanical and functional outputs. For example, a minus-end-directed kinesin-14 motor, *Drosophila* Ncd, has been shown by cryo-electron microscopy to have a coiled-coil mechanical element that swings like a lever-arm toward the minus-end of the microtubule upon ATP binding (Endres et al., 2006). Increased lever-arm length led to increased velocity in microtubule gliding assays, whereas decreased length led to decreased velocity. Ncd is a nonprocessive motor and is responsible for microtubule crossbridging and tension development in the mitotic spindle. The authors suggest that Ncd and tension-generating myosin II motors in muscle convergently evolved to arive at the same force-generating element.

By comparing general properties of myosins and kinesins, and specific kinesins within the superfamily, we can gain a better understanding of how their individual structural and motility properties allow them to carry out their cellular functions optimally.

4.2 Future outlook

4.2.1 Regulation of motor-cargo interaction

One limitation to our study, and indeed to most methods linking multiple motors together, is the fact that the motors bind to the cargo irreversibly (Kapitein et al., 2010b). *In vivo*, there are important regulatory mechanisms that modulate

cargo unloading and motor/adaptor abundance on the cargo. For example, there is evidence that in *Drosophila melanogaster*, the MAPK signalling pathway actively regulates kinesin-1 binding to JIP scaffolding proteins (Horiuchi et al., 2007) (for a review of kinesin regulation, see Verhey and Hammond (2009)). In *Saccharomyces cerevisiae*, Inp2p is the peroxisome-specific receptor for myosin V motor Myo2p. One study showed that whereas total Inp2p levels are regulated by cell cycle progression, Inp2p levels on individual peroxisomes are controlled by peroxisome positioning (Fagarasanu et al., 2009). Thus, both the multi-protein scaffold assemblies from Chapter 2 and the artificial cargo trafficking assays in Chapter 3 would benefit from having dynamic control over motor-cargo binding. This would allow for more dynamic, well-controlled studies on, for example, the effect of motor number on an individual cargo's transport.

Efremov and coworkers improved upon the peroxisome dispersion assay by using a genetic approach with a doxycycline-inducible promoter to tune receptor densities on the peroxisome surface with different concentrations of doxycycline (Efremov et al., 2014). Although this control over receptor densities on a cargo is certainly beneficial, it would also help to have a strategy to induce unbinding of motors.

4.2.2 Porters vs. rowers: cooperativity

We have shown that monomers from the kinesin-1, -2, and -3 families can collectively transport membrane-bound cargoes from the perinuclear region to the periphery of COS-7 cells, with select monomers generating enough force to disperse a high-load cargo and KIF3B monomers generating up to 10 pN of force in the optical trap. However, many questions remain open on the details of this transport by monomers compared to dimers. Most of our cargo dispersion observations were done on fixed cells, which enabled collecting a much higher sample size but also prevented us from measuring the dynamics that live-cell imaging would allow.

Thus, future work will use live-cell imaging for further investigations of how porters and rowers cooperate for intracellular cargo transport. This will involve performing live-cell imaging to track the movement of cargoes along microtubules before and after rapamycin-based recruitment of motor proteins. Measuring the fluorescence signal from motors, which is directly proportional to motor number, will provide important information about the number of motors driving the transport event. We can also measure dynamic parameters of the transport event such as speed and pause frequency. This will enable a comparison of motors from different families to determine how well they cooperate as dimers and monomers. These experiments would also allow us to test theoretical predictions that rowers and porters display different levels of cooperativity. Specifically, multiple porters have been shown to combine additively to generate higher forces but not speeds, whereas we would expect rowers to have a nonlinear response in relating speed and force production to an increase in motor number. We could also test this prediction with myosin motors, comparing myosins that actually function as porters vs. rowers.

A complementary approach could also be taken *in vitro*. To directly correlate motor number with cargo speed and force production, one could bind fluorescently-labeled motors to unlabeled beads. For each bead, it would then be possible to measure the speed and/or force while simultaneously measuring total fluorescence intensity and photobleaching steps, indicating the number of motors present on that particular bead. Compared to live-cell imaging of cellular cargoes, this would enable more precise measurement of the number of motors on each bead. One drawback is that the motor-bead linkage is not physiological, and several groups have begun to use a membrane-coated bead to allow for motor diffusion in the cargo.

4.2.3 Force generation by kinesin-2 motors

KIF5A monomers displayed a drastically better ability to transport high-load cargo than the other kinesin-1 motors, KIF5B and KIF5C. The fact that these motors are highly homologous yet behave vastly different in cells underscores the need to study motors using both reductionist and cell biological methods.

The ability of teams of monomeric KIF3B motors to withstand up to 11 pN of force is striking; previous studies showed that teams of KIF5B (kinesin-1) and KIF1A (kinesin-3) motors can only withstand average forces of 2.7 pN (Kamei et al., 2005) and 2.5 pN (Okada et al., 2003), respectively, at comparable concentrations. In the future, it will be interesting to identify the key force-generating elements of KIF3B and uncover their features. The mechanical element of kinesins is the neck linker, but sequence comparisons of the neck linker of KIF3B (kinesin-2) and KIF5C (kinesin-1) do not reveal any obvious differences that could account for the higher force generation of KIF3B monomers. It is possible that interactions of the neck linker with other structural features of the KIF3B motor domain enable the high force generation, and mutational analysis could be used to probe this possibility.

It will also be interesting to determine how the features of KIF3B revealed in these assays impact the functional output of the kinesin-2 KIF3A/KIF3B/KAP motor in cells. The kinesin-2 motor is best known for its role in the assembly, maintenance, and function of cilia and eukaryotic flagella. Unpublished work shows that cells expressing KIF3A/KIF3B motors that contain only one motor domain are unable to generate cilia, suggesting that dimerization is critical. It may be that ciliary cargoes only bind a couple of KIF3A/KIF3B motors and this small team cannot generate the high forces seen in our assays. It may also be that the dimeric version is required for walking on the special doublet microtubules in cilia.

4.2.4 Other features that modulate multi-motor cooperativity

The work described here investigated the ability of teams of dimeric and monomeric kinesin motors to transport cargoes in a cellular environment and the influence of force generation and motor protein length on this transport. Based on *in vitro* experiments, other motor features are also likely to influence the ability of motors to work in teams, and it will be interesting to investigate this in the future. For example, that the kinesin-2 motor KIF17 is ineffective in transport is surprising since this motor has been shown to be fast, processive, and continue stepping against a 6 pN hindering force when attached to beads and measured in an optical trap (Milic et al., 2014), so one would naively expect it to perform like kinesin-1 in cells. Sequence analysis of the KIF17 neck linker indicates that it has all of the features needed for force generation. Future experiments could examine whether KIF17 has a low on-rate to the microtubules or a high load-dependent off-rate that hinder its ability to work effectively under high-load situations, even in teams.

In fact, features that are seen as detrimental for single motors may help motors work more productively in a multi-motor scenario. Kinesin-1 can walk against loads, whereas kinesin-2 and kinesin-3 detach more readily under load. However, as monomers, it is kinesin-2 and -3 that tend to be stronger in teams than kinesin-1.

Two studies investigated the effect of single-motor velocity on multi-motor travel distance (Xu et al., 2012, 2013).

Duty ratio is an example of a motor property that has the opposite effect on transport efficiency of individual porters vs. multiple rowers – high duty ratio is better for individual porters, and low duty ratio is better for rowers in teams.

4.2.5 Use of SAH domains as building blocks

The work in this dissertation provides two examples of how the SAH domain can be used as a building block in synthetic biology: creating multi-protein assemblies

(Chapter 2) and extending the length of the kinesin "lever arm" (Chapter 3). The SAH domain has also been used by others to engineer chimeric myosin motors with different mechanical properties (Hariadi et al., 2014) or to systematically regulate protein-protein interactions, forming the basis for a FRET biosensor (Sivaramakrishnan and Spudich, 2011) (for a review, see Swanson and Sivaramakrishnan (2014)).

As we have shown in Chapter 2, combining SAH domains with tunable regulation, such as inducible chemical dimerization, offers a versatile and powerful method for modulating and monitoring dynamics *in vitro* and in cells. In the future, this structural element is likely to be useful to construct artificial motors for use in drug delivery, lab-on-chip, or nanodevices, i.e. in directed molecular assembly (Hess et al., 2004).

4.3 Conclusions

Numerous studies over the last few decades have shown the importance of coordination between the two motor domains for kinesin's processive motility. However, until now it was unknown whether dimerization was required for kinesin motors to transport cargo in a cellular context. Here we have shown, across the kinesin-1, -2, and -3 families, that although dimerization is indeed required for single-molecule processivity, monomeric kinesins can overcome their lack of processivity when they are grouped in teams, generating motion and in some cases large forces.

Our data demonstrate that the ability of kinesins to transport membrane-bound cargo requires only the catalytic motor domain and the neck linker. These minimal elements enable the motors to work as rowers in which each member of the team briefly binds to the track, generates an impulse of force, and then releases from the track. Although a minimal motor is sufficient for transport in all three families studied, there is large variability in cargo transport by monomers as well as dimers. Some monomeric kinesins go even further and generate high forces collectively, both

in cells and in the optical trap.

The fact that the relative transport efficiency of a dimeric motor is not a good predictor of its performance as a monomer (i.e. KIF5A is the weakest of the kinesin-1 dimers but the strongest of the kinesin-1 monomers) supports the reductionist approach of studying monomeric kinesin motors to better isolate motor domain-specific factors contributing to motility while also investigating them in a cellular context. Given their highly homologous motor domains, it is surprising that KIF5A monomers displayed such a drastically better ability to transport high-load cargo than the other kinesin-1 motors, KIF5B and KIF5C. This dimer vs. monomer approach is especially critical for the case of KIF3AB, which is unique with its heterodimerization of two different motor domains; understanding how they behave individually can lend insight into their distinct roles in the full-length molecule.

On the other hand, the finding that single-molecule motility assays do not predict the performance of motors in teams underscores the importance of studying motors in their native cellular environment with membrane-bound cargoes, microtubule-associated proteins, post-translational modifications, and all the cellular complexity that may affect their functioning. This is especially obvious in the kinesin-2 family. KIF17 *in vitro* is fast, processive, and can step against 6 pN hindering loads. In contrast, KIF3AB is slower, less processive, and detaches under an even lower load (Milic et al., 2014; Andreasson et al., 2015). In cells, however, this is reversed, with KIF3AB dispersing the Golgi well and KIF17 performing poorly.

Taken together, our study demonstrates the importance of using complementary approaches – *in vitro* and in cells – to thoroughly dissect motor function.

APPENDIX

APPENDIX A

A method for tethering single viral particles for virus-cell interaction studies with optical tweezers

This work was done in the laboratory of Wei Cheng at the University of Michigan.

A.1 Introduction

Human immunodeficiency virus type 1 (HIV-1) is an enveloped retrovirus that primarily infects T lymphocytes and macrophages *in vivo*. As the etiological agent of acquired immunodeficiency syndrome (AIDS), the HIV-1 replication cycle has been the subject of intense research over the last thirty years. Despite considerable advances, the mechanistic details for many steps in the cycle remain elusive due to inadequate techniques.

HIV-1 has a lipid bilayer that is derived from the host cell plasma membrane during viral assembly and budding. It holds 15 viral proteins, 2 copies of single-stranded RNA (Frankel and Young, 1998), and numerous incorporated cellular proteins (Arthur et al., 1992). As an enveloped virus, HIV-1 requires a cellular entry scheme that will liberate its contents from the protective viral membrane in order

to initiate infection. Entry is mediated by envelope glycoproteins (Env) in the viral membrane, which bind to cell surface receptors in a coordinated, sequential fashion and cause fusion of viral and cell membranes (for a review, see Gallo SA, Finnegan CM, Viard M, Raviv Y, Dimitrov A, Rawat SS, Puri A, Durell S, 2003). The viral core can then enter the cytoplasm and initiate replication.

Env functions as a trimer of heterodimers composed of noncovalently associated surface gp120 and transmembrane gp41 subunits. gp120 binding to a CD4 receptor on the target cell surface induces a conformational change in gp120 that exposes a binding site for a chemokine coreceptor, most commonly CCR5 or CXCR4. gp120 binding to the coreceptor causes additional conformational changes, which trigger the fusogenic machinery in gp41, leading to virus-cell membrane fusion and delivery of the viral payload into the cytoplasm.

In addition to its essential role in productive cellular entry, Env is the only viral immunogen on HIV-1 surface, making it the sole target for neutralizing antibodies produced by the humoral immune system. Therefore, it is a focus for the development of neutralizing antibody-eliciting vaccines and entry inhibitors. Moreover, Env-mediated cellular entry can reveal general features applicable to other systems, including receptor-mediated signaling, membrane fusion, and binding cooperativity.

Elegant structural and biochemical studies have provided significant insight into the sequence of receptor engagement and corresponding Env remodeling prior to and during cellular entry. However, several fundamental issues pertaining to virus-cell interactions and subsequent entry remain controversial. Clarifying these issues is crucial for understanding basic HIV-1 entry mechanisms and informing rational drug design.

Strikingly, HIV-1 Env is sparsely distributed on the viral surface compared to glycoproteins on other enveloped viruses such as influenza (Klein and Bjorkman, 2010). Nevertheless, HIV-1 is still able to infect cells, raising the question of potential

compensatory mechanisms. Recent studies suggest that maturation-dependent clustering of Env in the viral membrane is correlated with fusion competence (Chojnacki et al., 2012). Superresolution fluorescence (Chojnacki et al., 2012) and cryo-electron microscopy (Sougrat et al., 2007) can visualize Env distribution on virions but are unable to quantify the extent of receptor engagement. Thus, the dynamics and functional role of Env clustering remain unclear.

It is possible that spontaneous clustering occurs independently of virus-cell interaction, merely as a byproduct of Gag proteolysis during structural maturation of virions after budding from the cell; dissolution of the lattice could allow Env clustering driven by self-association of the gp41 cytoplasmic tail (CT). Alternatively, specific interactions with cellular CD4 receptors could induce Env clustering. Distinguishing between these two models motivates the development of a technique that can monitor high-resolution dynamics of Env clustering and probe cellular interactions while retaining the native states of the virus and cell.

Force spectroscopy has been used extensively to quantify receptor-ligand interactions (Bell, 1978). By varying external loading rates, it is possible to link bond strength to molecular-scale chemistry. Atomic force microscopy (AFM) has been used to measure interactions between HIV-1 and cellular receptors (Dobrowsky et al., 2008). However, this study used a cantilever with attached virions to force contact with a cell, which imposed artificial constraints on the geometry and number of bonds formed. They report that their virus functionalization, using LC-SMCC treatment of gp120, had no noticeable effect on viral infection. However, it is possible that modification of gp120 could still affect binding properties, and the long spacer arm in LC-SMCC has an unknown effect on force measurements. Furthermore, attaching virions to a cantilever via gp120 prevents an unknown number of Env from interacting with cells. Therefore, this study was unable to reliably investigate dynamical binding of multiple Env over long time courses.

Optical tweezers (OTs) offer significant advantages over AFM for this functional investigation; they can isolate a single virion in solution that is free to rotate and interact with a cell diffusively, they have superior force sensitivity and dynamic range, and they allow monitoring of virion internalization.

We thus set out to design an optical tweezers-based technique with which we can manipulate a single virion in solution by linking it to an optically trapped bead via a DNA tether (Figure A.1). It will then be possible to measure near-native, physical interactions of the virion with the surface of a micropipette-immobilized cell (not to scale).

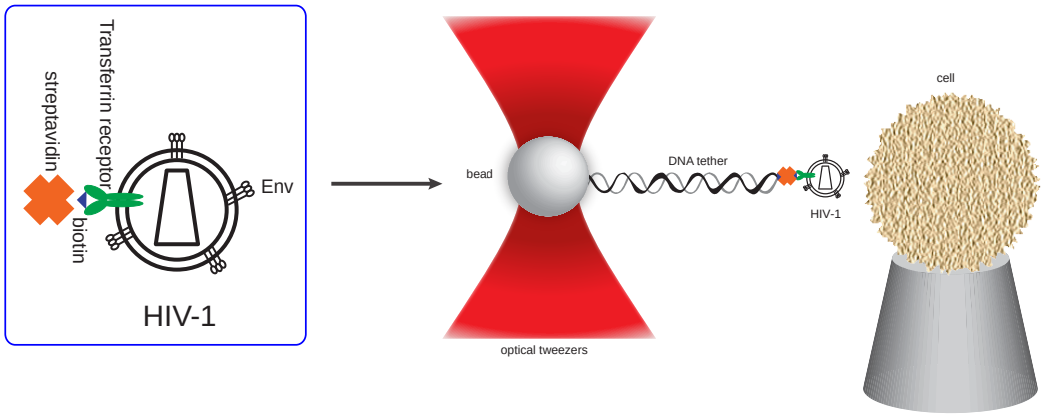

Figure A.1: **Single-virion optical trapping assay schematic.**

A.2 Materials and methods

Cell culture

Human embryonic kidney 293T cells were maintained at 37°C with 5% CO2 in Dulbeccos Modified Eagles Medium (DMEM, ATCC, Manassas, VA). TZM-bl cells were maintained at 37°C with 5% CO2 in DMEM (HyClone, Logan, UT). Both cell lines were supplemented with 10% Defined Fetal Bovine Serum (HyClone, Logan, UT). Complete medium refers to DMEM with 10% Defined Fetal Bovine Serum.

Production of HIV-1 virions with incorporated biotinylated transferrin receptors

pTfR-AP-IRES-BirA-ER (hereafter pTfR, for simplicity) (Liu et al., 2010) was subcloned into the pcDNA3.1(+) vector for expression in 293T cells using EcoRI and NotI restriction sites. HIV-1 virions were produced as described (Kim et al., 2013) with modifications. 293T cells were seeded in 2 mL culture volumes in 35 mm wells the day before transfection. The following plasmid amounts were added to each 35 mm well. For EGFP-Vpr virions, 293T cells were transfected with 1 ug pNL4-3R-E-, 1 ug pREC, 0.3 ug pEGFP-Vpr (Kim et al., 2013) and varying amounts of pTfR with TransIT LT-1 transfection reagent (Mirus Bio, Madison, WI). For iGFP virions, 293T cells were transfected with 1 ug pNL4-3-iGFP2 and different envelope plasmids. Before transfection, medium was supplemented with 100 uM biotin, which was previously shown to be saturating for BirA in 293T cells (Nesbeth et al., 2006). Medium was changed 6 hours post-transfection, maintaining the 100 uM biotin supplement. 24 hours post-transfection, culture supernatant was collected and filtered through a 0.45 um syringe filter. Virus preparations were then either aliquoted on ice and flash-frozen in liquid nitrogen, or dialyzed against PBS at 4°C in Spectra/Por Float-A-Lyzer G2 dialysis devices (Spectrum Laboratories, Inc., Rancho Dominguez, CA) with different molecular weight cutoffs (MWCOs) against PBS pH 7.4 for varying times. Immediately after collection, they were flash-frozen in liquid nitrogen. All viruses were stored at -80°C.

HIV-1 concentration was assayed with a p24 enzyme-linked immunosorbent assay (ELISA) as previously described (Kim et al., 2013) using the HIV-1 p24 Antigen Capture Kit (Advanced Bioscience Laboratories, Rockville, MD), following the manufacturers instructions. p24 concentration was converted to virion concentration via the assumption of 10 million virions per ng p24 (Kim et al., 2013). The concentration of infectious virions (titer) was measured using the TZM-bl indicator cell

line, as described (Kim et al., 2013). Infectivity was calculated by taking the ratio of infectious virion concentration to total virion concentration (titer/p24). Conditions were chosen with the goal of maintaining infectivity and maximizing biotinylated TfR (bTfR) incorporation.

Before HIV-1 was dialyzed, a feasibility experiment was performed to assess its stability when diluted in PBS or complete media at 4°C. The virus pool was diluted 25.5-fold, which brought the concentration to 4 x 10^7 particles/mL so that the results would be relevant for virometry. After incubation in the tube at 4°C and before flash-freezing, HIV-1 was further diluted 1:10 in complete media, bringing the total dilution to 1:255.

To test for expression of biotinylated TfR in 293T cells, cell lysates were also prepared. 293T cells were transfected with pTfR-AP-IRES-BirA-ER under the same conditions as virus-producing cells. Cells were washed with cold PBS and then incubated with 200 uL RIPA Lysis and Extraction Buffer (Thermo Scientific) containing protease inhibitor on ice for 15 minutes. Cells were collected and centrifuged at 12,000 rpm for 20 minutes at 4°C. The supernatant was collected and samples were stored at -80°C.

Western blotting

Virus samples were mixed with 6x SDS-PAGE sample loading buffer containing 9% β-mercaptoethanol and cell lysates were mixed with 2x Laemmli sample buffer containing 5% β-mercaptoethanol. Samples were heated at 95°C for 5 minutes. After cooling to room temperature, samples were run on 10% SDS-PAGE. Bands were then transferred onto supported nitrocellulose membranes.

Streptavidin-alkaline phosphatase conjugate (Invitrogen, Catalog #43-4322) at a concentration of 1.5 ug/mL was used to detect biotinylated protein. Protein bands were colorimetrically detected with nitro blue tetrazolium chloride and

5-bromo-4-chloro-3-indolyl-phosphate, toluidine salt substrates (NBT/BCIP, Roche) in a buffer containing 0.1 M Tris-HCl, 0.1 M NaCl, and 0.05 M MgCl2 at pH 9.5.

Virometry

Virometry to quantify bTfR copy number per virion was performed as described (Pang et al., 2014) with modifications. Alexa Fluor 594 streptavidin conjugate (Molecular Probes, Invitrogen) (SVD-Alexa 594) was used to detect and quantify bTfR in optically trapped virions. Briefly, dialyzed HIV-1 with incorporated bTfR was thawed from -80°C and incubated with 10 nM SVD-Alexa 594 for 1 hour at 20°C in the dark. The mixture was then diluted in PBS prior to injection into the flow chamber such that the final concentrations were 2 nM SVD-Alexa 594 and 0.8 - 1.3 x 10^8 virions/mL. These virus concentrations are higher than those found to aggregate in Pang et al., 2014 because here, dialysis removed much of the protein from the culture media that may have promoted aggregation in the previous study. This allowed higher-throughput measurements.

The refractive index of each trapped particle was calculated as described (Pang et al., 2016). All trapping experiments were conducted at 20.0 ± 0.2°C.

Preparation of DNA tethers

Doubly-labeled, double-stranded DNA tethers were prepared to link a virion to a bead. To generate Digoxigenin handles, a 510 bp fragment of Lambda DNA (New England BioLabs (NEB), Ipswich, MA) was PCR amplified using Taq polymerase. Digoxigenin (Dig)-dUTP was incorporated during PCR. The PCR product was purified with QIAquick PCR Purification Kit (Qiagen, Germantown, MD) and digested with XbaI (NEB). The digestion reaction was then treated with Antarctic phosphatase (NEB) and subsequently purified again with QIAquick PCR Purification Kit. To generate the long, biotinylated part of the tether, Lambda DNA was heated

at 65°C for 5 minutes to melt the cos sites and immediately quenched on ice to form hairpins. Klenow Fragment ($3' -> 5'$ exo-) (NEB) was used to incorporate Biotin-14-dATP and Biotin-14-dCTP (Invitrogen, Carlsbad, CA), after which the reaction was passed through a Micro Bio-Spin P-6 Gel Column (Bio-Rad, Hercules, CA) equilibrated with 1x New England Buffer 2 (NEB). This product was then digested by XbaI and ligated with the phosphatase-treated Dig handle at a molar ratio of Dig handle : Lambda DNA of 2:1. The length of the final DNA tethers was 8 um.

To form linkages for virion binding , doubly-labeled DNA tethers were incubated with 115 nM streptavidin, a 50-fold molar excess over DNA, for 30 minutes at 20°C and then 1 hour on ice. However, since unbound streptavidin would compete for virion binding, free streptavidin was removed by dialyzing DNA tethers against PBS for 87.5 hours at 4°C in 1000 kD MWCO membranes, with a total of four buffer exchanges.

Assembly of bead-DNA tether-virion complex

Here, we report the conditions used to obtain Video 1, in which an optically trapped bead attached to a DNA tether drags a fluorescent HIV-1 virion through a microfluidic chamber. Reproducibly forming the three-body complex proved to be difficult, so further optimization is necessary. Dig antibody-coated beads, DNA tethers, and virions were mixed as follows. First, 1 volume dual-labeled DNA tethers was incubated with 1 volume Dig antibody-coated beads and 3 volumes PBS overnight at 4°C, which was a ratio of 1735 tethers/bead. The next day, biotinylated, dialyzed HIV-1 was added to the bead-DNA mixture at an excess of 100 virions/bead and incubated on ice 3.5 hours. To remove unbound virions, the mixture was then centrifuged 3 times at 6000g for 5 minutes, resuspended in 40 uL PBS after each spin, and resuspended in 10 uL PBS after the final spin. 5 uL of this was then diluted in 395 uL PBS before injection into the microfluidic OTs chamber.

A.3 Results

Metabolically biotinylating an HIV-1-incorporated cellular protein in virus-producing cells

Isolating a virion for cellular delivery requires a labeling scheme with high specificity and minimal structural perturbation. As new virions bud from the cell, they incorporate host cellular proteins (Arthur et al., 1992). In order to target single virions without disrupting Env structure or function, we hypothesized that we could utilize the natural viral budding process to incorporate a biotinylated cell surface protein into nascent HIV-1 virions. This would serve as an anchoring target in the virion, leaving viral proteins intact. We could then use dual-labeled DNA tethers to link biotinylated virions to an optically trapped bead. Steering this bead would allow us to move the virion close to a cell, but the flexible DNA tether would allow the virion to freely diffuse and interact with the cell.

Among other labeling methods that commonly rely on *in vitro* manipulation of the virus pool, we chose metabolic biotinylation because it enabled site-specific labeling within the cell to occur simultaneously with virion production. We wanted to maximize the strength of the bond between the protein anchor and the DNA tether so that upon pulling, we would measure protein-protein interactions between viral and cellular proteins rather than simply rupturing the DNA from the virion. The strong affinity between biotin and streptavidin would allow for this. The small size of biotin (244.3 Da) was also less likely to interfere with protein incorporation than larger tags and an excess would be efficient to remove.

Previous studies have incorporated biotin into the membrane of enveloped viruses such as influenza (Liu et al., 2012) and infectious hematopoietic necrosis virus (Liu et al., 2011) in order to label virions with quantum dots for tracking. However, these studies treated purified viruses *in vitro* with Sulfo-NHS-LC-Biotin,

which labels primary amino groups rather than a specific peptide sequence. Another study made use of the natural viral budding process by adding 1,2-dioleoyl-sn-glycero-3-phosphoethanolamine-N-(cap biotinyl) (sodium salt) (Biotin-Cap-PE) to virus-producing cells to produce biotinylated pseudorabies virus (Huang et al., 2012). This strategy avoided excessive *in vitro* handling that could perturb viral stability, but again, biotin was incorporated nonspecifically into membranes.

Traditional biotinylation methods suffer from nonspecificity. *In vivo* biotinylation techniques circumvent this issue by using an Escherichia coli biotin ligase, BirA, for sequence-specific ligation of biotin to a lysine in a 15 amino acid acceptor peptide (AP) (Beckett et al., 1999; Schatz, 1993). When AP is fused to the extracellular domain of a protein of interest, this metabolic approach facilitates specific, high-efficiency biotinylation of cell surface proteins (Chen et al., 2005; de Boer et al., 2003). These biotinylated proteins can then be incorporated into budding virions when BirA and TfR-AP are coexpressed in virus-producing cells (a similar strategy was used in Nesbeth et al., 2006). This will allow high-affinity binding to a streptavidin-conjugated DNA tether linked to a trapped bead to manipulate single virions. It also avoids subjecting the virus pool to harsh post-purification labeling methods. To our knowledge, ours is the first study to biotinylate a virus for use in force spectroscopy.

In order to select a cellular protein to biotinylate, we wrote a MATLAB script to compare the expression library of 293T virus-producing cells (54,675 proteins) with the list of cellular proteins found in HIV-1 (Ott, 2008) (Cellular Proteins in HIV-1, https://ncifrederick.cancer.gov/research/avp/protein_db.asp) (303 proteins), narrowed to those localized to HIV-1 surface (131 proteins). We further restricted the list by protein structure and function, hypothesizing that transmembrane proteins with substantial cytoplasmic domains would be more difficult to pull from the viral membrane upon applied force. We also sought a protein whose overexpression has

not been shown to influence viral infectivity. We chose the transferrin receptor (TfR) on the basis of its demonstrated incorporation into the viral membrane (Orentas and Hildreth, 1993), endogenous expression in virus-producing cells, expected stability in the membrane, and functional insignificance to the virus.

We speculated that the sizable 67 amino acid cytoplasmic domain of TfR would stably anchor it in the viral membrane. TfR is a type II transmembrane protein, so its C-terminal ectodomain is a prime site for biotinylation. By expressing transferrin receptor fused with AP and BirA in virus-producing cells, it would be possible for nascent HIV-1 virions to incorporate biotinylated transferrin receptors as they bud from the plasma membrane.

Biotinylated TfR is present in HIV-1 preparations

To test whether our HIV-1 virions had indeed incorporated biotinylated transferrin receptors, we performed western blotting on iGFP virus preparations produced with 1 ug BG505 pEnv per well and varying amounts of TfR plasmid transfected. Our results indicate the presence of increasing bTfR in virus preparations with increasing plasmid input (Fig. 1A). Prior to this, we also optimized transfection conditions, including timing of biotin supplementation and transfection order.

Virometry reveals heterogeneity in biotinylated TfR incorporation per virion

Although western blots show the presence of biotinylated transferrin receptor in bulk virus preparations, they do not necessarily indicate viral incorporation; transferrin receptors could be present in non-viral microvesicles that bud off from the plasma membrane. Additionally, assessing the heterogeneity of TfR copy number per virion requires a more sensitive method. To quantify the number of biotinylated TfR on each virion, we used virometry, a technique recently developed in our lab

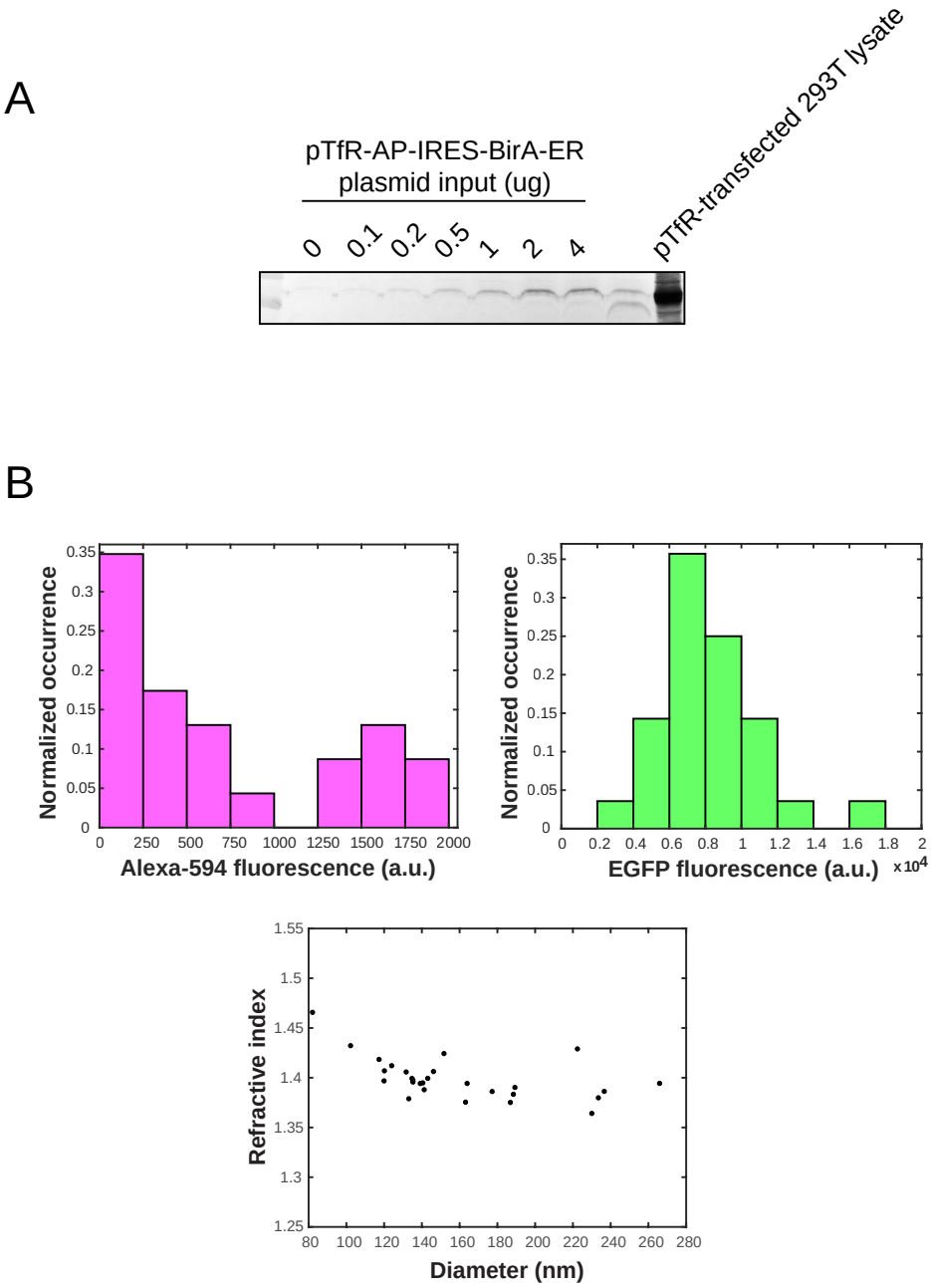

Figure A.2: **Production of HIV-1 with incorporated biotinylated transferrin receptors.**
(A) Western blot showing the presence of biotinylated TfR in HIV-1 preparations (iGFP virions with BG505 Env) detected with streptavidin-alkaline phosphatase conjugate. Loaded samples were diluted to have equal p24 concentrations. Lysate from 293T cells transfected with pTfR-AP-IRES-BirA-ER (pTfR) serves as a positive control. (B) Left: histogram of Alexa 594 fluorescence, proportional to the number of biotinylated transferrin receptors, in individually trapped virions. Right: histogram of EGFP fluorescence in individually trapped virions. Bottom: refractive index versus diameter of individually trapped particles. N = 28 virions trapped on the same day.

(Pang et al., 2014). Briefly, virions pumped into a flow chamber can be individually trapped by an 830 nm laser, whereupon their EGFP and Alexa 594 fluorescence can be simultaneously measured along with their size and refractive index (Fig. 1B, bottom), which were consistent with previous studies (Pang et al., 2014, 2016). We used these parameters to distinguish virions from other particles or debris, and only included viral particles in our analysis. From the size of a single Alexa 594 fluorophore photobleaching step, it is then possible to estimate the number of biotinylated TfR molecules per virion.

Fluorescence measurements of Alexa 594 per virion comprise a broad distribution (Figure 1B, left) and are uncorrelated with EGFP fluorescence (Figure 1B, right). Many virions have no Alexa 594 signal. Importantly, HIV-1 produced in the absence of pTfR does not nonspecifically bind to SVD-Alexa 594 when measured by virometry. Based on the mean Alexa 594 fluorescence, scaled for labeling stoichiometry on streptavidin, this pool of HIV-1 has a mean of 4 bTfR molecules per virion.

Incorporation of TfR preserves HIV-1 infectivity

For future applications of this technique, it is crucially important to maintain the infectivity of HIV-1 containing bTfR. We analyzed the effect of TfR overexpression and incorporation into the viral membrane by transfecting different amounts of TfR plasmid into 293T virus-producing cells along with fixed amounts of viral plasmids. We performed infectivity assays using TZM-bl cells, as described (Kim et al., 2013). To assess the effect of TfR expression and the presence of exogenous biotin on virus production in 293T cells, we performed an enzyme-linked immunosorbent assay (ELISA) to detect HIV-1 p24 capsid protein. Figure 2A shows the concentration of virion particles as a function of pTfR plasmid input during transfection for two strains of HIV-1 with two different envelopes. Although p24 concentration decreases with increasing TfR plasmid input, there is a concomitant decrease in the concentra-

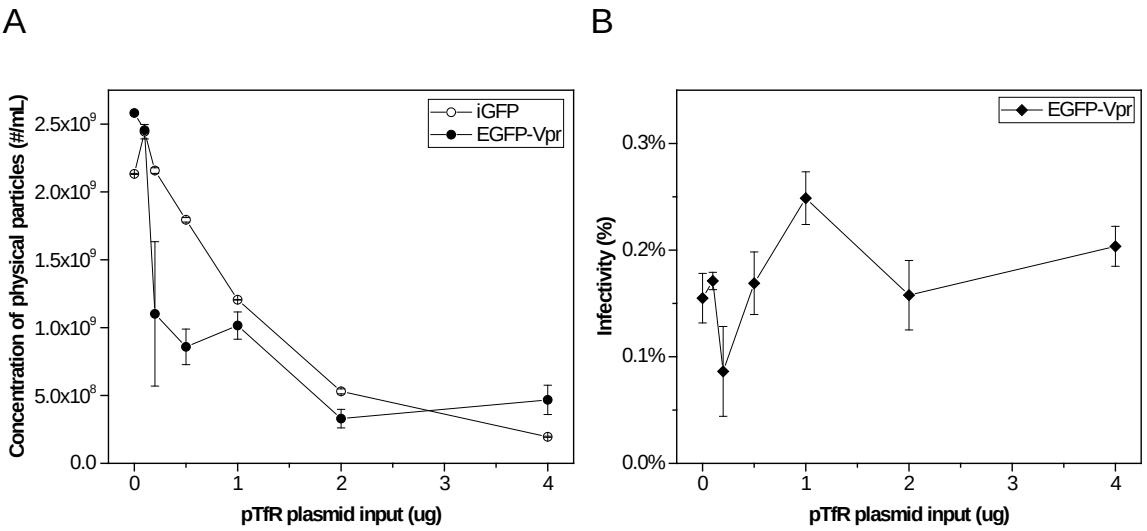

Figure A.3: **Effect of bTfR incorporation on HIV-1 production and infectivity.**
(A) Concentration of physical virion particles as a function of pTfR-AP-IRES-BirA-ER plasmid input, as measured by p24 ELISA. Open circles: iGFP backbone with 1 ug BG505 pEnv; black circles: EGFP-Vpr backbone with 1 ug NL4-3 pEnv. (B) Infectivity of EGFP-Vpr virions as a function of pTfR plasmid input. Titer is measured by TZM-bl cell assay. Infectivity is the percentage of infectious virions in a sample.

tion of infectious virions; thus, the infectivity remains relatively stable (Figure 2B). The similar trend in reduction of virus production with increasing pTfR between the two strains suggests that this may be a fundamental feature of competition between different overexpressed proteins. Indeed, when we equalized the total DNA of two different pTfR conditions by adding carrier DNA (pcDNA3.1), the p24 also equalized. Trypan blue staining of virus-producing cells indicated that 100 uM biotin was not cytotoxic compared to complete media alone, regardless of when it was added.

Dialysis reduces HIV-1 infectivity in a molecular weight cutoff-dependent manner

In order to achieve efficient binding to streptavidin, which would be the bridge between the biotinylated virion and the biotinylated DNA tether, it was necessary to remove unbound biotin from virus preparations while still preserving viral stability.

As a preliminary experiment, we first investigated whether HIV-1 is stable when diluted in PBS or complete media and stored at 4°C. We found that p24 (Figure 3A, left) and infectivity (Figure 3A, right) are fairly stable over 24 hours when HIV-1 is diluted in either PBS (black symbols) or complete media (red symbols) and stored at 4°C. This gave an upper-bound prediction for the time over which HIV-1 infectivity would remain stable. Of note, the samples corresponding to open symbols in Figure 3A were freshly thawed before the assays, so the additional freeze-thaw cycle experienced by the diluted and dialyzed samples may have partly contributed to the apparent decrease in p24 and titer.

We then tested dialysis membranes with several different molecular weight cutoffs, corresponding to varying pore sizes, using infectivity as a readout of HIV-1 stability. First, we tried a 10 kD molecular-weight-cutoff (MWCO) membrane because we wanted to maintain as many proteins as possible that might stabilize the virus. Although infectivity remained stable over 24 hours of dialysis in a 10 kD molecular-weight-cutoff (MWCO) membrane (Figure 3A, right, blue symbols), virometry revealed poor binding of SVD-Alexa 594 to virions, suggesting that free biotin may still be present and competing with bTfR for SVD binding.

However, after 24 hours, the infectivity of virions diluted in PBS (black), diluted in complete media (red), and dialyzed in PBS (blue) all showed a similar trend of decay (Figure 3A, right). This indicated that biotin removal needed to be more efficient in order to maintain HIV-1 stability and that loss of protein through the membrane was not the cause of infectivity decrease. Thus, we tried dialysis membranes with larger pore sizes to more rapidly remove biotin, at the possible expense of losing larger proteins (Figure 3B, C). We also took samples from the same pool to be dialyzed and instead stored them in a tube at 4°C for the entire dialysis time. Consistent with the results for 10 kD MWCO in Figure 3, samples that were dialyzed in 1000 kD MWCO maintained nearly the same infectivity as those stored

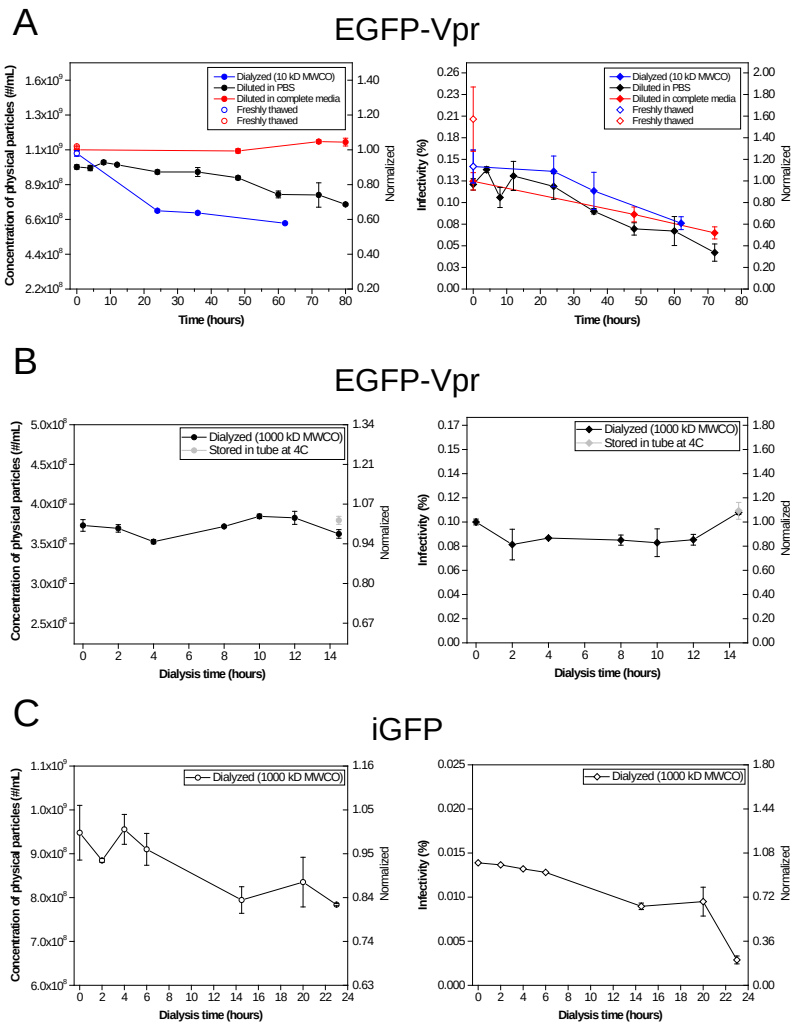

Figure A.4: **Effect of dialysis on HIV-1 stability.**
Left column: concentration of physical virion particles as measured by p24 ELISA. Error bars are standard deviations of duplicate trials. Right column: infectivity of virions. Error bars are propagated uncertainties using standard deviations of p24 and titer. All are plotted as a function of incubation or dialysis time in PBS at 4°C. The right y-axis is normalized by the sample diluted in complete media at 0 h of incubation. (A) EGFP-Vpr virions (with 1 ug NL4-3 pEnv and 1 ug pTfR) as a function of dialysis time in PBS in 10 kD MWCO membrane. Open symbols correspond to the sample of the same color that was diluted or dialyzed, except they were freshly thawed before the p24 and titer assays, rather than being frozen and thawed once more. Infectivity error bars are propagated uncertainties using standard deviations of p24 (N = 2) and titer (N = 3). (B) EGFP-Vpr virions (with 2 ug BG505 pEnv and 4 ug pTfR) as a function of dialysis time in PBS in 1000 kD MWCO membrane. Gray circles represent identical samples to those dialyzed, except they were stored in a tube at 4°C as a control for 14.5 hours. (C) iGFP virions (with 1 ug BG505 pEnv and 2 ug pTfR) as a function of dialysis time in PBS in 1000 kD MWCO membrane.

in a tube. Therefore, at least over these time scales, loss of protein does not seem to significantly affect HIV-1 stability during dialysis in PBS.

p24 and infectivity of EGFP-Vpr virions were stable over 14.5 hours (Figure 3B), but here again, this was insufficient time to adequately remove free biotin from the virus pool. Next, we decided to begin using iGFP virions because 100% of them are labeled with GFP, in contrast to EGFP-Vpr virions, which contain a nontrivial fraction of nonfluorescent particles. iGFP facilitated more confident identification of HIV-1 virions versus debris or microvesicles in the optical tweezers. After iGFP HIV-1 production, we dialyzed the virus pool in a 1000 kD MWCO membrane, allowing it to proceed for 23.5 hours this time for more complete biotin removal. The p24 and infectivity both decayed more rapidly for iGFP virions (Figure 3C) than for EGFP-Vpr virions (Figure 3B), despite using the same MWCO and dialysis conditions. One possible explanation for this is that iGFP virions with 1 ug BG505 pEnv are intrinsically less stable than EGFP-Vpr virions with 2 ug BG505 pEnv. The initial infectivity of iGFP virions also starts about ten-fold lower than that of EGFP-Vpr virions. Although the infectivity had significantly decayed after 23.5 hours of dialysis, we used these virions in virometry (Figure 1B) to test whether free biotin had at least been adequately removed so that we could quantify bTfR incorporation. Indeed, SVD-Alexa 594 binding improved after extended dialysis in a 1000 kD MWCO membrane.

Because dialysis in low MWCO membranes does not remove biotin thoroughly enough, a higher MWCO is required, but the dialysis time must be carefully tuned so as to preserve HIV-1 infectivity.

Biotinylated DNA tethers bind streptavidin

To test whether biotinylated DNA tethers bound streptavidin, we compared the migration in an agarose gel of unbound tethers alongside tethers that had been

incubated with streptavidin and then dialyzed. Indeed, streptavidin binding retarded the migration of the treated tethers compared to the untreated tethers. We further tested the dual labeling by force-extension curves in the optical tweezers using Dig antibody-coated beads and streptavidin-coated beads. These followed the characteristic trend for DNA stretching, indicating the presence of a dual-labeled DNA tether bound to two beads.

Bead-DNA tether-virion complex can be used to manipulate single HIV-1 virions in solution using optical tweezers

By combining biotinylated HIV-1 with dual-labeled DNA tethers and polystyrene beads, it is possible to move the virion around in the flow chamber and deliver it to a living cell immobilized on a micropipette. In Video 1, a Dig antibody-coated polystyrene bead is optically trapped and moved around the flow chamber. A fluorescent particle (virion) can be visualized at a distance from the bead approximately equal to the length of the DNA tether, 8 um. This video is a proof of principle of our technique. However, further optimization of conditions is required to increase reliability of forming the three-body complex before cellular delivery experiments can be performed.

A.4 Discussion

HIV-1 entry into cells is a highly coordinated and dynamic process. Much has been revealed about the coordination of key players during entry, but limitations on techniques have hindered further mechanistic insight. These details may be crucial to entry inhibitor development.

HIV-1 entry has mainly been studied in bulk, with many cells and many virions. Using optical tweezers to study single virus-cell interactions at the single-molecule level is unprecedented. The technique described here allows the possibility

of probing virus-cell interactions via rupture force measurements at varying loading rates, allowing decomposition of multiple simultaneous interactions. By isolating selective steps with inhibitors, one could decipher the physical framework for different HIV-1 entry pathways. This experimental geometry could also reveal the probability of nonspecific interactions versus specific Env-receptor binding at a single-particle level; optical tweezers allow the virion to sample the surface of the cell freely, maintaining physiological conditions.

The technique introduced here has unique potential to uncover the dynamics of Env clustering and cooperative binding. We expect that it will lend insight into essential viral entry mechanisms applicable to other viruses. It is also ideally suited to compare binding of different envelope glycoproteins across different viral strains at high resolution. Because it is able to directly probe the magnitude of interactions, our technique could be adapted to other fundamental questions in biology, such as protein-protein interactions and receptor-mediated membrane fusion.

This study also demonstrates the feasibility of using virometry (Pang et al., 2014) to quantify the copy number of cellular proteins incorporated into the viral membrane at a single-virion, single-molecule level. Although the incorporation of cellular proteins into HIV-1 has been well established, the identity, copy number, and heterogeneity among virions remain elusive due to lack of techniques available. The abundance of certain cellular proteins in HIV-1 may have a functional importance in enhancing cellular interactions, for example (Arhel and Kirchhoff, 2010; Liao et al., 2000; Sato et al., 2008). Thus, it is possible to use virometry to quantify protein copy number and associate this with physical interactions that our technique can directly measure.

A.5 Conclusion

We have described the development of a novel single-molecule technique that can be used to study interactions between single virions and living cells (Figure A.1). This technique opens the door to many previously inaccessible questions about viral entry and more broadly, receptor-ligand interactions in the context of live cells.

Overall, this technique and the principles discovered will potentially elucidate mechanisms of viral entry, reveal fundamental information on the cooperativity of receptor-ligand interactions, and have broad applicability to other systems.

A.6 Acknowledgments

This work was supported by a National Institutes of Health (NIH) Directors New Innovator Award (1DP2OD008693-01, to W.C.), a National Science Foundation CAREER Award (CHE1149670, to W.C.), and a research grant from the March of Dimes Foundation (5-FY10-490, to W.C.). We acknowledge Yuanjie Pang and Michael DeSantis and for writing virometry analysis code in MATLAB. We thank Allen Liu for the pTfR-AP-IRES-BirA-ER plasmid and Margaret Gnegy for the pcDNA3.1(+) vector. We thank Benjamin Chen for the pNL4-3-iGFP2 plasmid. We thank members of the Cheng lab for thoughtful discussions. The following reagents were obtained through the AIDS Research and Reference Reagent Program, Division of AIDS, National Institute of Allergy and Infectious Diseases (NIAID), National Institutes of Health (NIH): pNL4-3 from Dr. Malcolm Martin; pNL4-3.Luc.R-E- from Dr. Nathaniel Landau; pEGFP-Vpr from Dr. Warner C. Greene; TZM-bl cells from Dr. John C. Kappes, Dr. Xiaoyun Wu, and Tranzyme Inc.

A.7 References

Arhel, N., Kirchhoff, F., 2010. Host proteins involved in HIV infection: new therapeutic targets. Biochim. Biophys. Acta 1802, 313-21. doi:10.1016/j.bbadis.2009.12.003

Arthur, L.O., Bess, J.W., Sowder, R.C., Benveniste, R.E., Mann, D.L., Chermann, J.C., Henderson, L.E., 1992. Cellular proteins bound to immunodeficiency viruses: implications for pathogenesis and vaccines. Science 258, 1935-8.

Beckett, D., Kovaleva, E., Schatz, P.J., 1999. A minimal peptide substrate in biotin holoenzyme synthetase-catalyzed biotinylation. Protein Sci. 8, 921-9. doi:10.1110/ps.8.4.921

Bell, G., 1978. Models for the specific adhesion of cells to cells. Science 200, 618-627. doi:10.1126/science.347575

Chen, I., Howarth, M., Lin, W., Ting, A.Y., 2005. Site-specific labeling of cell surface proteins with biophysical probes using biotin ligase 2, 99-104. doi:10.1038/NMETH735

Chojnacki, J., Staudt, T., Glass, B., Bingen, P., Engelhardt, J., Anders, M., Schneider, J., Mller, B., Hell, S.W., Krusslich, H.-G., 2012. Maturation-dependent HIV-1 surface protein redistribution revealed by fluorescence nanoscopy. Science 338, 524-8. doi:10.1126/science.1226359

de Boer, E., Rodriguez, P., Bonte, E., Krijgsveld, J., Katsantoni, E., Heck, A., Grosveld, F., Strouboulis, J., 2003. Efficient biotinylation and single-step purification of tagged transcription factors in mammalian cells and transgenic mice. Proc. Natl. Acad. Sci. U. S. A. 100, 7480-5. doi:10.1073/pnas.1332608100

Dobrowsky, T.M., Zhou, Y., Sun, S.X., Siliciano, R.F., Wirtz, D., 2008. Monitoring early fusion dynamics of human immunodeficiency virus type 1 at single-molecule resolution. J. Virol. 82, 7022-33. doi:10.1128/JVI.00053-08

Frankel, a D., Young, J. a, 1998. HIV-1: fifteen proteins and an RNA. Annu. Rev. Biochem. 67, 1-25. doi:10.1146/annurev.biochem.67.1.1

Gallo SA, Finnegan CM, Viard M, Raviv Y, Dimitrov A, Rawat SS, Puri A, Durell S, B.R., 2003. The HIV Env-mediated fusion reaction. Biochim. Biophys. Acta - Biomembr. 1614, 36-50. doi:10.1016/S0005-2736(03)00161-5

Huang, B.H., Lin, Y., Zhang, Z.L., Zhuan, F., Liu, A.A., Xie, M., Tian, Z.Q., Zhang, Z., Wang, H., Pang, D.W., 2012. Surface labeling of enveloped viruses assisted by host cells. ACS Chem. Biol. 7, 683-688. doi:10.1021/cb2001878

Joo, K. Il, Lei, Y., Lee, C.L., Lo, J., Xie, J., Hamm-Alvarez, S.F., Wang, P., 2008.

Site-specific labeling of enveloped viruses with quantum dots for single virus tracking. ACS Nano 2, 1553-1562. doi:10.1021/nn8002136

Kim, J.H., Song, H., Austin, J.L., Cheng, W., 2013. Optimized Infectivity of the Cell-Free Single-Cycle Human Immunodeficiency Viruses Type 1 (HIV-1) and Its Restriction by Host Cells. PLoS One 8, e67170. doi:10.1371/journal.pone.0067170

Klein, J.S., Bjorkman, P.J., 2010. Few and far between: how HIV may be evading antibody avidity. PLoS Pathog. 6, e1000908. doi:10.1371/journal.ppat.1000908

Liao, Z., Roos, J.W., Hildreth, J.E.K., 2000. Increased Infectivity of HIV Type 1 Particles Bound to Cell Surface and Solid-Phase ICAM-1 and VCAM-1 through Acquired Adhesion Molecules LFA-1 and VLA-4 16, 355-366.

Liu, A.P., Aguet, F., Danuser, G., Schmid, S.L., 2010. Local clustering of transferrin receptors promotes clathrin-coated pit initiation. J. Cell Biol. 191, 1381-93. doi:10.1083/jcb.201008117

Liu, H., Liu, Y., Liu, S., Pang, D.-W., Xiao, G., 2011. Clathrin-mediated endocytosis in living host cells visualized through quantum dot labeling of infectious hematopoietic necrosis virus. J. Virol. 85, 625262. doi:10.1128/JVI.00109-11

Liu, S.L., Zhang, Z.L., Tian, Z.Q., Zhao, H.S., Liu, H., Sun, E.Z., Xiao, G.F., Zhang, W., Wang, H.Z., Pang, D.W., 2012. Effectively and efficiently dissecting the infection of influenza virus by quantum-dot-based single-particle tracking. ACS Nano 6, 141150. doi:10.1021/nn2031353

Nesbeth, D., Williams, S.L., Chan, L., Brain, T., Slater, N.K.H., Farzaneh, F., Darling, D., 2006. Metabolic biotinylation of lentiviral pseudotypes for scalable paramagnetic microparticle-dependent manipulation. Mol. Ther. 13, 814-22. doi:10.1016/j.ymthe.2005.09.016

Orentas, R.J., Hildreth, J.E., 1993. Association of host cell surface adhesion receptors and other membrane proteins with HIV and SIV. AIDS Res. Hum. Retroviruses 9, 1157-65.

Ott, D.E., 2008. Cellular proteins detected in HIV-1. Rev. Med. Virol. 18, 159-175. doi:10.1002/rmv

Pang, Y., Song, H., Cheng, W., 2016. Using optical trap to measure the refractive index of a single animal virus in culture fluid with high precision. Biomed. Opt. Express 7, 1672. doi:10.1364/BOE.7.001672

Pang, Y., Song, H., Kim, J.H., Hou, X., Cheng, W., 2014. Optical trapping of individual human immunodeficiency viruses in culture fluid reveals heterogeneity with single-molecule resolution. Nat. Nanotechnol. 9, 624-630. doi:10.1038/nnano.2014.140

Sato, K., Aoki, J., Misawa, N., Daikoku, E., Sano, K., Tanaka, Y., Koyanagi, Y., 2008. Modulation of human immunodeficiency virus type 1 infectivity through incorporation of tetraspanin proteins. J. Virol. 82, 1021-33. doi:10.1128/JVI.01044-07

Schatz, P.J., 1993. Use of Peptide Libraries to Map the Substrate Specificity of a Peptide-Modifying Enzyme: A 13 Residue Consensus Peptide Specifies Biotinylation in Escherichia coli. Nat. Biotechnol. 11, 1138-1143.

Sougrat, R., Bartesaghi, A., Lifson, J.D., Bennett, A.E., Bess, J.W., Zabransky, D.J., Subramaniam, S., 2007. Electron tomography of the contact between T cells and SIV/HIV-1: implications for viral entry. PLoS Pathog. 3, e63. doi:10.1371/journal.ppat.0030063

REFERENCES

REFERENCES

Akhmanova, A. and Hammer, J. A. Linking molecular motors to membrane cargo. *Current Opinion in Cell Biology*, 22(4):479–487, 2010. doi: 10.1016/j.ceb.2010.04.008.

Albracht, C. D., Rank, K. C., Obrzut, S., Rayment, I., and Gilbert, S. P. Kinesin-2 KIF3AB Exhibits Novel ATPase Characteristics. *Journal of Biological Chemistry*, 289(40):27836–27848, 2014. doi: 10.1074/jbc.M114.583914.

Ally, S., Larson, A. G., Barlan, K., Rice, S. E., and Gelfand, V. I. Opposite-polarity motors activate one another to trigger cargo transport in live cells. *Journal of Cell Biology*, 187(7):1071–1082, 2009. doi: 10.1083/jcb.200908075.

Andreasson, J. O. L., Shastry, S., Hancock, W. O., and Block, S. M. The mechanochemical cycle of mammalian kinesin-2 KIF3A/B under load. *Current Biology*, 25(9):1166–1175, 2015. doi: 10.1016/j.cub.2015.03.013.

Ashkin, A., Dziedzic, J. M., Bjorkholm, J. E., and Chu, S. Observation of a single-beam gradient force optical trap for dielectric particles. *Optics Letters*, 11(5): 288, 1986. doi: 10.1364/OL.11.000288.

Ashkin, A., Schütze, K., Dziedzic, J. M., Euteneuer, U., and Schliwa, M. Force generation of organelle transport measured in vivo by an infrared laser trap. *Nature*, 348(6299):346–8, 1990. doi: 10.1038/348346a0.

Axelrod, D. Cell-substrate Contacts Illuminated by Total-Internal Reflection Fluorescence. *Journal of Cell Biology*, 89(9):141–145, 1981. doi: 10.1083/jcb.89.1.141.

Axelrod, D. Total internal reflection fluorescence microscopy. *Methods in Cell Biology*, 30:245–70, 1989. doi: http://dx.doi.org/10.1016/S0091-679X(08)60982-6.

Baboolal, T. G., Sakamoto, T., Forgacs, E., White, H. D., Jackson, S. M., Takagi, Y., Farrow, R. E., Molloy, J. E., Knight, P. J., Sellers, J. R., and Peckham, M. The SAH domain extends the functional length of the myosin lever. *Proceedings of the National Academy of Sciences*, 106(52):22193–22198, 2009. doi: 10.1073/pnas.0909851106.

Barak, P., Rai, A., Rai, P., and Mallik, R. Quantitative optical trapping on single organelles in cell extract. *Nature Methods*, 10(1):68–70, 2013. doi: 10.1038/nmeth.2287.

Bartsch, T. F., Longoria, R. A., Florin, E. L., and Shubeita, G. T. Lipid droplets purified from drosophila embryos as an endogenous handle for precise motor transport measurements. *Biophysical Journal*, 105(5):1182–1191, 2013. doi: 10.1016/j.bpj.2013.07.026.

Belyy, V., Schlager, M. A., Foster, H., Reimer, A. E., Carter, A. P., and Yildiz, A. The mammalian dynein-dynactin complex is a strong opponent to kinesin in a tug-of-war competition. *Nature Cell Biology*, 18(9):1018–1024, 2016. doi: 10.1038/ncb3393.

Berliner, E., Mahtani, H. K., Karki, S., Chu, L. F., Cronan, J. E., and Gelles, J. Microtubule Movement by a Biotinated Kinesin Bound to a Streptavidin-coated Surface. *Journal of Biological Chemistry*, 269(11):8610–8615, 1994.

Berliner, E., Young, E. C., Anderson, K., Mahtani, H. K., and Gelles, J. Failure of a single-headed kinesin to track parallel to microtubule protofilaments. *Nature*, 373:718–721, 1995.

Bhabha, G., Johnson, G. T., Schroeder, C. M., and Vale, R. D. How Dynein Moves Along Microtubules. *Trends in Biochemical Sciences*, 41(1):94–105, 2016. doi: 10.1016/j.tibs.2015.11.004.

Bieling, P., Telley, I. A., Piehler, J., and Surrey, T. Processive kinesins require loose mechanical coupling for efficient collective motility. *EMBO reports*, 9(11): 1121–7, 2008. doi: 10.1038/embor.2008.169.

Blair, M. A., Ma, S., and Hedera, P. Mutation in KIF5A can also cause adult-onset hereditary spastic paraplegia. *Neurogenetics*, 7(1):47–50, 2006. doi: 10.1007/s10048-005-0027-8.

Blehm, B. H., Schroer, T. A., Trybus, K. M., Chemla, Y. R., Selvin, P. R., Blehm, B. H., Schroer, T. A., Trybus, K. M., Chemla, Y. R., and Selvin, P. R. In vivo optical trapping indicates kinesin's stall force is reduced by dynein during intracellular transport. *Proceedings of the National Academy of Sciences*, 110 (9):3381–3386, 2013. doi: 10.1073/pnas.1308350110.

Block, S. M., Goldstein, L. S. B., and Schnapp, B. J. Bead movement by single kinesin molecules studied with optical tweezers. *Nature*, 348(6299):348–352, 1990. doi: 10.1038/348348a0.

Brawley, C. M. and Rock, R. S. Unconventional myosin traffic in cells reveals a selective actin cytoskeleton. *Proceedings of the National Academy of Sciences of the United States of America*, 106(24):9685–9690, 2009. doi: 10.1073/pnas.0810451106.

Brownhill, K., Wood, L., and Allan, V. Molecular motors and the Golgi complex: Staying put and moving through. *Seminars in Cell and Developmental Biology*, 20(7):784–792, 2009. doi: 10.1016/j.semcdb.2009.03.019.

Brunnbauer, M., Dombi, R., Ho, T. H., Schliwa, M., Rief, M., and Ökten, Z. Torque Generation of Kinesin Motors Is Governed by the Stability of the Neck Domain. *Molecular Cell*, 46(2):147–158, 2012. doi: 10.1016/j.molcel.2012.04.005.

Burkhard, P., Ivaninskii, S., and Lustig, A. Improving coiled-coil stability by optimizing ionic interactions. *Journal of Molecular Biology*, 318(3):901–910, 2002. doi: 10.1016/S0022-2836(02)00114-6.

Bustamante, C., Cheng, W., Mejia, Y. X., and Meija, Y. X. Revisiting the central dogma one molecule at a time. *Cell*, 144(4):480–97, feb 2011. doi: 10.1016/j.cell.2011.01.033.

Cai, D., Verhey, K. J., and Meyhöfer, E. Tracking single Kinesin molecules in the cytoplasm of mammalian cells. *Biophysical Journal*, 92(12):4137–4144, 2007. doi: 10.1529/biophysj.106.100206.

Cai, D., McEwen, D. P., Martens, J. R., Meyhofer, E., and Verhey, K. J. Single molecule imaging reveals differences in microtubule track selection between kinesin motors. *PLoS Biology*, 7(10), 2009. doi: 10.1371/journal.pbio.1000216.

Case, R. B., Pierce, D. W., Hom-Booher, N., Hart, C. L., and Vale, R. D. The directional preference of kinesin motors is specified by an element outside of the motor catalytic domain. *Cell*, 90(5):959–966, 1997. doi: 10.1016/S0092-8674(00)80360-8.

Chowdhury, D. Stochastic mechano-chemical kinetics of molecular motors: A multidisciplinary enterprise from a physicist's perspective. *Physics Reports*, 529(1):1–197, 2013. doi: 10.1016/j.physrep.2013.03.005.

Clackson, T., Yang, W., Rozamus, L. W., Hatada, M., Amara, J. F., Rollins, C. T., Stevenson, L. F., Magari, S. R., Wood, S. A., Courage, N. L., Lu, X., Cerasoli, F., Gilman, M., and Holt, D. A. Redesigning an FKBP-ligand interface to generate chemical dimerizers with novel specificity. *Proceedings of the National Academy of Sciences*, 95(18):10437–10442, 1998. doi: 10.1073/pnas.95.18.10437.

Cole, D. G. Kinesin-II , the heteromeric kinesin. *Cell. Mol. Life Sci.*, 56:217–226, 1999.

Cole, D. G., Cande, W. Z., Baskin, R. J., Skoufias, D. a., Hogan, C. J., and Scholey, J. M. Isolation of a sea urchin egg kinesin-related protein using peptide antibodies. *Journal of Cell Science*, 101:291–301, 1992.

Cole, D. G., Chinn, S. W., Wedaman, K. P., Hall, K., Vuong, T., and Scholey, J. M. Novel heterotrimeric kinesin-related protein purified from sea urchin eggs. *Nature*, 366(6452):268–270, 1993. doi: 10.1038/366268a0.

Crimella, C., Baschirotto, C., Arnoldi, A., Tonelli, A., Tenderini, E., Airoldi, G., Martinuzzi, A., Trabacca, A., Losito, L., Scarlato, M., Benedetti, S., Scarpini, E., Spinicci, G., Bresolin, N., and Bassi, M. T. Mutations in the motor and stalk domains of KIF5A in spastic paraplegia type 10 and in axonal Charcot-Marie-Tooth type 2. *Clinical Genetics*, 82(2):157–164, 2012. doi: 10.1111/j.1399-0004.2011.01717.x.

Cross, R. A. The kinetic mechanism of kinesin. *TRENDS in Biochemical Sciences*, 29(6):301–309, 2004. doi: 10.1016/j.tibs.2004.04.010.

DeBoer, S. R., You, Y. M., Szodorai, A., Kaminska, A., Pigino, G., Nwabuisi, E., Wang, B., Estrada-Hernandez, T., Kins, S., Brady, S. T., and Morfini, G. Conventional kinesin holoenzymes are composed of heavy and light chain homodimers. *Biochemistry*, 47(15):4535–4543, 2008. doi: 10.1021/bi702445j.

Delevoye, C., Miserey-Lenkei, S., Montagnac, G., Gilles-Marsens, F., Paul-Gilloteaux, P., Giordano, F., Waharte, F., Marks, M. S., Goud, B., and Raposo, G. Recycling endosome tubule morphogenesis from sorting endosomes requires the kinesin motor KIF13A. *Cell Reports*, 6(3):445–454, 2014. doi: 10.1016/j.celrep.2014.01.002.

DeRose, R., Miyamoto, T., and Inoue, T. Manipulating signaling at will: Chemically-inducible dimerization (CID) techniques resolve problems in cell biology. *Pflugers Archiv European Journal of Physiology*, 465(3):409–417, 2013. doi: 10.1007/s00424-012-1208-6.

Derr, N. D., Goodman, B. S., Jungmann, R., Leschziner, A. E., Shih, W. M., and Reck-Peterson, S. L. Tug-of-War in Motor Protein Ensembles Revealed with a Programmable DNA Origami Scaffold. *Science*, 338(November 2):662–666, 2012. doi: 10.1126/science.1226734.

Dunn, B. D., Sakamoto, T., Hong, M. S. S., Sellers, J. R., and Takizawa, P. A. Myo4p is a monomeric myosin with motility uniquely adapted to transport mRNA. *Journal of Cell Biology*, 178(7):1193–1206, 2007. doi: 10.1083/jcb.200707080.

Efremov, A. K., Radhakrishnan, A., Tsao, D. S., Bookwalter, C. S., Trybus, K. M., and Diehl, M. R. Delineating cooperative responses of processive motors in living cells. *Proceedings of the National Academy of Sciences of the United States of America*, 111(3):E334–43, 2014. doi: 10.1073/pnas.1313569111.

Egea, G. and Serra-Peinado, C. Golgi apparatus: Finally mechanics comes to play in the secretory pathway. *Current Biology*, 24(16):R741–R743, 2014. doi: 10.1016/j.cub.2014.07.002.

Encalada, S. E., Szpankowski, L., Xia, C. H., and Goldstein, L. S. B. Stable kinesin and dynein assemblies drive the axonal transport of mammalian prion protein vesicles. *Cell*, 144(4):551–565, 2011. doi: 10.1016/j.cell.2011.01.021.

Endres, N. F., Yoshioka, C., Milligan, R. A., and Vale, R. D. A lever-arm rotation drives motility of the minus-end-directed kinesin Ncd. *Nature*, 439(7078):875–878, 2006. doi: 10.1038/nature04320.

Engelke, M. F., Winding, M., Yue, Y., Shastry, S., Teloni, F., Reddy, S., Blasius, T. L., Soppina, P., Hancock, W. O., Gelfand, V. I., and Kristen, J. Engineered kinesin motor proteins amenable to small molecule inhibition. *Nature Communications*, 7:1–12, 2016. doi: 10.1038/ncomms11159.

Fagarasanu, A., Mast, F. D., Knoblach, B., Jin, Y., Brunner, M. J., Logan, M. R., Glover, J. N. M., Eitzen, G. A., Aitchison, J. D., Weisman, L. S., and Rachubinski, R. A. Myosin-driven peroxisome partitioning in S. cerevisiae. *Journal of Cell Biology*, 186(4):541–554, 2009. doi: 10.1083/jcb.200904050.

Feng, Q., Mickolajczyk, K. J., Chen, G.-Y., and Hancock, W. O. Motor Reattachment Kinetics Play a Dominant Role in Multimotor-Driven Cargo Transport. *Biophysical Journal*, 114(2):400–409, 2018. doi: 10.1016/j.bpj.2017.11.016.

Fletcher, D. A. and Mullins, R. D. Cell mechanics and the cytoskeleton. *Nature*, 463 (7280):485–492, 2010. doi: 10.1038/nature08908.

Fulton, A. B. How crowded is the cytoplasm? *Cell*, 30(2):345–347, 1982. doi: 10.1016/0092-8674(82)90231-8.

Funatsu, T., Harada, Y., Tokunaga, M., Saito, K., and Yanagida, T. Imaging of single fluorescent molecules and individual ATP turnovers by single myosin molecules in aqueous solution. *Nature*, 374:555–559, 1995. doi: 10.1038/374555a0.

Furuta, K., Furuta, A., Toyoshima, Y. Y., Amino, M., Oiwa, K., and Kojima, H. Measuring collective transport by defined numbers of processive and nonprocessive kinesin motors. *Proceedings of the National Academy of Sciences of the United States of America*, 110(2):501–6, 2013. doi: 10.1073/pnas.1201390110.

Gilbert, S. P., Guzik-Lendrum, S., and Rayment, I. Kinesin-2 motors: Kinetics and biophysics. *Journal of Biological Chemistry*, 293(12):4510–4518, 2018. doi: 10.1074/jbc.R117.001324.

Grover, R., Fischer, J., Schwarz, F. W., Walter, W. J., Schwille, P., and Diez, S. Transport efficiency of membrane-anchored kinesin-1 motors depends on motor density and diffusivity. *Proceedings of the National Academy of Sciences*, 113 (46):E7185–E7193, 2016. doi: 10.1073/pnas.1611398113.

Guet, D., Mandal, K., Pinot, M., Hoffmann, J., Abidine, Y., Sigaut, W., Bardin, S., Schauer, K., Goud, B., and Manneville, J. B. Mechanical role of actin dynamics in the rheology of the Golgi complex and in Golgi-associated trafficking events. *Current Biology*, 24(15):1700–1711, 2014. doi: 10.1016/j.cub.2014.06.048.

Hackney, D. D. Evidence for alternating head catalysis by kinesin during microtubule-stimulated ATP hydrolysis. *Proc Natl Acad Sci U S A*, 91(15):6865–6869, 1994. doi: 10.1073/pnas.91.15.6865.

Hackney, D. D. The kinetic cycles of myosin, kinesin, and dynein. *Annual review of physiology*, 58:731–50, 1996.

Hakimi, M. A., Speicher, D. W., and Shiekhattar, R. The motor protein kinesin-1 links neurofibromin and merlin in a common cellular pathway of neurofibromatosis. *Journal of Biological Chemistry*, 277(40):36909–36912, 2002. doi: 10.1074/jbc.C200434200.

Hammond, J. W., Cai, D., Blasius, T. L., Li, Z., Jiang, Y., Jih, G. T., Meyhofer, E., and Verhey, K. J. Mammalian Kinesin-3 motors are dimeric in vivo and move by processive motility upon release of autoinhibition. *PLoS Biology*, 7 (3):0650–0663, 2009. doi: 10.1371/journal.pbio.1000072.

Hammond, J. W., Blasius, T. L., Soppina, V., Cai, D., and Verhey, K. J. Autoinhibition of the kinesin-2 motor KIF17 via dual intramolecular mechanisms. *Journal of Cell Biology*, 189(6):1013–1025, 2010. doi: 10.1083/jcb.201001057.

Hancock, W. O. and Howard, J. Processivity of the Motor Protein Kinesin Requires Two Heads. *Journal of Cell Biology*, 140(6):1395–1406, 1998.

Hariadi, R. F., Cale, M., and Sivaramakrishnan, S. Myosin lever arm directs collective motion on cellular actin network. *Proceedings of the National Academy of Sciences*, 111(11):4091–4096, 2014. doi: 10.1073/pnas.1315923111.

Hariharan, V. and Hancock, W. O. Insights into the Mechanical Properties of the Kinesin Neck Linker Domain from Sequence Analysis and Molecular Dynamics Simulations. *Cellular and molecular bioengineering*, 2(2):177–189, 2009. doi: 10.1007/s12195-009-0059-5.

Hartman, M. A. and Spudich, J. A. The myosin superfamily at a glance. *Journal of Cell Science*, 125(7):1627–1632, 2012. doi: 10.1242/jcs.094300.

Hendricks, A. G., Perlson, E., Ross, J. L., Schroeder, H. W., Tokito, M., and Holzbaur, E. L. F. Motor Coordination via a Tug-of-War Mechanism Drives Bidirectional Vesicle Transport. *Current Biology*, 20(8):697–702, 2010. doi: 10.1016/j.cub.2010.02.058.

Hendricks, A. G., Holzbaur, E. L. F., and Goldman, Y. E. Force measurements on cargoes in living cells reveal collective dynamics of microtubule motors. *Proceedings of the National Academy of Sciences of the United States of America*, 109(45):18447–52, 2012. doi: 10.1073/pnas.1215462109.

Hendricks, A. G., Goldman, Y. E., and Holzbaur, E. L. F. *Reconstituting the motility of isolated intracellular cargoes*, volume 540. Elsevier Inc., 1 edition, 2014.

ISBN 9780123979247. doi: 10.1016/B978-0-12-397924-7.00014-5. URL http://dx.doi.org/10.1016/B978-0-12-397924-7.00014-5.

Hess, H., Bachand, G. D., and Vogel, V. Powering Nanodevices with Biomolecular Motors. *Chemistry - A European Journal*, 10(9):2110–2116, 2004. doi: 10.1002/chem.200305712.

Hirokawa, N., Sato-Yoshitake, R., Kobayashi, N., Pfister, K. K., Bloom, G. S., and Brady, S. T. Kinesin associates with anterogradely transported membranous organelles in vivo. *Journal of Cell Biology*, 114(2):295–302, 1991. doi: 10.1083/jcb.114.2.295.

Hirokawa, N. and Noda, Y. Intracellular Transport and Kinesin Superfamily Proteins : Structure Dynamics and Function. *Physiology Review*, 88:1089–1118, 2008. doi: 10.1152/physrev.00023.2007.

Hirokawa, N., Noda, Y., Tanaka, Y., and Niwa, S. Kinesin superfamily motor proteins and intracellular transport. *Nature Reviews Molecular Cell Biology*, 10:682–696, 2009. doi: 10.1038/nrm2774.

Hirokawa, N., Niwa, S., and Tanaka, Y. Molecular motors in neurons: Transport mechanisms and roles in brain function, development, and disease. *Neuron*, 68(4):610–638, 2010. doi: 10.1016/j.neuron.2010.09.039.

Hoepfner, S., Severin, F., Cabezas, A., Habermann, B., Runge, A., Gillooly, D., Stenmark, H., and Zerial, M. Modulation of receptor recycling and degradation by the endosomal kinesin KIF16B. *Cell*, 121(3):437–450, 2005. doi: 10.1016/j.cell.2005.02.017.

Holton, J. and Alber, T. Automated protein crystal structure determination using ELVES. *Proceedings of the National Academy of Sciences of the United States of America*, 101(6):1537–1542, 2004. doi: 10.1073/pnas.0306241101.

Holzbaur, E. L. and Goldman, Y. E. Coordination of molecular motors: from in vitro assays to intracellular dynamics. *Current Opinion in Cell Biology*, 22(1):4–13, 2010. doi: 10.1016/j.ceb.2009.12.014.

Horiuchi, D., Collins, C. A., Bhat, P., Barkus, R. V., DiAntonio, A., and Saxton, W. M. Control of a Kinesin-Cargo Linkage Mechanism by JNK Pathway Kinases. *Current Biology*, 17(15):1313–1317, 2007. doi: 10.1016/j.cub.2007.06.062.

Howard, J., Hudspeth, A. J., and Vale, R. D. Movement of microtubules by single kinesin molecules. *Nature*, 342(6246):154–158, 1989. doi: 10.1038/342154a0.

Hwang, W., Lang, M. J., and Karplus, M. Force Generation in Kinesin Hinges on Cover-Neck Bundle Formation. *Structure*, 16:62–71, 2008. doi: 10.1016/j.str.2007.11.008.

Infante, C., Ramos-morales, F., Fedriani, C., Bornens, M., and Rios, R. M. GMAP-210, A Cis-Golgi Network-associated Protein, Is a Minus End Microtubule-binding Protein. *Journal of Cell Biology*, 145(1):83–98, 1999.

Inoue, Y., Toyoshima, Y. Y., Hikikoshi Iwane, A., Morimoto, S., Higuchi, H., and Yanagida, T. Movements of truncated kinesin fragments with a short or an artificial flexible neck. *Proc. Natl. Acad. Sci. USA*, 94(July):7275–7280, 1997.

Jamison, D. K., Driver, J. W., Rogers, A. R., Constantinou, P. E., and Diehl, M. R. Two kinesins transport cargo primarily via the action of one motor: Implications for intracellular transport. *Biophysical Journal*, 99(9):2967–2977, 2010. doi: 10.1016/j.bpj.2010.08.025.

Jamison, D. K., Driver, J. W., and Diehl, M. R. Cooperative responses of multiple kinesins to variable and constant loads. *Journal of Biological Chemistry*, 287 (5):3357–3365, 2012. doi: 10.1074/jbc.M111.296582.

Jeppesen, G. M. and Hoerber, J. K. H. The mechanical properties of kinesin-1: a holistic approach. *Biochemical Society transactions*, 40(2):438–43, 2012. doi: 10.1042/BST20110768.

Jonsson, E., Yamada, M., Vale, R. D., and Goshima, G. Clustering of a kinesin-14 motor enables processive retrograde microtubule-based transport in plants. *Nature Plants*, 1(7):1–7, 2015. doi: 10.1038/nplants.2015.87.

Kamal, A., Stokin, G. B., Yang, Z., Xia, C. H., and Goldstein, L. S. Axonal transport of amyloid precursor protein is mediated by direct binding to the kinesin light chain subunit of kinesin-1. *Neuron*, 28:449–459, 2000.

Kamei, T., Kakuta, S., and Higuchi, H. Biased Binding of Single Molecules and Continuous Movement of Multiple Molecules of Truncated Single-Headed Kinesin. *Biophysical Journal*, 88(3):2068–2077, 2005. doi: 10.1529/biophysj.104.049759.

Kamm, C., Boston, H., Hewett, J., Wilbur, J., Corey, D. P., Hanson, P. I., Ramesh, V., and Breakefield, X. O. The Early Onset Dystonia Protein TorsinA Interacts with Kinesin Light Chain 1. *Journal of Biological Chemistry*, 279(19): 19882–19892, 2004. doi: 10.1074/jbc.M401332200.

Kammerer, R. A., Kostrewa, D., Progias, P., Honnappa, S., Avila, D., Lustig, A., Winkler, F. K., Pieters, J., and Steinmetz, M. O. A conserved trimerization motif controls the topology of short coiled coils. *Proceedings of the National Academy of Sciences*, 102(39):13891–13896, 2005. doi: 10.1073/pnas.0502390102.

Kanai, Y., Okada, Y., Tanaka, Y., Harada, A., Terada, S., and Hirokawa, N. KIF5C, a Novel Neuronal Kinesin Enriched in Motor Neurons. *J. Neurosci.*, 20(17): 6374–6384, 2000. doi: 10.1016/S0168-0102(00)81149-9.

Kapitein, L. C., Schlager, M. A., Kuijpers, M., Wulf, P. S., van Spronsen, M., MacKintosh, F. C., and Hoogenraad, C. C. Mixed Microtubules Steer Dynein-Driven Cargo Transport into Dendrites. *Current Biology*, 20(4):290–299, 2010a. doi: 10.1016/j.cub.2009.12.052.

Kapitein, L. C., Schlager, M. a., Van Der Zwan, W. a., Wulf, P. S., Keijzer, N., and Hoogenraad, C. C. Probing intracellular motor protein activity using an inducible cargo trafficking assay. *Biophysical Journal*, 99(7):2143–2152, 2010b. doi: 10.1016/j.bpj.2010.07.055.

Kiyokawa, T., Kanaori, K., Tajima, K., Kawaguchi, M., Mizuno, T., Oku, J. I., and Tanaka, T. Selective formation of AAB- and ABC-type heterotrimeric α-helical coiled coils. *Chemistry - A European Journal*, 10(14):3548–3554, 2004. doi: 10.1002/chem.200305729.

Klopfenstein, D. R., Tomishige, M., Stuurman, N., and Vale, R. D. Role of phosphatidylinositol(4,5)bisphosphate organization in membrane transport by the Unc104 kinesin motor. *Cell*, 109(3):347–358, 2002. doi: 10.1016/S0092-8674(02)00708-0.

Knight, A. E. and Molloy, J. E. Coupling ATP hydrolysis to mechanical work. *Nature Cell Biology*, 1(4):E87–E89, 1999. doi: 10.1038/12083.

Knight, P. J., Thirumurugan, K., Xu, Y., Wang, F., Kalverda, A. P., Stafford, W. F., Sellers, J. R., and Peckham, M. The predicted coiled-coil domain of myosin 10 forms a novel elongated domain that lengthens the head. *Journal of Biological Chemistry*, 280(41):34702–34708, 2005. doi: 10.1074/jbc.M504887200.

Kron, S. J. and Spudich, J. a. Fluorescent actin filaments move on myosin fixed to a glass surface. *Proceedings of the National Academy of Sciences of the United States of America*, 83(17):6272–6276, 1986. doi: 10.1073/pnas.83.17.6272.

Kull, F. J., Sablin, E. P., Lau, R., Fletterick, R. J., and Vale, R. D. Crystal structure of the kinesin motor domain reveals a structural similarity to myosin., 1996. ISSN 0028-0836.

Kull, F. J., Vale, R. D., and Fletterick, R. J. The case for a common ancestor: Kinesin and myosin motor proteins and G proteins. *Journal of Muscle Research and Cell Motility*, 19(8):877–886, 1998. doi: 10.1023/A:1005489907021.

Kural, C., Kim, H., Syed, S., Goshima, G., Gelfand, V. I., and Selvin, P. R. Kinesin and dynein move a peroxisome in vivo: a tug-of-war or coordinated movement? *Science (New York, N.Y.)*, 308(5727):1469–72, 2005. doi: 10.1126/science.1108408.

Laib, J. A., Marin, J. A., Bloodgood, R. A., and Guilford, W. H. The reciprocal coordination and mechanics of molecular motors in living cells. *Proceedings of the National Academy of Sciences of the United States of America*, 106(9):3190–5, 2009. doi: 10.1073/pnas.0809849106.

Lakadamyali, M. Navigating the cell: how motors overcome roadblocks and traffic jams to efficiently transport cargo. *Physical chemistry chemical physics : PCCP*, 16(13):5907–16, 2014. doi: 10.1039/c3cp55271c.

Landry, M. P., McCall, P. M., Qi, Z., and Chemla, Y. R. Characterization of photoactivated singlet oxygen damage in single-molecule optical trap experiments. *Biophysical Journal*, 97(8):2128–2136, 2009. doi: 10.1016/j.bpj.2009.07.048.

Leibler, S. and Huse, D. A. Porters versus rowers: A unified stochastic model of motor proteins. *Journal of Cell Biology*, 121(6):1357–1368, 1993. doi: 10.1083/jcb.121.6.1357.

Leidel, C., Longoria, R. A., Gutierrez, F. M., and Shubeita, G. T. Measuring Molecular Motor Forces In Vivo: Implications for Tug-of-War Models of Bidirectional Transport. *Biophysical Journal*, 103(3):492–500, 2012. doi: 10.1016/j.bpj.2012.06.038.

Li, R. and Gundersen, G. G. Beyond polymer polarity: How the cytoskeleton builds a polarized cell. *Nature Reviews Molecular Cell Biology*, 9(11):860–873, 2008. doi: 10.1038/nrm2522.

Li, X. and DiFiglia, M. The recycling endosome and its role in neurological disorders. *Progress in Neurobiology*, 97(2):127–141, 2012. doi: 10.1016/j.pneurobio.2011.10.002.

Lin, F., Hiesberger, T., Cordes, K., Sinclair, A. M., Goldstein, L. S. B., Somlo, S., and Igarashi, P. Kidney-specific inactivation of the KIF3A subunit of kinesin-II inhibits renal ciliogenesis and produces polycystic kidney disease. *Proceedings of the National Academy of Sciences*, 100(9):5286–5291, 2003. doi: 10.1073/pnas.0836980100.

Lindman, S., Johansson, I., Thulin, E., and Linse, S. Green fluorescence induced by EF-hand assembly in a split GFP system. *Protein Science*, 18(6):1221–1229, 2009. doi: 10.1002/pro.131.

Litowski, J. R. and Hodges, R. S. Designing heterodimeric two-stranded α-helical coiled-coils. Effects of hydrophobicity and α-helical propensity on protein folding, stability, and specificity. *Journal of Biological Chemistry*, 277(40):37272–37279, 2002. doi: 10.1074/jbc.M204257200.

Mallik, R., Carter, B. C., Lex, S. A., King, S. J., and Gross, S. P. Cytoplasmic dynein functions as a gear in response to load. *Nature*, 427(6975):649–652, 2004. doi: 10.1038/nature02293.

Marszalek, J. R., Ruiz-Lozano, P., Roberts, E., Chien, K. R., and Goldstein, L. S. B. Situs inversus and embryonic ciliary morphogenesis defects in mouse mutants lacking the KIF3A subunit of kinesin-II. *Proceedings of the National Academy of Sciences of the United States of America*, 96(9):5043–5048, 1999. doi: Doi10.1073/Pnas.96.9.5043.

McGuire, J. R., Rong, J., Li, S. H., and Li, X. J. Interaction of Huntingtin-associated protein-1 with kinesin light chain: Implications in intracellular trafficking in neurons. *Journal of Biological Chemistry*, 281(6):3552–3559, 2006. doi: 10.1074/jbc.M509806200.

Mehta, A. D., Finer, J. T., and Spudich, J. A. Chapter 4 Reflections of a Lucid Dreamer: Optical Trap Design Considerations. *Methods in Cell Biology*, 55 (C):47–69, 1997. doi: 10.1016/S0091-679X(08)60402-1.

meng Fu, M. and Holzbaur, E. L. F. Integrated regulation of motor-driven organelle transport by scaffolding proteins. *Trends in Cell Biology*, 24(10):564–574, 2014. doi: 10.1016/j.tcb.2014.05.002.

Milic, B., Andreasson, J. O. L., Hancock, W. O., and Block, S. M. Kinesin processivity is gated by phosphate release. *Proceedings of the National Academy of Sciences*, 111(39):14136–14140, 2014. doi: 10.1073/pnas.1410943111.

Milic, B., Andreasson, J. O. L., Hogan, D. W., and Block, S. M. Intraflagellar transport velocity is governed by the number of active KIF17 and KIF3AB motors and their motility properties under load. *Proceedings of the National Academy of Sciences*, page 201708157, 2017. doi: 10.1073/pnas.1708157114.

Miller, R. H. and Lasek, R. I. Cross-bridges mediate anterograde and retrograde vesicle transport along microtubules in squid axoplasm. *Journal of Cell Biology*, 101(6):2181–2193, 1985. doi: 10.1083/jcb.101.6.2181.

Miyata, H., Yoshikawa, H., Hakozaki, H., Suzuki, N., Furuno, T., Ikegami, a., Kinosita, K., Nishizaka, T., and Ishiwata, S. Mechanical measurements of single actomyosin motor force. *Biophysical journal*, 68(4 Suppl):286S–289S; discussion 289S–290S, 1995.

Molloy, J. E., Burns, J. E., Kendrick-Jones, B., Tregear, R. T., and White, D. C. S. Movement and force produced by a single myosin head, 1995. ISSN 00280836.

Mukherjea, M., Ali, M. Y., Kikuti, C., Safer, D., Yang, Z., Sirkia, H., Ropars, V., Houdusse, A., Warshaw, D. M., and Sweeney, H. L. Myosin VI Must Dimerize and Deploy Its Unusual Lever Arm in Order to Perform Its Cellular Roles. *Cell Reports*, 8(5):1522–1532,, 2014. doi: 10.1016/j.celrep.2014.07.041.

Nakajima, K., Yin, X., Takei, Y., Seog, D. H., Homma, N., and Hirokawa, N. Molecular Motor KIF5A Is Essential for GABAA Receptor Transport, and KIF5A Deletion Causes Epilepsy. *Neuron*, 76(5):945–961, 2012. doi: 10.1016/j.neuron.2012.10.012.

Nambiar, R., McConnell, R. E., and Tyska, M. J. Control of cell membrane tension by myosin-I. *Proceedings of the National Academy of Sciences*, 106(29):11972–11977, 2009. doi: 10.1073/pnas.0901641106.

Nelson, S. R., Trybus, K. M., and Warshaw, D. M. Motor coupling through lipid membranes enhances transport velocities for ensembles of myosin Va. *Proceedings of the National Academy of Sciences*, 111(38):E3986–E3995, 2014. doi: 10.1073/pnas.1406535111.

Neuman, K. C., Chadd, E. H., Liou, G. F., Bergman, K., and Block, S. M. Characterization of photodamage to Escherichia coli in optical traps. *Biophysical Journal*, 77(5):2856–2863, 1999. doi: 10.1016/S0006-3495(99)77117-1.

Nguyen, M. M., McCracken, C. J., Milner, E. S., Goetschius, D. J., Weiner, A. T., Long, M. K., Michael, N. L., Munro, S., and Rolls, M. M. γ-tubulin controls neuronal microtubule polarity independently of Golgi outposts. *Molecular biology of the cell*, 25(13):2039–50, 2014. doi: 10.1091/mbc.E13-09-0515.

Norris, S. R., Soppina, V., Dizaji, A. S., Schimert, K. I., Sept, D., Cai, D., Sivaramakrishnan, S., and Verhey, K. J. A method for multiprotein assembly in cells reveals independent action of kinesins in complex. *Journal of Cell Biology*, 207 (3):393–406, 2014. doi: 10.1083/jcb.201407086.

Norris, S. R., Núñez, M. F., and Verhey, K. J. Influence of fluorescent tag on the motility properties of kinesin-1 in single-molecule assays. *Biophysical Journal*, 108(5):1133–1143, 2015. doi: 10.1016/j.bpj.2015.01.031.

Okada, Y. and Hirokawa, N. A processive single-headed motor: kinesin superfamily protein KIF1A. *Science (New York, N.Y.)*, 283(1999):1152–1157, 1999. doi: 10.1126/science.283.5405.1152.

Okada, Y. and Hirokawa, N. Mechanism of the single-headed processivity: diffusional anchoring between the K-loop of kinesin and the C terminus of tubulin. *Proceedings of the National Academy of Sciences*, 97(2):640–5, 2000. doi: 10.1073/pnas.97.2.640.

Okada, Y., Yamazaki, H., Sekine-Aizawa, Y., and Hirokawa, N. The neuron-specific kinesin superfamily protein KIF1A is a unique monomeric motor for anterograde axonal transport of synaptic vesicle precursors. *Cell*, 81(5):769–780, 1995. doi: 10.1016/0092-8674(95)90538-3.

Okada, Y., Higuchi, H., and Hirokawa, N. Processivity of the single-headed kinesin KIF1A through biased binding to tubulin. *Nature*, 424(May):574–577, 2003. doi: 10.1038/nature01804.

Otsuka, A. J., Jeyaprakash, A., García-Añoveros, J., Tang, L. Z., Fisk, G., Hartshorne, T., Franco, R., and Bornt, T. The C. elegans unc-104 gene encodes a putative kinesin heavy chain-like protein. *Neuron*, 6(1):113–122, 1991. doi: 10.1016/0896-6273(91)90126-K.

Peckham, M. Coiled coils and SAH domains in cytoskeletal molecular motors. *Biochemical Society Transactions*, 39(5):1142–1148, 2011. doi: 10.1042/BST0391142.

Phichith, D., Travaglia, M., Yang, Z., Liu, X., Zong, A. B., Safer, D., and Sweeney, H. L. Cargo binding induces dimerization of myosin VI. *Proceedings of the National Academy of Sciences of the United States of America*, 106(41):17320–17324, 2009. doi: 10.1073/pnas.0909748106.

Phillips, R. K., Peter, L. G., Gilbert, S. P., and Rayment, I. Family-specific kinesin structures reveal neck-linker length based on initiation of the coiled-coil. *Journal of Biological Chemistry*, 291(39):20372–20386, 2016. doi: 10.1074/jbc.M116.737577.

Pinaud, F. and Dahan, M. Targeting and imaging single biomolecules in living cells by complementation-activated light microscopy with split-fluorescent proteins. *Proceedings of the National Academy of Sciences*, 108(24):E201–E210, 2011. doi: 10.1073/pnas.1101929108.

Post, P. L., Tyska, M. J., O'Connell, C. B., Johung, K., Hayward, A., and Mooseker, M. S. Myosin-IXb is a single-headed and processive motor. *Journal of Biological Chemistry*, 277(14):11679–11683, 2002. doi: 10.1074/jbc.M111173200.

Pyrpassopoulos, S., Arpa, G., Feeser, E. A., Shuman, H., Tüzel, E., and Ostap, E. M. Force Generation by Membrane-Associated Myosin-I. *Scientific Reports*, pages 1–14, 2016. doi: 10.1038/srep25524.

Rai, A. K., Rai, A., Ramaiya, A. J., Jha, R., and Mallik, R. Molecular adaptations allow dynein to generate large collective forces inside cells. *Cell*, 152(1-2): 172–182, 2013. doi: 10.1016/j.cell.2012.11.044.

Ramos-Nascimento, A., Kellen, B., Ferreira, F., Alenquer, M., Vale-Costa, S., Raposo, G., Delevoye, C., and Amorim, M. J. KIF13A mediates trafficking of influenza A virus ribonucleoproteins. *Journal of Cell Science*, 130(23):4038–4050, 2017. doi: 10.1242/jcs.210807.

Ray, S., Meyhöfer, E., Milligan, R. A., and Howard, J. Kinesin follows the microtubule's protofilament axis. *Journal of Cell Biology*, 121(5):1083–1093, 1993. doi: 10.1083/jcb.121.5.1083.

Reck-Peterson, S. L., Tyska, M. J., Novick, P. J., and Mooseker, M. S. The Yeast Class V Myosins, Myo2p and Myo4p, Are Nonprocessive Actin-based Motors. *Journal of Cell Biology*, 153(5):1121–1126, 2001.

Reid, E., Kloos, M., Ashley-Koch, A., Hughes, L., Bevan, S., Svenson, I. K., Graham, F. L., Gaskell, P. C., Dearlove, A., Pericak-Vance, M. A., Rubinsztein, D. C., and Marchuk, D. A. A Kinesin Heavy Chain (KIF5A) Mutation in Hereditary Spastic Paraplegia (SPG10). *The American Journal of Human Genetics*, 71 (5):1189–1194, 2002. doi: 10.1086/344210.

Rice, S., Lin, A. W., Safer, D., Hart, C. L., Naber, N., Carragher, B. O., Cain, S. M., Pechatnikova, E., Wilson-kubalek, E. M., Whittaker, M., I, E. P., Cooke, R.,

Taylor, E. W., Milligan, R. A., and Vale, R. D. A structural change in the kinesin motor protein that drives motility. *Nature*, 402:778–784, 1999.

Rogers, A. R., Driver, J. W., Constantinou, P. E., Jamison, D. K., and Diehl, M. R. Negative interference dominates collective transport of kinesin motors in the absence of load. *Physical Chemistry Chemical Physics*, 11(24):4800–4803, 2009. doi: 10.1039/b901646e.

Rosenfeld, S. S., Fordyce, P. M., Jefferson, G. M., King, P. H., and Block, S. M. Stepping and stretching. How kinesin uses internal strain to walk processively. *Journal of Biological Chemistry*, 278(20):18550–18556, 2003. doi: 10.1074/jbc.M300849200.

Ross, J. L., Ali, M. Y., and Warshaw, D. M. Cargo transport: molecular motors navigate a complex cytoskeleton. *Current Opinion in Cell Biology*, 20(1):41–47, 2008. doi: 10.1016/j.ceb.2007.11.006.

Roth, S., Dogterom, M., Casademunt, J., and Oriola, D. Formation of helical membrane tubes around microtubules by single-headed kinesin KIF1A. *Nature Communications*, 6:1–8, 2015. doi: 10.1038/ncomms9025.

Sakamoto, T., Webb, M. R., Forgacs, E., White, H. D., and Sellers, J. R. Direct observation of the mechanochemical coupling in myosin Va during processive movement. *Nature*, 455(7209):128–132, 2008. doi: 10.1038/nature07188.

Schindler, T. D., Chen, L., Lebel, P., Nakamura, M., and Bryant, Z. Engineering myosins for long-range transport on actin filaments. *Nature Nanotechnology*, 9(1):33–38, 2014. doi: 10.1038/nnano.2013.229.

Schnitzer, M. J. and Block, S. M. Kinesin hydrolyses one ATP per 8-nm step. *Nature*, 388(6640):386–390, 1997. doi: 10.1038/41111.

Scholey, J. M. Intraflagellar transport motors in cilia: Moving along the cell's antenna. *Journal of Cell Biology*, 180(1):23–29, 2008. doi: 10.1083/jcb.200709133.

Scholey, J. M. Kinesin-2: a family of heterotrimeric and homodimeric motors with diverse intracellular transport functions. *Annual Review of Cell and Developmental Biology*, 29(May):443–69, 2013. doi: 10.1146/annurev-cellbio-101512-122335.

Sellers, J. R. Myosins: A diverse superfamily. *Biochimica et Biophysica Acta - Molecular Cell Research*, 1496(1):3–22, 2000. doi: 10.1016/S0167-4889(00)00005-7.

Setou, M., Setou, M., Nakagawa, T., and Seog, D.-h. Kinesin Superfamily Motor Protein KIF17 and mLin-10 in NMDA Receptor Containing Vesicle Transport. *Science*, 288(2000):1796–1803, 2000. doi: 10.1126/science.288.5472.1796.

Sheetz, M. P. and Spudich, J. A. Movement of myosin-coated fluorescent beads on actin cables in vitro. *Nature*, 303(5912):31–35, 1983. doi: 10.1038/303031a0.

Shubeita, G. T., Tran, S. L., Xu, J., Vershinin, M., Cermelli, S., Cotton, S. L., Welte, M. a., and Gross, S. P. Consequences of Motor Copy Number on the Intracellular Transport of Kinesin-1-Driven Lipid Droplets. *Cell*, 135(6): 1098–1107, 2008. doi: 10.1016/j.cell.2008.10.021.

Sivaramakrishnan, S. and Spudich, J. A. Systematic control of protein interaction using a modular ER/K α-helix linker. *Proceedings of the National Academy of Sciences*, 108(51):20467–20472, 2011. doi: 10.1073/pnas.1116066108.

Sivaramakrishnan, S., Sung, J., Ali, M., Doniach, S., Flyvbjerg, H., and Spudich, J. A. Combining single-molecule optical trapping and small-angle x-ray scattering measurements to compute the persistence length of a protein ER/K α-helix. *Biophysical Journal*, 97(11):2993–2999, 2009. doi: 10.1016/j.bpj.2009.09.009.

Sivaramakrishnan, S. and Spudich, J. A. Coupled myosin VI motors facilitate unidirectional movement on an F-actin network. *Journal of Cell Biology*, 187(1): 53–60, 2009. doi: 10.1083/jcb.200906133.

Sivaramakrishnan, S., Spink, B. J., Sim, A. Y. L., Doniach, S., and Spudich, J. A. Dynamic charge interactions create surprising rigidity in the ER/K alpha-helical protein motif. *Proceedings of the National Academy of Sciences of the United States of America*, 105(36):13356–61, 2008. doi: 10.1073/pnas.0806256105.

Smith, J. J. and Aitchison, J. D. Peroxisomes take shape. *Nature Reviews Molecular Cell Biology*, 14(12):803–817, 2013. doi: 10.1038/nrm3700.

Soppina, V. and Verhey, K. J. The family-specific K-loop influences the microtubule on-rate but not the superprocessivity of kinesin-3 motors. *Molecular biology of the cell*, 25(14):2161–70, 2014. doi: 10.1091/mbc.E14-01-0696.

Soppina, V., Rai, A. K., Ramaiya, A. J., Barak, P., and Mallik, R. Tug-of-war between dissimilar teams of microtubule motors regulates transport and fission of endosomes. *Proc. Natl. Acad. Sci. USA*, 106(46):19381–6, 2009. doi: 10.1073/pnas.0906524106.

Soppina, V., Norris, S. R., Dizaji, A. S., Kortus, M., Veatch, S., and Peckham, M. Dimerization of mammalian kinesin-3 motors results in superprocessive motion. *Proceedings of the National Academy of Sciences*, 111(15), 2014. doi: 10.1073/pnas.1400759111.

Spudich, J. A., Rice, S. E., Rock, R. S., Purcell, T. J., and Warrick, H. M. Optical traps to study properties of molecular motors. *Cold Spring Harbor Protocols*, 6(11):1305–1318, 2011a. doi: 10.1101/pdb.top066662.

Spudich, J. A., Rice, S. E., Rock, R. S., Purcell, T. J., and Warrick, H. M. Optical traps to study properties of molecular motors. *Cold Spring Harbor Protocols*, 6(11):1305–1318, 2011b. doi: 10.1101/pdb.top066662.

Stauber, T., Simpson, J. C., Pepperkok, R., and Vernos, I. A Role for Kinesin-2 in COPI-Dependent Recycling between the ER and the Golgi Complex. *Current Biology*, 16(22):2245–2251, 2006. doi: 10.1016/j.cub.2006.09.060.

Stewart, R. J., Thaler, J. P., and Goldstein, L. S. Direction of microtubule movement is an intrinsic property of the motor domains of kinesin heavy chain and Drosophila ncd protein. *Proceedings of the National Academy of Sciences of the United States of America*, 90(11):5209–5213, 1993. doi: 10.1073/pnas.90.11.5209.

Svoboda, K. and Block, S. M. Force and velocity measured for single kinesin molecules. *Cell*, 77(5):773–84, jun 1994.

Svodoba, K., Schmidt, C. F., Schnapp, B. J., and Block, S. M. Direct observation of kinesin stepping by optical trapping interferometry. *Nature*, 365:721–727, 1993.

Swanson, C. J. and Sivaramakrishnan, S. Harnessing the unique structural properties of isolated α-helices. *Journal of Biological Chemistry*, 289(37):25460–25467, 2014. doi: 10.1074/jbc.R114.583906.

Takeda, S., Yonekawa, Y., Tanaka, Y., Okada, Y., Nonaka, S., and Hirokawa, N. New Insights in Determination of Laterality and Mesoderm Induction by. *The Journal of cell biology*, 145(4):825–836, 1999. doi: 10.1083/jcb.145.4.825.

Tanaka, Y., Kanai, Y., Okada, Y., Nonaka, S., Takeda, S., Harada, A., and Hirokawa, N. Targeted disruption of mouse conventional kinesin heavy chain, kif5B, results in abnormal perinuclear clustering of mitochondria. *Cell*, 93(7):1147–1158, 1998. doi: 10.1016/S0092-8674(00)81459-2.

Tao, L., Fasulo, B., Warecki, B., and Sullivan, W. Tum/RacGAP functions as a switch activating the Pav/kinesin-6 motor. *Nature Communications*, 7, 2016. doi: 10.1038/ncomms11182.

Teng, J., Rai, T., Tanaka, Y., Takei, Y., Nakata, T., Hirasawa, M., Kulkarni, A. B., and Hirokawa, N. The KIF3 motor transports N-cadherin and organizes the developing neuroepithelium. *Nature Cell Biology*, 7(5):474–482, 2005. doi: 10.1038/ncb1249.

Tomishige, M., Klopfenstein, D. R., and Vale, R. D. Conversion of Unc104/KIF1A kinesin into a processive motor after dimerization. *Science*, 297:2263–2267, 2002. doi: 10.1126/science.1073386.

Tseng, K. F., Wang, P., Lee, Y. R. J., Bowen, J., Gicking, A. M., Guo, L., Liu, B., and Qiu, W. The preprophase band-associated kinesin-14 OsKCH2 is a processive minus-end-directed microtubule motor. *Nature Communications*, 9 (1):1–11, 2018. doi: 10.1038/s41467-018-03480-w.

Tuma, M. C., Zill, A., Le Bot, N., Vernos, I., and Gelfand, V. Heterotrimeric kinesin II is the microtubule motor protein responsible for pigment dispersion in Xenopus melanophores. *Journal of Cell Biology*, 143(6):1547–1558, 1998. doi: 10.1083/jcb.143.6.1547.

Uyeda, T. Q., Abramson, P. D., and Spudich, J. a. The neck region of the myosin motor domain acts as a lever arm to generate movement. *Proceedings of the National Academy of Sciences of the United States of America*, 93(April): 4459–4464, 1996. doi: 10.1073/pnas.93.9.4459.

Uyeda, T. Q., Warrick, H. M., Kron, S. J., and Spudich, J. A. Quantized velocities at low myosin densities in an in vitro motility, 1991. ISSN 00280836.

Vale, R. D. and Milligan, R. a. The way things move: looking under the hood of molecular motor proteins. *Science (New York, N.Y.)*, 288(5463):88–95, 2000. doi: 10.1126/science.288.5463.88.

Vale, R. D. The molecular motor toolbox for intracellular transport. *Cell*, 112(4): 467–480, 2003. doi: 10.1016/S0092-8674(03)00111-9.

Vale, R. D., Reese, T. S., and Sheetz, M. P. Identification of a Novel Force-Generating Protein, Kinesin, Involved in Microtubule-Based Motility. *Cell*, 42:39–50, 1985.

Vale, R. D., Funatsu, T., Pierce, D. W., Romberg, L., Harada, Y., and Yanagida, T. Direct observation of single kinesin molecules moving along microtubules. *Nature*, 380:451–453, 1996.

Veigel, C. and Schmidt, C. F. Moving into the cell: single-molecule studies of molecular motors in complex environments. *Nature Reviews Molecular Cell Biology*, 12:163–176, mar 2011. doi: 10.1038/nrm3062.

Verhey, K. J. and Hammond, J. W. Traffic control: regulation of kinesin motors. *Nature Reviews Molecular Cell Biology*, 10(11):765–777, 2009. doi: 10.1038/nrm2782.

Verhey, K. J., Kaul, N., and Soppina, V. Kinesin Assembly and Movement in Cells. *Annu. Rev. Biophys*, 40:267–88, 2011. doi: 10.1146/annurev-biophys-042910-155310.

Vershinin, M., Carter, B. C., Razafsky, D. S., King, S. J., and Gross, S. P. Multiple-motor based transport and its regulation by Tau. *Proc. Natl. Acad. Sci. USA*, 104(1):87–92, 2007.

Visscher, K., Schnitzer, M. J., and Block, S. M. Single kinesin molecules studied with a molecular force clamp. *Nature*, 400(6740):184–9, 1999. doi: 10.1038/22146.

Walter, W. J., MacHens, I., Rafieian, F., and Diez, S. The non-processive rice kinesin-14 OsKCH1 transports actin filaments along microtubules with two distinct velocities. *Nature Plants*, 1(August):1–5, 2015. doi: 10.1038/nplants.2015.111.

Wang, W., Cao, L., Wang, C., Gigant, B., and Knossow, M. Kinesin, 30 years later: Recent insights from structural studies. *Protein Science*, 24:1047–1056, 2015. doi: 10.1002/pro.2697.

Wei, J. H. and Seemann, J. Golgi ribbon disassembly during mitosis, differentiation and disease progression. *Current Opinion in Cell Biology*, 47:43–51, 2017. doi: 10.1016/j.ceb.2017.03.008.

Wiemer, E. A., Wenzel, T., Deerinck, T. J., Ellisman, M. H., and Subramani, S. Visualization of the peroxisomal compartment in living mammalian cells: Dynamic behavior and association with microtubules. *Journal of Cell Biology*, 136(1):71–80, 1997. doi: 10.1083/jcb.136.1.71.

Woehlke, G. and Schliwa, M. Directional motility of kinesin motor proteins. *Biochimica et Biophysica Acta - Molecular Cell Research*, 1496(1):117–127, 2000. doi: 10.1016/S0167-4889(00)00013-6.

Wong, R. W.-C., Setou, M., Teng, J., Takei, Y., and Hirokawa, N. Overexpression of motor protein KIF17 enhances spatial and working memory in transgenic mice. *Proceedings of the National Academy of Sciences*, 99(22):14500–14505, 2002. doi: 10.1073/pnas.222371099.

Xia, C. H., Roberts, E. A., Her, L. S., Liu, X., Williams, D. S., Cleveland, D. W., and Goldstein, L. S. Abnormal neurofilament transport caused by targeted disruption of neuronal kinesin heavy chain KIF5A. *Journal of Cell Biology*, 161(1):55–66, 2003. doi: 10.1083/jcb.200301026.

Xu, J., Shu, Z., King, S. J., and Gross, S. P. Tuning Multiple Motor Travel via Single Motor Velocity. *Traffic*, 13(9):1198–1205, 2012. doi: 10.1111/j.1600-0854.2012.01385.x.

Xu, J., King, S. J., Lapierre-Landry, M., and Nemec, B. Interplay between velocity and travel distance of Kinesin-based transport in the presence of tau. *Biophysical Journal*, 105(10):L23–L25, 2013. doi: 10.1016/j.bpj.2013.10.006.

Yamazaki, H., Nakata, T., Okada, Y., and Hirokawa, N. KIF3A/B: A heterodimeric kinesin superfamily protein that works as a microtubule plus end-directed motor for membrane organelle transport. *Journal of Cell Biology*, 130(6):1387–1399, 1995. doi: 10.1083/jcb.130.6.1387.

Yildiz, A., Forkey, J. N., McKinney, S. A., Taekjip, H., Goldman, Y. E., and Selvin, P. R. Myosin V Walks Hand-Over-Hand: Single Fluorophore Imaging with 1.5-nm Localization. *Science*, 300:2061–2065, 2003.

Yildiz, A., Tomishige, M., Vale, R. D., and Selvin, P. R. Kinesin walks hand-over-hand. *Science*, 303(5658):676–678, 2004. doi: 10.1126/science.1093753.

Yildiz, A., Tomishige, M., Gennerich, A., and Vale, R. D. Intramolecular Strain Coordinates Kinesin Stepping Behavior along Microtubules. *Cell*, 134(6):1030–1041, 2008. doi: 10.1016/j.cell.2008.07.018.

Young, E. C., Mahtani, H. K., and Gelles, J. One-headed kinesin derivatives move by a nonprocessive, low-duty ratio mechanism unlike that of two-headed kinesin. *Biochemistry*, 37(10):3467–3479, 1998. doi: 10.1021/bi972172n.

Yu, C., Feng, W., Wei, Z., Miyanoiri, Y., Wen, W., Zhao, Y., and Zhang, M. Myosin VI Undergoes Cargo-Mediated Dimerization. *Cell*, 138(3):537–548, 2009. doi: 10.1016/j.cell.2009.05.030.

Zhang, P., Rayment, I., and Gilbert, S. P. Fast or Slow, Either Head Can Start the Processive Run of Kinesin-2 KIF3AC. *Journal of Biological Chemistry*, 291 (9):4407–4416, 2016. doi: 10.1074/jbc.M115.705970.

Zhang, Y. and Hancock, W. O. The two motor domains of KIF3A/B coordinate for processive motility and move at different speeds. *Biophysical Journal*, 87(3): 1795–1804, 2004. doi: 10.1529/biophysj.104.039842.

Zhao, C., Takita, J., Tanaka, Y., Setou, M., Nakagawa, T., Takeda, S., Yang, H. W., Terada, S., Nakata, T., Takei, Y., Saito, M., Tsuji, S., Hayashi, Y., and Hirokawa, N. Charcot-Marie-Tooth disease type 2A caused by mutation in a microtubule motor KIF1Bbeta. *Cell*, 105(5):587–97, 2001. doi: S0092-8674(01)00363-4[pii].